

SEDIMENTOLOGY OF THE VIKING FORMATION,  
GILBY A AND B FIELDS, ALBERTA

SEDIMENTOLOGY OF THE VIKING FORMATION,  
(LOWER CRETACEOUS),  
GILBY A AND B FIELDS, ALBERTA

By

HOLLY KATHERINE RADDYSH, B.E.S.

A Thesis

Submitted to the Department of Geology  
in Partial Fulfillment of the Requirements  
for the degree of  
Bachelor of Science

McMaster University

1986

C Holly K. Raddysh, 1986

BACHELOR OF SCIENCE (1986)  
(Geology)

McMASTER UNIVERSITY  
Hamilton, Ontario

TITLE: Sedimentology of the Viking Formation (Lower  
Cretaceous), Gilby A and B Fields, Alberta

AUTHOR: Holly Katherine Raddysh, B.E.S.  
(University of Waterloo)

SUPERVISOR: Professor R. G. Walker

NUMBER OF PAGES: 241

## ABSTRACT

Examination of 80 cores from the Viking Formation in the Gilby A and B Field area allows sub-division into eleven facies: 2 of which are predominantly mudstone, 2 fine to medium grained sandstone facies, 2 laminated-burrowed mudstone-sandstone facies, 2 pebbly sandstone facies, 2 conglomeratic facies and 1 facies (sideritized muddy siltstone with Skolithos) which represents an erosional or scoured surface. Trough cross-bedding is the dominant sedimentary structure preserved in the sandy facies. Low angle trough cross-bedding is observed in the pebbly sandstone facies. The conglomeratic facies lack stratification. Sandstone and conglomeratic facies are referred to as the Viking Formation "coarse sediment package" which is enveloped with sharp contacts by underlying siltstones and overlying mudstones.

Both lateral and vertical variation of the facies sequence occur over the Gilby A and B fields. The Gilby A field may be delineated into 3 facies assemblages and the Gilby B field as 1 facies assemblage. The vertical variation in facies sequence of the coarse sediment package is observed across the width of the Gilby A and B fields, where 1 to 3 coarsening-upward sequences are observed.

Detailed study of log markers (using 450 logs) and facies variations throughout the study region has revealed a scour beginning along the southwestern margin of the Gilby A and B fields. This scour surface is coincident with the

lower surface of the coarse sediment package - represented by a chert pebble veneer to the southeast of the fields. The surface is also coincident with the sideritized muddy siltstone (with Skolithos) facies (immediately underlying the pebble veneer) found to the south and along the southwest margins of the fields, although the scour has removed this facies to the northwest. The scour surface drops stratigraphically towards the northeast margin of the fields and gently rises stratigraphically approximately 4.8-6.4 km beyond the northeastern margin of the fields.

The development of this scoured surface is problematic. A transgressive period or relative rise in sea level could have eroded the shoreface (presuming the area was near the shoreface) leaving the scoured topography. This topography being subsequently infilled by the Viking coarse sediment package during a regressive period or relative drop in sea level. Conversely, a rapid drop in sea level could have resulted in the development of the scoured topography. This was followed by scour topography infilling during a continued, though slower regression possibly under influence of a longshore current system.

## ACKNOWLEDGEMENTS

There are a number of individuals and companies whose contributions have aided this study.

I thank R. G. Walker for his supervision of the study. His critical editing and knowledge of sedimentology was of great benefit to the research.

I thank A. G. Plint (University of Western Ontario) for his useful comments and criticisms.

G. Pemberton (University of Alberta) helped identify trace fossils and significantly aided the authors understanding of the depositional history of the study area.

The identification of trace fossils by M. Risk (McMaster University) was greatly appreciated.

I acknowledge the support of fellow McMaster University students K. P. Downing, M. Franklyn, J. G. Pozzobon and M. Rutka for their interest, comments and criticisms. The study benefited greatly from discussions with K. P. Downing and J. G. Pozzobon. I especially thank R. Rice for his assistance and comments involving the petrography and Markov chain analysis, as well as G. Rice for his assistance involving the cathode luminescent microscopy.

G. Nadon (University of Toronto) assisted in acquiring data used in the study and provided useful suggestions and criticisms.

I acknowledge the support of Texaco Canada Resources Ltd. who provided base maps, well logs and core analysis used in the study. I thank G. Dillabough of Texaco and S.

Greer (Luscar Ltd.) for their suggestions and assistance.

Gulf Canada Corp. kindly provided map reductions, reproductions and copies. Gulf geologists D. Bardwell, D. Inkster and K. Stromquist made useful suggestions and criticisms.

From McMaster University, J. J. Whorwood developed core photographs and photomicrographs, L. Zwicker prepared all thin-sections and J. Ceker assisted in the use of microscopes.

J. W. Keith (Consulting Geologist) provided technical support and useful comments on the study.

I thank Gulf Canada Corp. in Calgary and R. G. Walker in Hamilton for providing use of word-processing facilities.

I acknowledge the very significant contribution to the thesis made by M. R. Keith who professionally drafted the majority of figures in the thesis.

D. A. Keith (Alberta Research Council) provided much assistance during the writing of this thesis, including help with word-processing and editorial comments.

The research was financially supported by a National Science and Engineering Research Council (NSERC) Scholarship to the author and a NSERC Grant to R. G. Walker.

Finally, I thank A. A. Raddysh, L. M. Raddysh, and J. A. Raddysh for their considerable moral and financial support. Most importantly I thank my parents Alexandra and Tony Raddysh for their continual assistance, patience and encouragement.

## Table of Contents

	PAGE
<b>CHAPTER 1. INTRODUCTION</b>	
1.1 The Problem .....	1
1.1.1 Shoreface Attached Sandbodies .....	1
1.1.2 Offshore Developed Sandbodies .....	2
1.2 General Introduction .....	3
1.2.1 Viking Formation .....	4
1.2.2 Gilby A and B Fields .....	4
1.3 Justification and Goals of Study .....	5
1.4 Data Base .....	8
1.5 Thesis Format .....	8
 <b>CHAPTER 2. STRATIGRAPHY AND SETTING</b>	
2.1 Viking Formation .....	10
2.1.1 Biostratigraphy and Chronostratigraphy .	10
2.1.2 Setting .....	11
2.1.3 Viking Stratigraphy .....	12
Internal Viking Stratigraphy .....	14
2.1.4 Previous Work .....	21
2.2 Gilby A and B Fields .....	25
2.2.1 History .....	25
2.2.2 Structural Setting .....	26
Paleogeographic Setting .....	27
 <b>CHAPTER 3. FACIES AND FACIES SEQUENCE</b> .....	
3.1 Method and Introduction .....	28
3.2 Facies Divisions .....	28
3.3 Facies Descriptions .....	29
3.3.1 Facies A: Homogenous Muddy Siltstones ..	29
3.3.2 Facies B: Sideritized Muddy Siltstones (With <u>Skolithos</u> ) .....	33
3.3.3 Facies C: Pervasively Bioturbated Muddy Sandstones .....	44

3.3.4	Facies D: Burrowed-Laminated Mudstones-Sandstones .....	47
3.3.5	Facies E: Cross Bedded Sandstones .....	52
3.3.6	Facies F: Pebbly Cross Bedded Sandstones .....	56
3.3.7	Facies G: Laminated Mudstone-Pebbly Sandstones .....	59
3.3.8	Facies H: Massive Pebbly Sandstones .....	63
3.3.9	Facies I: Laminated Mudstones and Conglomerates .....	66
3.3.10	Facies J: Conglomerates .....	69
3.3.11	Facies K: Black Mudstones .....	72
3.4	Generalized Facies Sequence .....	76
3.4.1	Introduction to Facies Sequence .....	76
3.4.2	Discussion .....	80
3.4.3	Gilby A-1 .....	82
3.4.4	Gilby A-3 .....	95
3.4.5	Gilby A-2 .....	101
3.4.6	Gilby B-1 .....	106
3.5	Summary .....	114
 CHAPTER 4. PETROGRAPHY		
4.1	Method .....	116
4.2	Results .....	117
4.2.1	Constituents .....	118
	Quartz .....	118
	Chert .....	125
	Rock Fragments .....	125
	Feldspars .....	128
	Glauconite .....	128
	Accessory Minerals .....	135
	Cements .....	135
 CHAPTER 5. FACIES DISTRIBUTION AND DETAILED FIELD GEOMETRY		
5.1	Introduction .....	143
5.2	Facies Distribution .....	143
5.2.1	Capping Conglomerate Distribution .....	143
5.2.2	Maximum Chert Pebble Length in Capping Conglomerate .....	147
5.2.3	Glauconite Distribution .....	150
5.3	Cross-Sections .....	153
5.3.1	Introduction .....	153
5.3.2	Section 1 .....	154
5.3.3	Section 2 .....	157

5.3.4	Section 3 .....	161
5.3.5	Section 4 .....	165
5.3.6	Section 5 .....	168
5.3.7	Datum Investigation and Normalization ...	172
5.3.8	Summary .....	182
5.4	Isopach Maps .....	185
5.4.1	Isopach of Viking Coarse Sediment Package	185
5.4.2	Isopach of Upper Datum to Lower Surface of Coarse Sediment Package .....	188
5.5	Summary .....	189
CHAPTER 6.	CONCLUSIONS .....	192
6.1	Introduction .....	192
6.2	Gilby A and B Scour .....	192
6.3	Review of the Gilby A and B Coarse Sediment Distribution and Scour .....	193
6.3.1	Introduction of Figures 6.1, 6.2 and 6.3.	193
6.3.2	Discussion of Figures 6.1, 6.2 and 6.3 ..	202
6.4	Development and Infill of the Gilby Scour .....	203
6.5	Development of the Viking Gilby A and B fields .	206
REFERENCES	.....	207
APPENDIX 1 - MARKOV CHAIN ANALYSIS - DATA AND RESULTS ..		212
APPENDIX 2 - WELL LOCATIONS OF EXAMINED CORE .....		217
APPENDIX 3 - DIAGRAMMATIC CORE DESCRIPTIONS .....		219

## List of Figures

	PAGE
1.1. Study Area Location Map .....	7
2.1. Stratigraphic Nomenclature .....	16
2.2. Internal Viking Stratigraphy .....	19
3.1. Dark Muddy Siltstone .....	32
3.2. Dark Muddy Siltstone .....	32
3.3. Bioturbated Muddy Siltstone .....	32
3.4. Bioturbated Siltstone .....	32
3.5. Sideritized Muddy Siltstone (with <u>Skolithos</u> ) .....	38
3.6. Sideritized Muddy Siltstone (with <u>Skolithos</u> ) .....	38
3.7. Sideritized Muddy Siltstone (with <u>Skolithos</u> ) .....	38
3.7a. Sideritized Muddy Siltstone (with <u>Skolithos</u> ) .....	40
3.7b. Photomicrograph of Sideritized Muddy Siltstone (with <u>Skolithos</u> ) .....	40
3.7c. Photomicrograph of Sideritized Muddy Siltstone (with <u>Skolithos</u> ) .....	43
3.7d. Photomicrograph of Sideritized Muddy Siltstone (with <u>Skolithos</u> ) .....	43
3.8. Bioturbated Muddy Sandstone .....	46
3.9. Bioturbated Muddy Sandstone .....	46
3.10. Bioturbated Muddy Sandstone .....	46
3.11. Burrowed-Laminated Mudstone-Sandstone .....	51
3.12. Burrowed-Laminated Sandstone-Mudstone .....	51
3.13. Burrowed-Laminated Mudstone-Sandstone .....	51
3.14. Burrowed-Laminated Mudstone-Sandstone .....	51
3.15. Cross-Bedded Sandstone .....	55
3.16. Cross-Bedded Sandstone .....	55

3.17. Pebbly Cross-Bedded Sandstone .....	58
3.18. Pebbly Cross-Bedded Sandstone .....	58
3.19. Pebbly Cross-Bedded Sandstone .....	58
3.20. Laminated Mudstone-Pebbly Sandstone .....	62
3.21. Laminated Mudstone-Pebbly Sandstone .....	62
3.22. Laminated Mudstone-Pebbly Sandstone .....	62
3.23. Massive Pebbly Sandstone .....	65
3.24. Massive Pebbly Sandstone .....	65
3.25. Laminated Mudstone and Conglomerate .....	68
3.26. Laminated Mudstone and Conglomerate .....	68
3.27. Conglomerate .....	71
3.28. Conglomerate .....	71
3.29. Conglomerate .....	71
3.30. Black Mudstone .....	75
3.31. Black Mudstone .....	75
3.32. Black Mudstone .....	75
3.33. Black Mudstone .....	75
3.34. Legend for Facies .....	77
3.35. Location Map for Core and Log Cross-Sections .....	79
3.36. Lithologic Cross-Section 1 .....	84
3.37. Lithologic Cross-Section 2 .....	88
3.38. Facies Relationship Diagram - Gilby A-1 area .....	92
3.39. Lithologic Cross-Section 4 .....	97
3.40. Facies Relationship Diagram - Gilby A-3 area .....	100
3.41. Lithologic Cross-Section 3 .....	103
3.42. Lithologic Cross-Section 5 .....	108
3.43. Facies Relationship Diagram - Gilby B-1 area .....	112

4.1.	Modal Percentages of Constituents from Point Counting .....	120
4.2.	Sandstone Classification .....	122
4.3.	Photomicrograph of Cross-bedded Sandstone .....	124
4.4.	Cathodoluminescent photomicrograph of Figure 4.3 .	124
4.5.	Photomicrograph of Cross-bedded Sandstone .....	127
4.6.	Photomicrograph of Cross-bedded Sandstone .....	127
4.7.	Photomicrograph of Cross-bedded Sandstone .....	130
4.8.	Cathodoluminescent photomicrograph of Figure 4.7 .	130
4.9.	Photomicrograph of Pervasively Bioturbated Muddy Sandstone .....	132
4.10.	Cathodoluminescent photomicrograph of Figure 4.9 .	132
4.11.	Photomicrograph of Massive Pebbly Sandstone .....	134
4.12.	Photomicrograph of Massive Pebbly Sandstone .....	134
4.13.	Photomicrograph of Massive Pebbly Sandstone .....	138
4.14.	Cathodoluminescent photomicrograph of Figure 4.13	138
4.15a and b.	Scanning Electron Photomicrograph of Massive Pebbly Sandstone .....	140
4.16a, b and c.	Scanning Electron Photomicrograph of Massive Pebbly Sandstone .....	142
5.1.	Isopach Map of Capping Conglomerate Distribution .	145
5.2.	Distribution of Maximum Chert Pebble Length in the Capping Conglomerates .....	149
5.3.	Distribution of Glauconite .....	152
5.4.	Cross-Section 1 .....	156
5.5.	Cross-Section 2 .....	159
5.6.	Cross-Section 3 .....	163
5.7.	Cross-Section 4 .....	167

5.8.	Cross-Section 5 .....	170
5.9.	Location Map of Facies B Boundary .....	174
5.10.	Structure Map of the Upper Datum (Marker A) .....	177
5.11.	Normalized Cross-Sections 2, 3, 4 and 5 .....	181
5.12.	Isopach Map of the Viking Coarse Sediment Package.	184
5.13.	Isopach Map of the Upper Datum to the Lower Surface of the Coarse Sediment Package .....	187
6.1.	Cross-Section 6.1 through Figures 5.12 and 5.13 ..	195
6.2.	Cross-Section 6.2 through Figures 5.12 and 5.13 ..	197
6.3.	Cross-Section 6.3 through Figures 5.12 and 5.13 ..	199

## CHAPTER 1: INTRODUCTION

### 1.1 The Problem

#### Development of Elongate Linear Sandstone Bodies - Cretaceous Interior Seaway

This study provides sedimentological information on two linear northwest-southeast trending shallow marine sandstone bodies deposited within the Interior Cretaceous Seaway of western North America. The development of ancient linear sandstone bodies is problematic, they may have formed either as shoreface attached bodies or developed as offshore bodies.

#### 1.1.1 Shoreface Attached Sandbodies

Studies of somewhat similar modern sandbodies show them to originate as shoreface-attached bodies which are detached during subsequent transgression (Swift and Field, 1981). Swift and Field (1981) have documented the off-shore migration of linear sandridges on the Maryland inner continental shelf. Direct comparison between modern linear sandstone bodies and ancient examples is difficult because of dissimilarities between them. Most ancient linear sandstone bodies have a gradational, coarsening-upward sequence (Walker, 1984; p.163), are completely encased in mud (Swift and Rice, 1984, p. 44) and may have been

deposited during regression. Modern sandstone bodies, such as those on the Atlantic Shelf or the Southern Bight of the North Sea "protrude from Holocene transgressive sand sheets through overlying Holocene mud deposits" (Swift and Rice, 1984; p.43) and as mentioned above were detached from the shoreface during transgression.

#### 1.1.2 Offshore Developed Sandbodies

Alternatively these sandbodies could develop offshore as suggested by a number of workers who have studied Cretaceous Interior Seaway sandbodies (e.g. Berg, 1975, Hobson et al., 1978; La Fon, 1981; Seeling, 1978; Spearing, 1976; and Walker, 1983a). If these bodies developed offshore problems arise as to mechanisms of sediment transport and reasons for the specific location of sandbody development.

1. Sediment transport offshore: Two possible mechanisms capable of transporting sediment offshore are storm-generated geostrophic currents and turbidity currents.

Storm-generated geostrophic currents have been shown to be important in sediment transport on the continental shelf of the eastern United States (e.g. Swift, 1984) and have been suggested to have been important to sediment transport in the Cretaceous Interior Seaway (Swift and Rice, 1984). Swift (1984) and Walker (1984) discuss geostrophic currents with respect to incremental shelf transport.

Wave loading on the shoreface is suggested by Walker (1984) to have been a possible mechanism of initiating turbidity currents in the Cretaceous Seaway. He has suggested turbidity currents were responsible for offshore sediment transport in several Mesozoic sandstone units in the Interior Seaway (Hamblin and Walker, 1979; Walker, 1986)

2. Offshore location: The location of sand ridge deposition is suggested by Swift and Rice (1984) to be influenced by depositional or structurally developed shelf topography. The initial topography induces further deposition, receiving sand incrementally during successive storms.

## 1.2 General Introduction

This thesis is part of a long term research project at McMaster University investigating shallow marine deposits in the Cretaceous Viking and Cardium Formations in the western Interior Seaway. These Formations are similar in that they generally coarsen upwards (mudstone - siltstone - sandstone +/- conglomerate) and are encased in marine shales. Numerous Viking and Cardium fields occur as long linear sandbodies. The study of specific fields in the Viking and Cardium Formations will provide further insight into the formation of shallow marine sandstone bodies.

This thesis documents the detailed sedimentology and geometry of two linear sandstone bodies - Viking Gilby A and B fields deposited in the Cretaceous Interior Seaway.

### 1.2.1 Viking Formation

The Viking Formation is limited in known outcrop exposure but is correlative with the Bow Island Formation in Southern Alberta and the Paddy and Cadotte Members of the Athabaska Formation in west-central Alberta. Since the Viking Formation is an important oil and gas producer in Western Canada a number of sufficient wells have penetrated the formation to provide excellent subsurface control in Alberta and Saskatchewan. This study was carried out in conjunction with Downing's (M.Sc. in prog., McMaster University) investigation of the Joffre, Mikwan and Fenn Viking fields and Pozzobon's (M.Sc. in prog., McMaster University) study of the Dodsland-Hoosier Viking fields in southwestern Saskatchewan.

### 1.2.2 Gilby A and B Fields

Detailed study of the Viking Formation within the Gilby A and B fields will provide further data on shallow marine sandstone bodies and add to the limited previously published work on these fields. Previous Gilby Viking studies include Love's (1959) brief descriptive review of Gilby-Bentley and Koldijk's (1976) investigation of Gilby B. Love (1959) referred to the southern portion of Gilby A as "Bentley" and

the northern portion as "Gilby". Koldijk's (1976) study will be discussed in more detail in chapter 2.

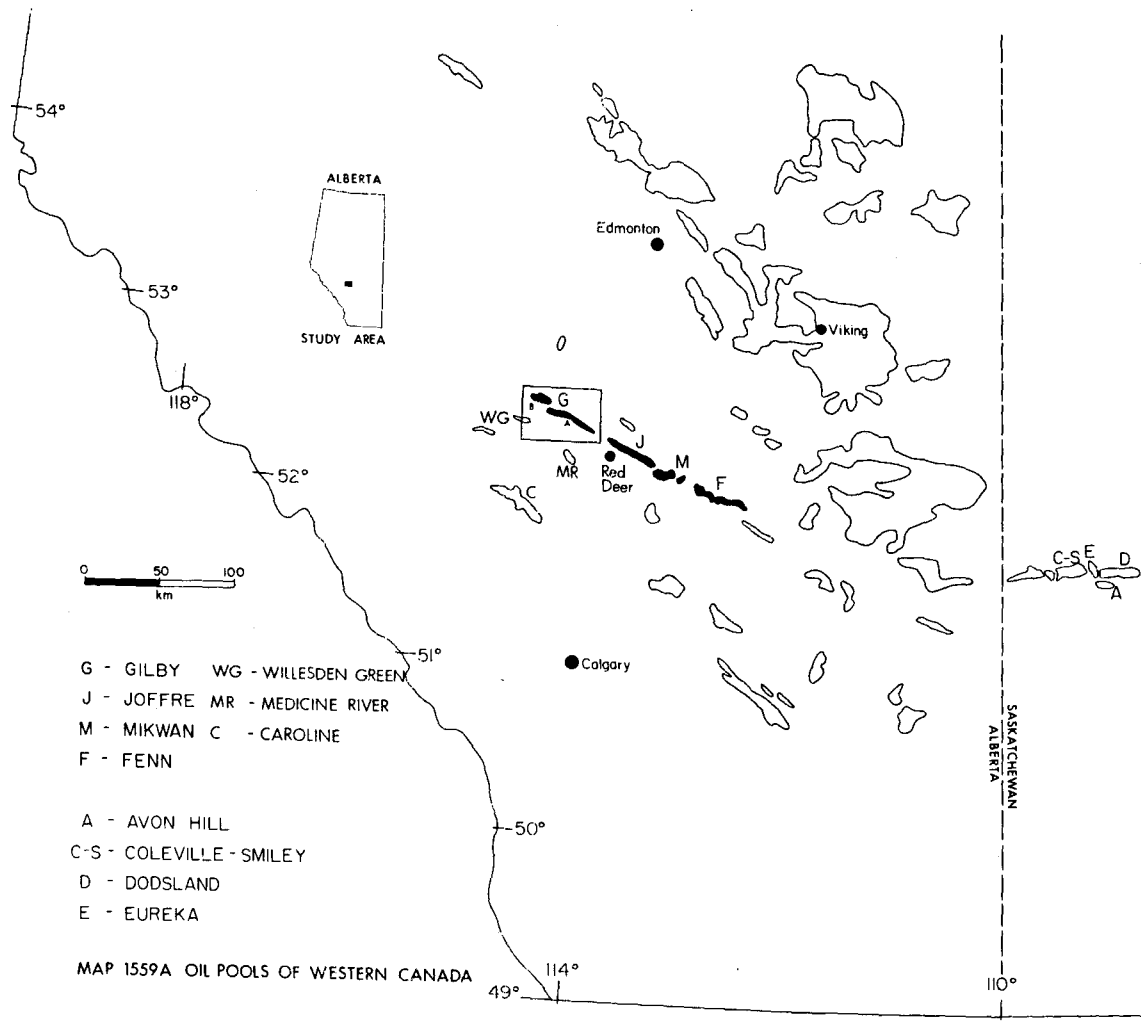
The Gilby A and B fields are located immediately northwest of Red Deer in south-central Alberta (see Figure 1.1). The Gilby fields trend northwest-southeast. Along this trend the Viking Joffre, Mikwan and Fenn fields occur to the southeast of Gilby.

Gilby A is the larger of the two pools covering 5,734 ha, while Gilby B is approximately half as large at 2,334 ha (Energy Resources Conservation Board of Alberta, 1984). The ERCB lists four smaller Viking Gilby pools (C {255 ha}, F {128 ha}, G {65 ha}, and H {64}) surrounding the Gilby A and B fields, these are included within the study area (see Figure 3.35). The total initial established reserves of conventional crude oil for the Gilby A, B, C, F, G and H pools is 3,125,000 m<sup>3</sup> (ERCB, 1984). Well log control is good to the east, west and south of the fields, but only fair to the north of the fields.

### 1.3 Justification and Goals of Study

This study provides detailed sedimentological information and documents geometrical configuration of facies in two linear sandstone bodies which will add information to a growing data base of these problematic shallow marine deposits.

Fig. 1.1. Study area location map. Viking oil fields are shown outlined. Study area shown in box (location in southern Alberta shown in inset), Gilby A and B fields and other adjacent Viking field areas shown darkened, these fields are labelled with key in lower left. From G.S.C. Map 1559A (1984).



The Viking Formation and other shallow marine sandbodies are important oil and gas producers. Additional information on these deposits may help in the exploration for undiscovered hydrocarbon bearing sandbodies and in secondary recovery from producing Viking fields.

#### 1.4 Data Base

The data base used for this study included all available Viking cores in the region (80 cores), which were examined at the Core Research Centre, Calgary. Approximately 450 well logs, specifically resistivity and some gamma responses, were examined. Resistivity logs were primarily used because they are the most available logs in the study area and best showed markers throughout the study area.

#### 1.5 Thesis Format

Chapter 1 has presented an introduction to the problems of elongate shallow marine sandbodies in the Cretaceous Seaway and to the nature and aims of this study. Chapter 2 provides information with respect to biostratigraphy, chronostratigraphy, setting, stratigraphy of the Viking Formation, previous work and history, emphasizing the Gilby

A and B fields. The first half of chapter 3 provides lithofacies description and interpretation. The second half of chapter three is devoted to the facies sequence, discussing both lateral and vertical variations. Chapter 4 provides the findings from petrographic and cathodoluminescence study. The detailed geometry of Gilby A and B, including isopach maps of facies distribution, description of 5 log cross-sections and an examination of the upper and lower surfaces of the coarser Viking sediments are presented in chapter 5. Chapter 6 provides conclusions about the sedimentology of the Viking Formation in the Gilby A and B fields based on the findings of this study.

## Chapter 2: STRATIGRAPHY AND SETTING

### 2.1 Viking Formation

#### 2.1.1 Biostratigraphy and Chronostratigraphy

The Viking Formation is difficult to date accurately, because the microfossils available are inadequate for correlation, and there are too few macrofossils within the Viking sand (Stelck, 1958). Viking stratigraphy is determined by the use of reliable fossil zones which enclose the formation.

The Viking sand member (Stelck, 1975; p.253, referred to in this study as the Viking coarse sediment package, see section 2.1.3 p.20) lies between the underlying Haplophragmoides gigas Zone of the Joli Fou Shale and the overlying Miliammina manitobensis Zone (Stelck, 1958). The M. manitobensis Zone is situated below the Base of Fish Scale marker (discussed in section 2.1.3, p.13) and above the Viking sand member. The macrofossils available for dating the Viking Formation in the Plains of Western Canada are the pelecypods Inoceramus comancheanus Cragin and I. bellvuensis Reeside both of which are found at the base of the Joli Fou Shale (Stelck, 1975).

The age of the Viking Formation must be determined from the upper shales of the Viking Formation within the M. manitobensis Zone. This Zone has been dated as just above

the (middle) Late Albian, about 98 Ma. (Stelck, 1975). Tizzard and Lerbekmo (1975) dated bentonites in the Viking Formation of south-central Alberta. These bentonites have an average K-Ar radiometric age of about 100 Ma which is agreeable with the middle Late Albian.

### 2.1.2 Setting

The Viking Formation was deposited in the Interior Cretaceous Seaway. The shelf area of the Seaway separates the northern Alberta and Williston basins (Boethling, 1977a). The Colorado Sea occupied the Seaway during deposition of the Viking Formation. During Viking time the Colorado Sea may have had its western shore somewhere near the present edge of the disturbed belt. Beach (1962) suggests this is indicated by the existence of the Viking as a "Grit Bed" in Turner Valley. The Viking Formation extends from the eastern margin of the Foothills through central Alberta, where it continues to the east and northeast until the sandstone eventually shales out

The Viking Formation is found to increase in thickness to the west, however, the sandstone thickness actually decreases. Towards the east and northeast the Viking becomes progressively thinner and finer grained. This thinning towards the east and northeast indicates that Cordilleran uplifts could have been the main source of sediment. Similar views are presented by Boethling (1977) who states that the Viking sand influx was initiated by an

increase in tectonism and by Tizzard and Lerbekmo (1975), who suggest that repeated regressions of the Colorado Sea or a decrease in the rate of subsidence of the basin could have caused deposition of the Viking sands.

The Viking sandstone laterally has been documented in studies as being a localized deposit, a widespread "sheet-like" deposit or a narrow elongated bar. Within a particular deposit the Viking commonly consists of multiple sand development (Amajor and Lerbekmo, 1980; Boethling, 1977a; Tizzard and Lerbekmo, 1980; Beaumont, 1984)

### 2.1.3 Viking Stratigraphy

The Viking Formation belongs to the (Lower) Colorado Group. Originally the Viking had been classified as a member of the Colorado Group but is now a formation (Amajor and Lerbekmo, 1980). The Colorado Group includes the lower Joli Fou Formation, the Viking Formation and the Upper Shale Formation.

The Joli Fou Formation occurs at the base of the Colorado Group in Alberta and consists of marine shales. This formation is about 150 ft (46 m) thick in Central Alberta. It loses its lithologic character towards the western and southern areas of Alberta (Glaister, 1959; Tizzard and Lerbekmo, 1975; Koldijk, 1976).

The Viking Formation overlies the Joli Fou Formation and consists of multiple sandstone units enclosed in marine shales. The Viking Formation, in much of central

Alberta, has a thickness of 50-100 ft (18-36 m) (Beaumont, 1984). The term Viking Formation is used in south-central Alberta; alternatively as the Peace River or Paddy in the northwest; the Pelican in the northeast and the Bow Island in the south (Boethling, 1977a). The Viking Formation extends to the northwestern United States but is called the Newcastle or Muddy Formations of Wyoming and Montana (Boethling, 1977a; Beaumont, 1984).

In previous work the upper shale above the Viking is referred to as the Lloydminster Shale, Mowry Formation and the Colorado Shale. These marine shales lie between the top of the Viking Formation and the Base of Fish Scale Marker. The Fish Scale Marker consists of mudstone layers alternating with graded sandstones composed up of fish-skeletal debris (Simpson, 1979). The upper shales consist of silty shale and siltstone and are about 200 ft (61 m) thick (Evans, 1970). This interval has been left unnamed in previous work on the Viking by Glaister (1959), Oliver (1960) and Dickie (1973). Evans (1970) comments that this shale is an "unnamed part of the Lower Colorado" and that due to its "silty shale and siltstone beds it can be correlated with certainty" through his area of study in Southwestern Saskatchewan. The upper shale interval has also been referred to as the Lloydminster Shale by Tizzard and Lerbekmo (1975), Amajor and Lerbekmo (1980) and Amajor (1980) on their correlation charts for central Alberta. Koldijk (1975) refers to these shales as the Mowry Formation

in his study area of the Gilby B field. The Mowry Formation is more commonly used to refer to this upper shale unit in South Dakota, Montana and Wyoming (Glaister, 1959; Boethling, 1977; Tizzard and Lerbekmo, 1975). Authors who have referred to the same interval as the Colorado Formation include Stelck (1958), Boethling (1977) and Beaumont (1984). In this study this upper shale will be referred to as the Colorado Formation after the most recently published work by Beaumont (1984) (see Figure 2.1).

### Internal Viking Stratigraphy

Stratigraphically the base of the Viking is normally defined as occurring at the base of the sandstone or sandy shale which overlies the Joli Fou Shale. The top of the Viking is placed at the top of a chert-rich sandstone. This top has been referred to as a " chert-pebble stringer" (Stelck, 1958; Glaister, 1959; Shelton, 1973; Tizzard and Lerbekmo, 1975; Amajor and Lerbekmo, 1980). Some workers have found the top of the Viking to be a fairly consistent stratigraphic horizon for electric-log correlations. However, in the area of south-western Saskatchewan Jones (1961) found the Viking top to have a lenticular and discontinuous nature. Amajor and Lerbekmo (1980) in their study area of south-central Alberta also found the Viking top to be regionally discontinuous.

Work on the Viking Formation within Alberta has internally subdivided the Formation. Stelck (1958) notes

Fig. 2.1. Stratigraphic nomenclature of the Viking Formation in Central Alberta. Nomenclature used in this study follows Beaumont (1984) and is shown on right of figure.

# CENTRAL ALBERTA

		KOLDIJK 1976	AMAJOR / LERBEKMO 1980	BEAUMONT 1984 THIS STUDY
UPPER CRETACEOUS			FISH SCALE BASE	
LOWER CRETACEOUS		MOWRY FORMATION	LLOYDMINSTER SHALE	COLORADO
COLORADO GROUP	UPPER ALBIAN	VIKING FORMATION	VIKING FORMATION	VIKING FORMATION
		JOLI FOU FORMATION	JOLI FOU FORMATION	JOLI FOU FORMATION

FIG. 2-1 STRATIGRAPHIC NOMENCLATURE

that the "Viking is broken into several separate stringers and locally these may be termed first, second and third Viking sands".

In his study of the Joffre Field, Shelton (1973) describes the Viking sandstone as containing several sandstone units. He further subdivided the productive sandstone zone into three separate units. Love (1955) previously described the Joffre productive zone as a single unit. Shelton (1973) divides the formation into the upper unit as the "thin chert-pebble conglomerate", the middle unit as the "productive sandstone or pay zone" (found 15-30 ft below the Viking top) and the basal unit as an "interbedded shale and shaley sandstone with two thin persistent bentonites".

Koldijk (1976) subdivided the Viking Formation of the Gilby B field into three intervals. He referred to these intervals as the "Lower Viking", the "Pay Zone" and the "Upper Viking". The "Lower Viking" consists of silty shales lying above the top of the Joli Fou Shales and below the base of the sandstone unit. The "Pay Zone" refers to the coarse sediment package (see Figure 2.2) which is composed of those sandstones which are normally hydrocarbon bearing and are capped by a thin, unproductive conglomerate. Koldijk determined that at Gilby B the capping conglomerates within the "Pay Zone" were the reservoir rather than the underlying fine sandstones. The "Upper Viking" is a dense silty shale placed above the "Pay Zone" to the top of the

Fig. 2.2. Internal Viking Stratigraphy. typical on-field electric log, spontaneous-potential (SP) curve on left side and resistivity log on right side, is employed to illustrate the internal stratigraphy of the Viking Formation in the study area. Regional Viking stratigraphy shown on left side of diagram (modified after Koldijk, 1976). All markers used in this study area are labelled on the resistivity log on the right side of the figure. Note that Marker "B" and "C" enclose the "coarse sediment package" (see text for discussion). Marker "A" is used as the Upper Datum throughout this study.



## Viking Formation.

The Viking Formation was subdivided in south-central Alberta by Amajor and Lerbekmo (1980) into the following units (in ascending order): the "Basal Viking sandstone"; the "Lower Viking sandstone"; the "Middle shale"; the "Upper Viking sandstone" and the "Viking Grit".

Figure 2.2 shows the internal stratigraphy of the Viking Formation (modified after Koldijk, 1976) and includes log markers (A through to H) used in this study.

The Viking "coarse sediment package" is defined throughout the study as the interval between markers B and C. The Base of Fish Scales was not used as a datum in this study since Marker A was found to be regionally reliable and in closer proximity to the Viking "coarse sediment package". Marker A is shown on resistivity logs by a stratigraphically lower, relatively higher resistivity kick within a double resistivity kick. Each of these kicks represents one or more siltstone beds (observed in core) within the muddy siltstones (Facies A, see section 3.3). Just a few feet above Marker A is the "Viking top" or chert pebble stringer (p.14) which was observed in core. The lower markers D, E and G are recognized on resistivity logs by a relatively small (higher resistivity) kick representing a muddy siltstone (Facies A, section 3.3) having a slightly higher percentage of siltstone, while lower markers F, and H are recognized by a lower resistivity representing a muddy siltstone having a slightly higher percentage of mudstone.

#### 2.1.4 Previous Work

Previous work on the Viking Formation in central Alberta and southwestern Saskatchewan has focused on the nature of the deposit (eg. offshore bar) and mechanisms of emplacement of the sediment. The types of deposits and emplacement mechanisms include storm emplacement, regressive and transgressive deposits, barrier islands and deltas. Listed in chronological order are a number of previous studies on the Viking, with particular emphasis placed on the type of deposit and depositional process suggested by the author.

Beach (1956 and 1962) studied the larger Viking oil and gas fields including Viking-Kinsella, Joarcam, Joffre, Kessler and Pendant d'Oreille in southwestern Alberta. Emplacement of the Viking sediment by turbidity currents is suggested by Beach (1956) to explain his observations of large rounded chert pebbles found within sand and shale, sand in offshore positions and bentonites. The bentonites are distributed over a wide area and would require deposition over a short period of time, Beach (1956) suggested this could be accomplished by turbidity current emplacement.

Stelck (1958) suggests that the Viking Formation was developed as shoreface and offshore bar deposits.

De Wiel (1965) compared the deposits in the Viking sea to those in the Grand Banks area of the Atlantic Ocean. He suggests that the Viking had been deposited under regressive

conditions where longshore currents distributed the sediment. He discounts the idea that turbidity currents deposited the Viking sands. The reasoning he used, which compliments a similar view by Jones (1961), is that the Viking sea could not provide the necessary slope and depths needed for turbidity current initiation. De Wiel (1956) also points out that turbidites are in-part represented by graded bedding and turbidity currents may produce channels which "lead down-dip from the source area" (after Gammel, 1965). He argues that the Viking sands have an inverse grading and the sandbody geometry strikes parallel to the structure on the Paleozoic sea floor. These observations would indicate that a turbidity current deposit is unlikely.

Evans (1970) studied the Dodsland-Hoosier and Smiley fields of southwestern Saskatchewan (Townships 29 to 32, Ranges 19 to 28W3M). He described thin sand units (which he termed members) within the study area which trend at high angles to the normal northwest to southeast trend of most Viking sandbodies. The study suggests that these sand units which are stacked in an imbricate fashion were deposited by tidal currents in an offshore setting.

Based on his study of the Joffre Field, Shelton (1973) describes the Viking deposit as a barrier bar. He based this interpretation upon the sediments gradational lower and lateral boundaries, a field width to thickness ratio of 500:1, mixed bedding, and the presence of glauconite. The study also concludes that the Jorcam field, which lies 70

miles to the northeast of Joffre, formed under regressive conditions. The Joffre field would have formed before the Jorcam field as the sea retreated toward the northeast under regressive conditions.

A barrier bar deposit was also suggested by Tizzard and Lerbekmos' (1975) work in southeast Alberta (between Townships 19 and 26 and Ranges 1 and 16W4M). They concluded that the study area represents a barrier bar complex.

Storm-surge was considered by Koldijk (1976) to be the mechanism responsible for the deposition of the Viking sediments at the Gilby B field. He suggests deposition at Gilby B by turbidity currents is unlikely since he found no evidence of graded bedding. Koldijk (1976) suggests that strong currents, generated by storms, could transport gravels to an offshore environment. A "linear, shoaling feature" is suggested to localize the pebbles (Koldijk, 1976). This shoaling feature is suggested to be an extension of the "sand bars" on the Joffre-Bentley-Gilby trend.

Boethling (1977b) suggested that Viking sediments are a redistributed bar and sheet sand complex which had two major basins on either side of the broad shelf where the formation was deposited. He refers to the "sill-like nature of the shelf" which directly influenced the southward flowing cold Boreal current and the northward flowing warm Gulfian current which he suggests influenced Viking sediment deposition.

Amajor's (1980) regional subsurface study of the Viking sandstones in central Alberta and part of southwestern Saskatchewan attempted to determine the patterns and environments of deposition by integrating all evidence regionally. He attempted to link the multiple interpretations of previous localized studies of the Viking Formation. The study suggests that deltas supplied the Viking sediment. These deltas are located in the southern Alberta - northern Montana Foothills and the Jasper area. He suggests that the sediment from the deltas was transported during a still-stand shoreline condition or during later sea level rise. The study provides a possible interpretation for both the shoreline and offshore Viking sandbodies. The "wave-dominated regressive meso-tidal barrier island systems" he suggests represent the "shoreline-nearshore sandstones" in the southwest of the study area. The offshore sandbodies (particularly the Dodsland - Hoosier area of southwest Saskatchewan) were suggested to be deposited in a "sub-tidal, tide dominated shallow offshore marine environment".

Based on Beaumont's (1984) study of the Viking sandstones in central Alberta, including the Joffre-Jorcam area, he concluded that the sediment was deposited during a change in sea level. He suggests that at the end of Joli Fou deposition a rapid regression occurred resulting in eastward (northeastward ?) sediment progradation; a later major transgression reworked the Viking sediment into its

present configurations. This transgression was "punctuated by a series of stillstands or minor regressions" (Beaumont, 1984).

A regional sedimentology study of the Viking Formation at the Caroline-Garrington-Harmatton fields in south-central Alberta has been conducted by Hein, Longstaffe, Dean, Delure, Grant and Robb of the University of Alberta. In particular, Robb (M.Sc., 1985) investigated the Viking Formation at the Garrington oil field in southwestern Alberta. He found it to be a laterally extensive coarsening-upward sequence of shale, sandstones and conglomerates. Robb (1985) concludes that a "regression associated with progradation of a shoreline-attached clastic wedge" caused the development of the Viking Garrington field.

## 2.2 Gilby A and B Fields

### 2.2.1 History

The Cretaceous - Viking sandstone was named by S. E. Slipper in 1918 to refer to the "gas producing sand of the Viking - Kinsella field in east central Alberta" (Stelck, 1958). The Gilby A field, as referred to by the Alberta Energy Resources Conservation Board (1983), has been called the "Gilby-Bentley" field in previous work (Love, 1959; Shelton, 1973; Koldijk, 1976). The "Gilby" field corresponds to the east-west trending northern part of the

Gilby A field. The "Bentley" field is the more southerly extension of the northwest-southeast trending Gilby A field. The discovery well for Gilby A is located at 10-4-41-3 W5M, and was drilled on November 8, 1953. The discovery well for the Gilby B field is located at 11-33-41-4 W5M and was drilled on December 4, 1961.

The Gilby A field (90 total wells) is approximately 22 mi (35.4 km) long and 1 mi (1.6 km) to 1.5 mi (2.4 km) in width. The Gilby B field is about 10 mi (16.1 km) long and 2 mi (3.2 km) in width. Gilby B is shorter than Gilby A but is equally as wide.

### 2.2.2 Structural Setting

The core examined for the Gilby A and B fields was structurally undisturbed. The two fields are stratigraphic traps where essentially porous sand is surrounded by impermeable shale (Love, 1955; Koldijk, 1976).

The Gilby B field has a regional dip of 50 ft/mi (10 m/km) towards the southwest (Koldijk, 1976). A mild flexure is found at the Gilby B field where the regional southwest dip changes from 40-50 ft/mi (8-10 m/km) (Koldijk, 1976). Koldijk (1976) suggests that this change in dip is due to structure or topography on the underlying Cretaceous surface. The Gilby A field has a regional dip of approximately 40 ft/mi (8 m/km) determined from the structure map of Marker A (Figure 5.10).

### Paleogeographic Setting

In published work on the Gilby and Joffre Viking fields there are few suggestions regarding the location of the paleoshoreline. For the Joffre field Shelton (1973) comments that the distance to the shoreline in the southwest is not known. Koldijk (1976) refers to Gilby B as having an "environmental setting, somewhere offshore". He also states that the epineritic Colorado Sea had offshore water depths considerably less than on modern shelves. Beaumont (1984) in his study of the Viking Formation in central Alberta which focused on the Joffre-Jorcam fields, gives a minimum distance of 200 miles (320 km) west to the paleoshoreline. The most substantial evidence for a paleoshoreline comes from Robb's (M.Sc., 1985) study of the Viking Garrington oil field. He observed rooted zones occurring to the west and southwest of Garrington, approximately 30-50 km from the Garrington oil field. Therefore the closest possible paleoshoreline to the Gilby Viking fields is suggested to be approximately 90 to 110 km to the west and southwest of the fields.

## Chapter 3: FACIES AND FACIES SEQUENCE

### 3.1 Method and Introduction

Core examined at the Core Research Center, Calgary, provided the basis for the following facies divisions. All cored wells in the study area were examined, a total of 61 core from the Gilby fields (A and B and other smaller fields) and 13 from off-field locations (see Fig. 5.9 for cored well locations). Following a discussion of the basis of facies divisions, the facies are described. Each facies is followed by a brief interpretation. Both lateral and vertical facies sequences are described with the aid of core cross-sections and Markov chain analysis. A brief summary of the facies and facies sequence concludes the chapter.

### 3.2 Facies Divisions

"Facies" is a term used to describe the unique aspects of a group of rocks designated as the lithology, sedimentary and biological features (body and trace fossils) (after De Raaf et al., 1965, in Walker, 1984a, p.1). The Viking sediments range from clay through to pebble-sized terrigenous material. The biological features consist mainly of a low diversity trace fossil assemblage. The

facies described are based solely on the work of this study. Similar facies were independently defined in the Viking Joffre, Mikwan and Fenn fields (K. Downing, M.Sc. in prog.). All core was measured in metric units and grain size measurements were performed with a hand lens and Canstrat (Canadian Stratigraphic Service) grain size card (phi scale)

### 3.3 Facies Descriptions

#### 3.3.1 Facies A: HOMOGENEOUS MUDDY SILTSTONES

Facies A (Figure 3.1) represents the Lower Viking Formation (Koldijk, 1976; p.64). It underlies all of the coarse facies and has a minimum thickness of 0.16 m. The homogeneous muddy siltstones were subdivided on the basis of their silt content into dark muddy siltstones, bioturbated muddy siltstones and bioturbated siltstones. These siltstones are characterized by their well mixed or homogeneous appearance and their lack of fissility in core. They range in colour from black to light grey, depending on their silt content. The unit contains preserved, sharp based silt beds (average 1-4 cm thick). The sharp bases are commonly irregular, probably due to loading, and often contain ripped-up mud clasts (Figure 3.2). The silt beds are parallel laminated with a few examples of ripple cross-lamination. These cross-lamination. These silt beds are colour graded due to a grain size change. Finer material occurs where the laminae are dark and coarser material where the laminae are

light in colour. The tops of the silt beds are sharp to irregular, the latter likely due to bioturbation.

Facies A has a well mixed or stirred appearance as a result of pervasive bioturbation. Individual burrows are dominantly horizontal and are recognized when the silt content is great enough to provide a colour contrast with the black clays. Dark green nodules of pyrite (occurring as clumps less than 2 cm in diameter) and sideritic concretions (averaging 7 cm in diameter) are common in the less silty subfacies of the unit. Bentonite beds (1-2 cm thick) and fishscales (5-10 mm in diameter) were both frequently found within this facies.

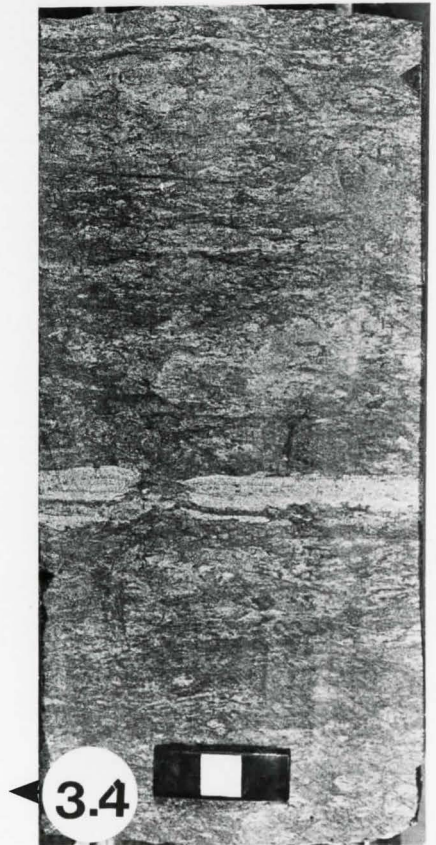
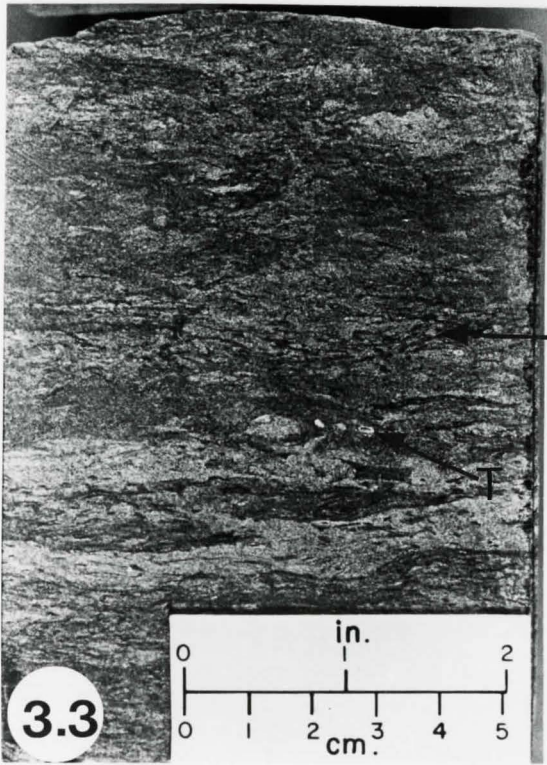
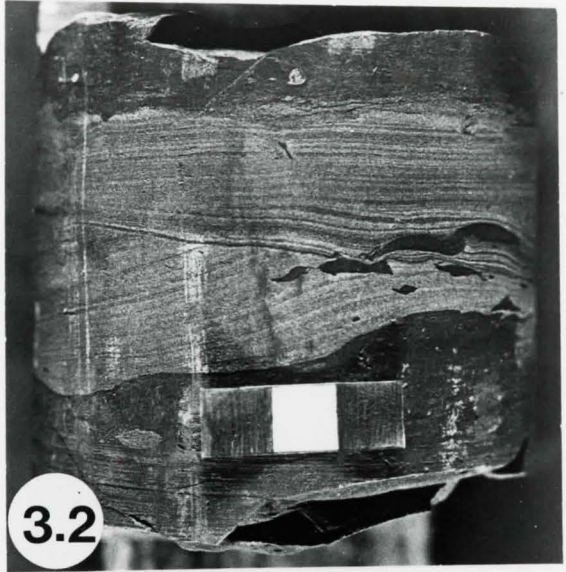
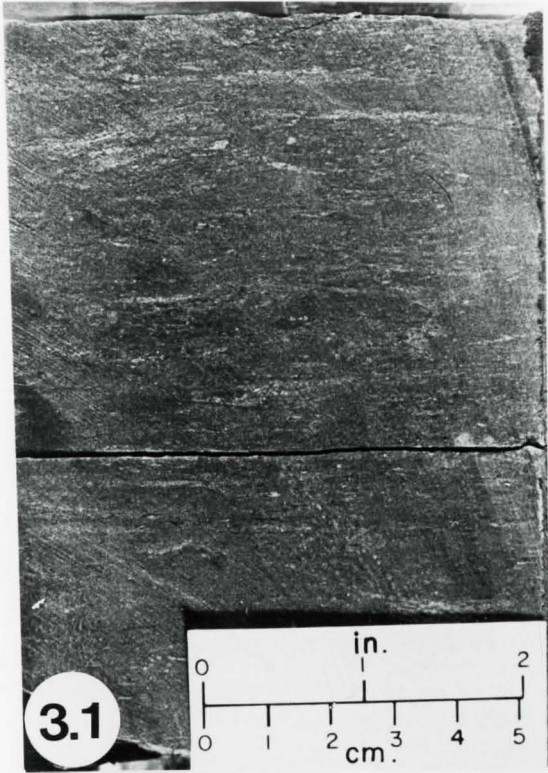
The three muddy siltstone subfacies have a gradational contact and are discussed below in order of increasing silt content: 1) Dark Muddy Siltstones (Facies A-1, Figure 3.1), is characterized by its very black color and low silt content (approximately 0-10%). The lack of color contrast suggests bioturbation may be absent. 2) Bioturbated Muddy Siltstones (Facies A-2, Figure 3.3), is characterized by its grey color and wide range in silt content (approximately 10-70%). The mottled, stirred appearance of this muddy siltstone subfacies is due to the pervasive bioturbation throughout. Recognized burrows include Terebellina, Skolithos (small vertical tubes), Palaeophycus and Helminthoida. 3) Bioturbated Siltstone (Facies A-3, Figure 3.4), is characterized by its light grey color and the high silt content (generally greater than 70%). This subfacies

Fig. 3.1. Dark Muddy Siltstone, Facies A-1. Note the patchy occurrence of siltstone (lighter colour) and absence of any lamination, 11-12-41-4W5, 6399 ft (1950.4 m). Scale in inches and cm.

Fig. 3.2. Dark Muddy Siltstone, Facies A-1. Note the rare preserved, sharp based silt to very fine sand ripple cross laminated beds (3 cm thick) containing ripped-up mud clasts, 12-16-40-1W5, 5649 ft (1721.8 m). Scale is 3 cm.

Fig. 3.3. Bioturbated Muddy Siltstone, Facies A-2. Note the abundance of discontinuous siltstone laminae suggesting bioturbation. The small, white flattened circles are Terebellina (T) and the small, black shredded forms may be Helminthoida (H). The continuous laminations have sharp to bioturbated bases and tops, 11-12-41-4W5, 6382 ft (1945.2 m). Scale in inches and cm.

Fig. 3.4. Bioturbated Siltstone, Facies A-3. Note the churned, thoroughly mixed appearance of siltstone with mudstone and very fine sandstone. The overall lighter colour of this siltstone is a result of the higher silt content. A thin (1 cm) silt to very fine sand bed is partially preserved. Compare with Figures 3.1 and 3.3, 12-8-41-3W5, 6326 ft (1928.2 m). Scale is 3 cm.



is pervasively bioturbated and also contains the traces listed in type 2, above.

Facies A is interpreted to have been deposited in a deep muddy basin where the originally sharply based silt beds were probably erosively emplaced by storm events. The colour grading or upward fining within the silt beds is evidence of deposition from a waning flow.

3.3.2 Facies B: SIDERITIZED MUDDY SILTSTONES  
(WITH SKOLITHOS)

Facies B (Figure 3.5) represents the commonly sideritized contact between the underlying facies A and the overlying coarse sediment (most frequently represented by facies C and H). Facies B is characterized by a sharp erosive contact, with coarse sediment above the contact and Skolithos burrows penetrating the contact into muddy siltstones (facies A) and sideritic muddy siltstones.

The frequency of the sideritization and Skolithos burrows through the contact is shown in Table 3.1 for Gilby A (42 wells penetrate the contact), Gilby B (10 wells penetrate the contact) and off-field (10 wells penetrate the contact) cored wells. Also shown are the length and range of lengths (cm) of the Skolithos burrows and the thickness of the sideritized zone.

Table 3.1

<u>LOCATION</u>	<u>%SIDERITE</u>	<u>%SKOLITHOS</u>	<u>%SIDERITE &amp; SKOLITHOS</u>
<u>GILBY A</u>	40	38	29
average (cm)	9.0	7.5	-
range	4.0-17.0	3.0-15.0	-
<u>GILBY B</u>	66	30	-
average (cm)	3.7	3.5	-
range (cm)	1.0-7.0	3.0-4.0	-
<u>OFF-FIELD</u>	40	10	10
(ERCB data)			
average (cm)	6.0	9.0	-
range (cm)	5.0-8.0	4.0-9.0	-

The above table illustrates that the siderite and Skolithos burrows have a slightly higher frequency of occurrence in the Gilby A and B fields, over the off-field wells.

The vertical Skolithos burrows (Figure 3.6) are the only type of burrow evident at the contact. These burrows have well-defined vertical walls, appear slightly bulbous at their bases and are filled with the same sediment that overlies the facies. This is usually a medium-grained

sandstone, being granule to pebble sized clasts of mudstone, sideritized mudstone and chert pebbles.

The siderite is dark brown in color (Figure 3.7) and commonly grades inward to a milky-white colour. This portion is softer than the surrounding darker siderite. The burrows which penetrate through the softer milky-white siderite appear to narrow in thickness.

Facies B represents a firmground (personal communication, G. Pemberton, 1985). Ekdale et al. (1984, p.306) define a firmground as a stiff, uncemented substrate. This is an important observation since a firmground represents a period of discontinuity or erosion (Bromley, 1975). The characteristics of facies B - the erosive contact and burrowing were used to formulate a sequence of events which lead to the development of facies B. A possible sequence of events are (G. Pemberton, personal communication):

1. Facies A, the underlying muddy siltstone was deposited and later burrowed, showing mainly Palaeophycus. These burrows are referred to as pre-omission suite (pre-firmground) burrows. Pre-omission suite burrows as suggested by Bromely (1975) refer to the time relationship they have with period of erosion or depositional hiatus, i.e. they pre-date it. Note that the horizontal Palaeophycus burrows are truncated by the vertical Skolithos burrows (post-omission suite burrows) implying they are pre-Skolithos (see Figure 3.7a and b).

Fig. 3.5. Sideritized Muddy Siltstone (with Skolithos), Facies B. Note the large vertical Skolithos burrows (3-10 cm in length) having sharp, straight boundaries and penetrating down through sideritic muddy siltstone and into muddy siltstone (Facies A). The Skolithos burrows are infilled with the overlying massive medium grained sandstone with pebbles (Facies H). The siderite is medium brown grading inwards to a milky-white colour. Note that the burrows which penetrate through the softer milky-white siderite narrow in thickness, 8-17-40-1W5, 5647 ft (1721.2 m). Scale in cm.

Fig. 3.6. Sideritized Muddy Siltstone (with Skolithos), Facies B. The longest Skolithos burrow (12 cm x 0.5 cm) in the photograph penetrates through the siderite and 6 cm into the muddy siltstone (Facies A). The burrow is infilled with medium grained sandstone containing granules. The wider Skolithos burrow (1 cm wide) to the left of the longer burrow is also infilled with the same size sandstone as the first, c.f. Figure 3.5, 16-19-40-1W5, 5854 ft (1784.3 m).

Fig. 3.7. Sideritized Muddy Siltstone (with Skolithos), Facies B. An off-field example of the Skolithos burrow (4 cm x 1 cm) penetrating into sideritized muddy siltstone. Infilling the burrow is the same material which sharply overlies it, a medium grained sandstone with granules and pebbles. The darker outlined veins below the burrow are cracks in the sideritized siltstone. Towards the top of the core the pebble size increases. This coarse sediment package is draped by black mudstone (Facies K) with silt laminae, 16-18-41-4W5, 6575 ft. (2004.0 m). The core is 3.5 inches in width.

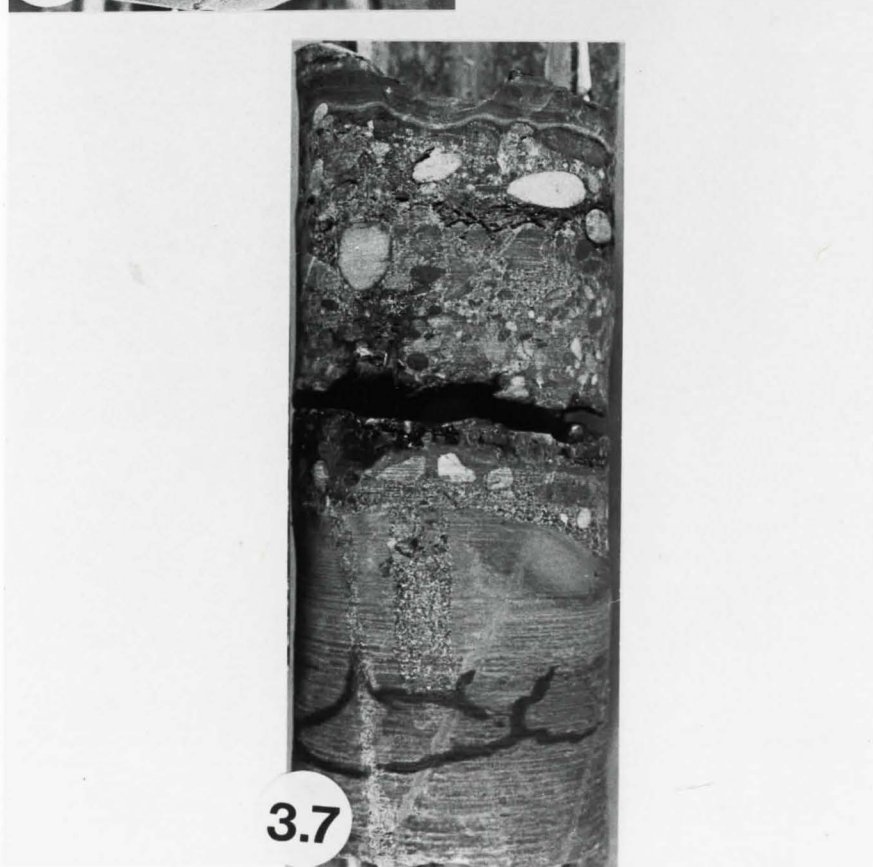
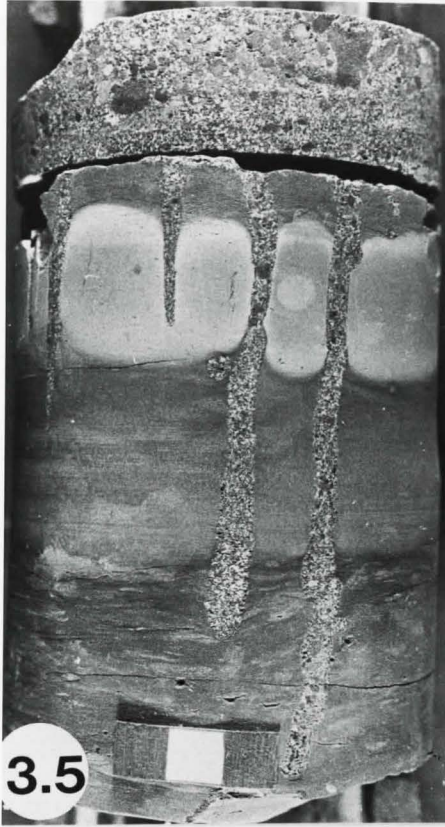
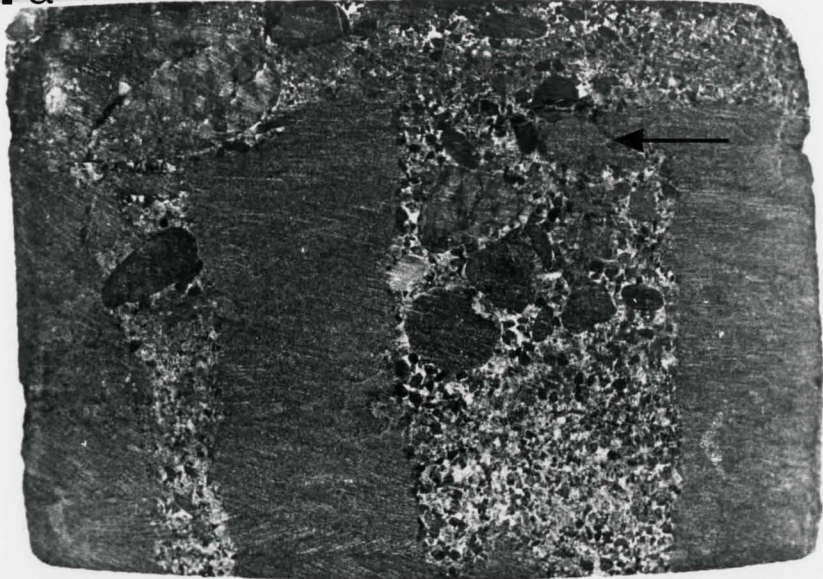


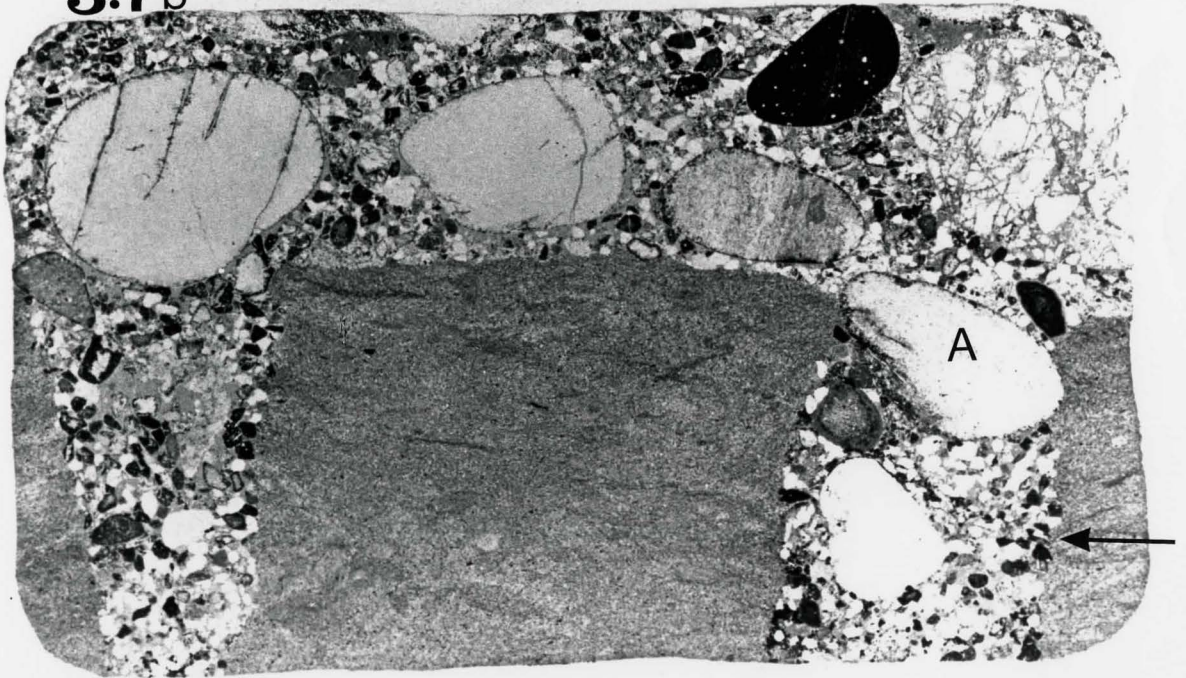
Fig. 3.7a. Sideritized Muddy Siltstone (with Skolithos), Facies B. Note the sharp contact of coarse sediment with sideritized muddy siltstone below. Skolithos burrows have sharp, straight margins with the sideritized muddy siltstone. Burrow is infilled with medium sandstone and pebble sized chert found above the burrows. The fine white material in the matrix was identified as kaolinite under thin section and SEM (see Chapter 4, Figure 4.14). The arrow denotes the position where siderite appears within burrow. This is evidence in favor of post-sideritization of the burrow, 16-18-41-4W5, 6575 ft. (2004.0 m). Core width is 4.3 cm.

Fig. 3.7b. Sideritized Muddy Siltstone (with Skolithos), Facies B. Photomicrograph (under plane-polarized light) of two Skolithos burrows penetrating through sideritized muddy siltstone. Note that the burrows are straight with vertical walls implying they were formed in firm sediment. The pebble (A) appears wedged in and confined by the burrow walls also implying formation in firm sediment. The arrow highlights where the horizontal burrows of Paleophycus (pre-Skolithos) are truncated against burrow wall, 16-18-41-4W5, 6575 ft. (2004.0 m). Length of photomicrograph is 2 cm.

3.7a



3.7b



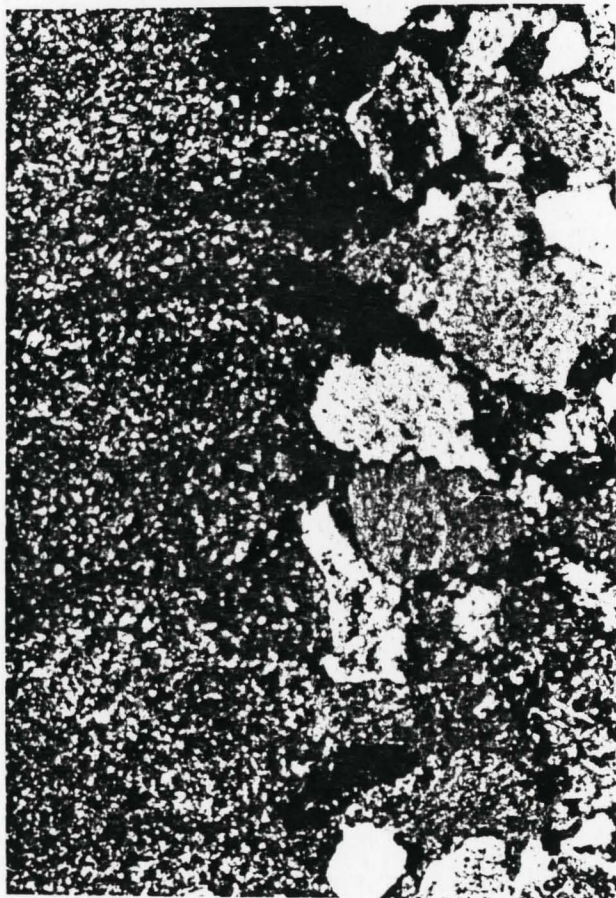
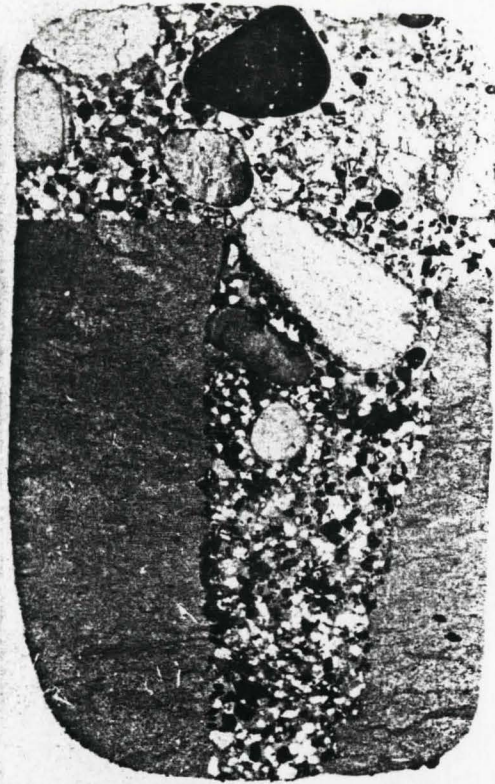
2. Facies A was partially consolidated and made more cohesive by the weight of overlying sediments. This partially consolidated horizon was later exhumed leaving a cohesive but non-lithified substrate, a "firmground".

3. Burrowing into the "firmground" by Skolithos occurred. The Skolithos burrows are straightwith well defined walls which imply that they burrowed into a stiff substrate, at least partially consolidated. Organisms capable of inhabiting modern firmgrounds include shrimp, crabs and polychaetes (Pemberton and Frey 1984b). These burrows were not immediately filled because surrounding sediment was firm. A concentration of iron-oxides (opaques) around the burrow developed (see Figure 3.7c and 3.7d).

4. Another period of erosion occurred at the top of the firmground, simultaneously depositing coarse sediment which in-fills the burrows. Evidence for this second period of erosion at the contact between Facies A and the overlying coarse sediment includes the absence of iron-oxides at the contact of Facies A and the coarse sediment and the presence of opaques around burrow walls (see Figure 3.7d). The chaotic, unsorted nature of the overlying coarse sediment in addition to the presence of ripped-up mud clasts found just above the contact imply rapid, erosive deposition, perhaps during a storm event. The limited occurrence of Facies B within the study area suggests erosion (see Chapter 5 for further discussion).

**Fig. 3.7c. Sideritized Muddy Siltstone (with Skolithos), Facies B. Photomicrograph (plane-polarized light) of Skolithos burrow having sharp vertical walls and concentration of iron oxides (black rounded grains) at wall margins. Note the absence of iron oxides at the horizontal contact of coarse sediment with sideritized muddy siltstone, 16-18-41-4W5, 6575 ft 2004.0 m). Width of photomicrograph is 2 cm.**

**Fig. 3.7d. Sideritized Muddy Siltstone (with Skolithos), Facies B. Photomicrograph (plane-polarized light, magnification is 25x) of square outlined in Fig. 3.7c. Note the iron oxides found along the margins of the burrow wall, 16-18-41-4W5, 6575 ft (2004 m). Width of photomicrograph is 0.3 mm.**



5. Sideritization of Facies A occurs, probably controlled by the porosity and permeability contrast at the contact with the overlying coarse sediment. The Skolithos burrows were developed before sideritization as they are not observed to burrow through siderite.

### 3.3.3 Facies C: PERVASIVELY BIOTURBATED MUDDY SANDSTONES

Facies C (Figure 3.8) has an average thickness of 0.44 m, ranging from 0.04-1.57 m. It normally occurs in the lower portion of the Viking coarse sediment. This facies is characterized by a very fine to lower medium size sand (with some upper medium sand size). The mud present represents less than 30% of the total unit. The mud occurs as thin wisps, originally deposited as mud laminae. These laminae were subsequently disrupted by bioturbation and therefore the facies lacks any preserved stratification. Rare sandstone beds were not burrowed preserving parallel to slightly inclined stratification.

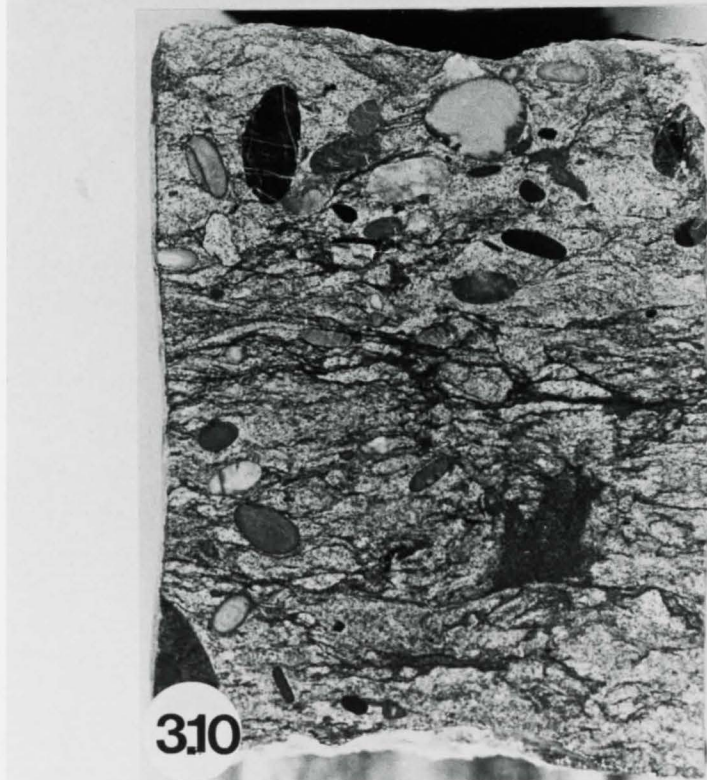
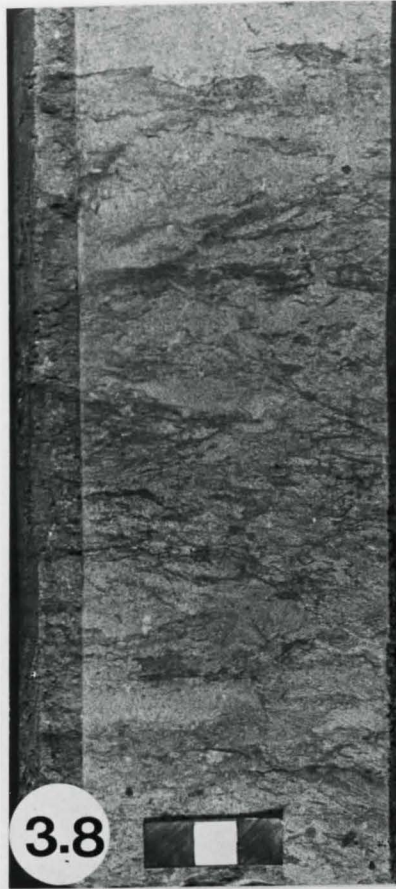
Burrows recognized include Terebellina and Skolithos, and several indistinct types. Terebellina burrows are white, doughnut-shaped structures (less than 5 mm in diameter). Skolithos burrows (range in length from 4-12 cm), have irregular, ragged walls and usually cross-cut the pervasively bioturbated sediment (Figure 3.9). These burrows are normally filled with lower to upper medium sand.

There are a few, chaotically scattered, polymictic pebbles (5-20 mm) occurring at the base of this facies.

Fig. 3.8. Bioturbated Muddy Sandstone, Facies C. Colour-mottling caused by mixed-in shaley material resulting from intensive bioturbation. There are no continuous mud laminations preserved, 12-1-40-1W5, 5489 ft (1673.0 m). Scale in cm.

Fig. 3.9. Bioturbated Muddy Sandstone, Facies C. Note how the Skolithos burrows (10 cm) crosscut all bioturbated muddy sandstone. These burrows are post bioturbation of the muddy sandstone. They have partially ragged margins and are generally vertical. The Skolithos are infilled with medium grained sandstone which is slighter coarser than outside the burrows. There are a few scattered chert granules and pebbles and the arrow denotes the Terebellina burrow, 4-30-40-1W5, 5745 ft (1715.1 m). Width across core is 3.5 in (8.9 cm).

Fig. 3.10. Bioturbated Muddy Sandstone, Facies C. Note the large chert pebbles scattered throughout the muddy bioturbated sandstone. The matrix is an upper fine sandstone, c.f. Fig. 3.8 and 3.9, 12-3-41-3W5, 6260 ft (1908.0 m). Width across core is 3.5 in (8.9 cm).



These pebbles are most frequently found where Facies C occurs at the base of the Viking coarse sediment. Locally, large oblong rounded polymictic pebbles occur at this horizon. These large pebbles are dispersed chaotically through the bioturbated muddy sandstone (Figure 3.10).

Facies C was probably deposited rather slowly, giving organisms time to bioturbate the sediment thoroughly. The mud wisps were originally thin mud laminations deposited under quiet conditions. The vertical burrows cross-cut already previously burrowed sediment and probably represent a second, later period of bioturbation. Texturally this facies resembles Facies D, except that Facies D is not thoroughly bioturbated and contains a higher percentage of mud.

#### 3.3.4 FACIES D: BURROWED-LAMINATED MUDSTONES-SANDSTONES

Facies D (Figure 3.11) has an average thickness of 0.5 m, ranging from 0.08-4.09 m. The facies commonly has a greater proportion of sandstone (approximately 60%) over mudstone (approximately 40%). If this is the case, then the Facies is referred to as D-1, a burrowed-laminated mudstone-sandstone. However, there are a few examples in Facies D where the amount of mudstone (approximately 60%) is greater than the amount of sandstone (approximately 40%) (Figure 3.12). In this case the facies is referred to as D-2, a burrowed-laminated sandstone-mudstone.

This facies is characterized by layers of bioturbated muddy sandstone interbedded with alternating mudstone and sandstone laminations and beds of sandstone. The bioturbated muddy sandstone (average thickness 5 cm, ranging 3-11 cm) layers in this facies are similar to Facies C. In Facies D, however, Skolithos burrows infrequently occur and are usually shorter in length (1-3 cm) than those developed in Facies C. The Skolithos burrows are similar in both Facies in that the walls are ragged and cross-cut through discontinuous mud laminations. Mudstone occurs mainly as discontinuous wisps which probably represent the remnants of horizontally laminated mudstone. The sandstone grains in the bioturbated beds are upper fine to medium sand size. These layers of muddy sandstone are pervasively bioturbated, with the recognizable traces being Skolithos and Terebellina.

The mudstone laminations (less than 3 mm thick) are black in colour and have sharp, flat bases. They may be burrowed giving them an irregular shape. The tops of these mud laminations are sharp to bioturbated.

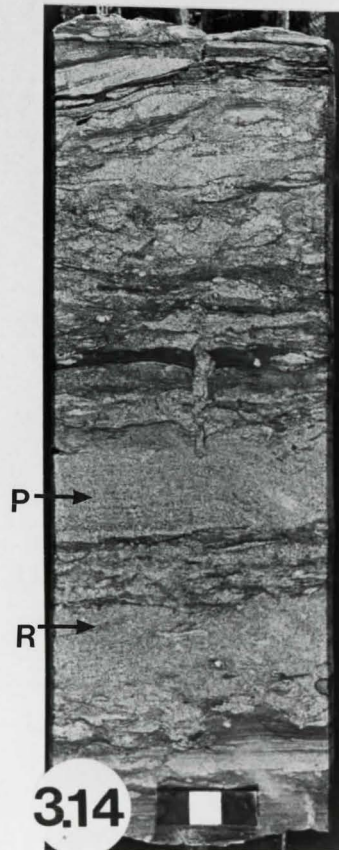
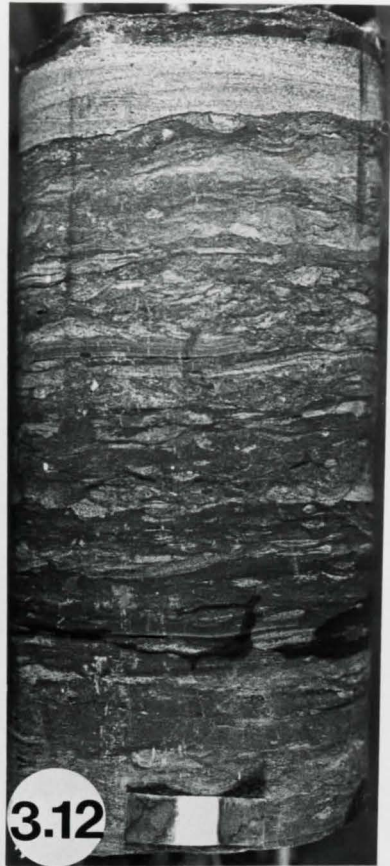
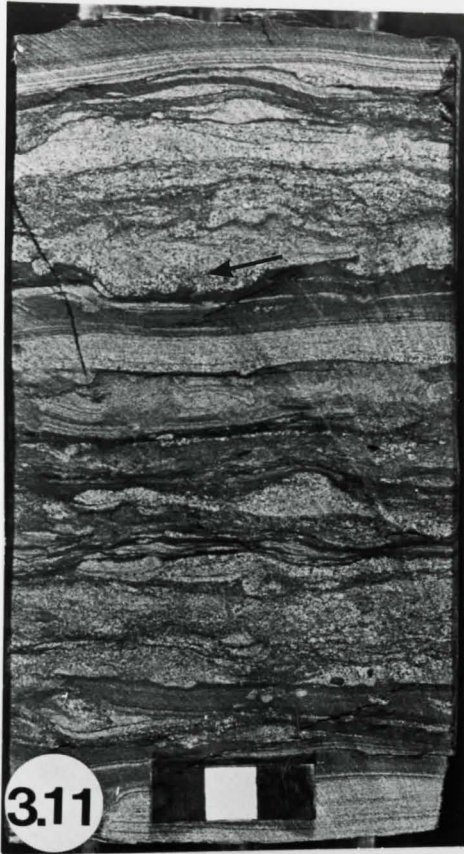
Sandstone laminae and beds are interlaminated with the mudstone. Sandstone grain sizes range from lower fine to upper coarse. This sandstone can exist as thin laminations (less than 1.0 mm thick) or as thicker beds (ranging 1-11 cm). The base of these sandstone beds are sharp to bioturbated. These beds are commonly graded (Figure 3.13). The grading is evident where the lighter-coloured coarse

Fig. 3.11. Burrowed-Laminated Mudstone-Sandstone, Facies D-1. Note the layers of bioturbated muddy sandstone alternating with mudstone and sandstone laminations and beds of sandstone. The bioturbated layers of muddy sandstone are identical to Facies C. Note the sharp to bioturbated bases and tops of the mudstone and sandstone laminations. The arrow denotes a graded sandstone in the bioturbated muddy sandstone layer. The alternating mudstone sandstone laminations at the top of the core are flat to slightly undulatory, 4-12-40-1W5, 5493 ft (1674.3 m). Scale in cm.

Fig. 3.12. Burrowed-Laminated Sandstone-Mudstone, Facies D-2. Note the greater proportion of mudstone here as compared to Fig. 3.11. The only continuous sandstone laminations are preserved at the top of the core. The laminations are slightly inclined and have both a sharp base and top, 16-19-40-1W5, 5850 ft (1783 m). Scale in cm.

Fig. 3.13 Burrowed-Laminated Mudstone-Sandstone, Facies D-1. Note that the sandstone laminae occur as both thin laminations (less than 2 mm) or as thicker beds (2 cm). The base of the sandstone beds are sharp and the tops are bioturbated. Note how (arrow) the sandstone bed is graded, the lighter-coloured sediment is coarse and the darker-coloured sediment is fine, 2-30-40-1W5, 5817.5 ft (1773.2 m). Scale in cm.

Fig. 3.14. Burrowed-Laminated Mudstone-Sandstone, Facies D-1. Note the suggestion of parallel lamination (P) and ripple cross-lamination (R) within the sandstone beds. There is a hint of bioturbation in the lower sandstone bed. The sandstone beds have sharp to bioturbated tops. Continuous mudstone laminations are absent except at the very top of the core. The vertical burrow may be Skolithos (3 cm), 4-12-40-1W5, 5496.5 ft (1675.3 m). Scale in cm.



sediment grades upward into the darker-coloured fine sediment. There is some evidence of horizontal, parallel lamination and ripple cross-laminations within the sandstone beds. The beds are normally not bioturbated but some burrowing is evident within the finer grain sizes. The sandstone laminae and beds have sharp to bioturbated tops. Note that mudstone laminae can be absent from the sandstone beds (Figure 3.14).

A few unsorted pebbles (granule size to 12.5 mm), mud clasts (1-3 cm in length) and pyritized mudstone clasts (1-2 cm in diameter) occur throughout the facies.

The bioturbated sandstone beds represent a slower period of sand deposition giving the bioturbators time to thoroughly mix the sediment. The laminations of mudstone/sandstone and sandstone beds represent alternation periods of slow and sudden deposition, possibly due to intermittent storm deposition. The normal grading within the sandstone beds are evidence for deposition from a current with waning flow.

### 3.3.5 Facies E: CROSS BEDDED SANDSTONES

In core, Facies E occurs as both a thin (E-1) (average thickness 0.19 m, ranging 0.04-0.77 m) or thick (E-2) (average thickness 0.48 m, ranging 0.12-1.14 m) cross-bedded sandstone. The thin cross-bedded type normally occurs below the thick cross-bedded type, however either type can occur individually in a core. Facies E has a salt and pepper-like

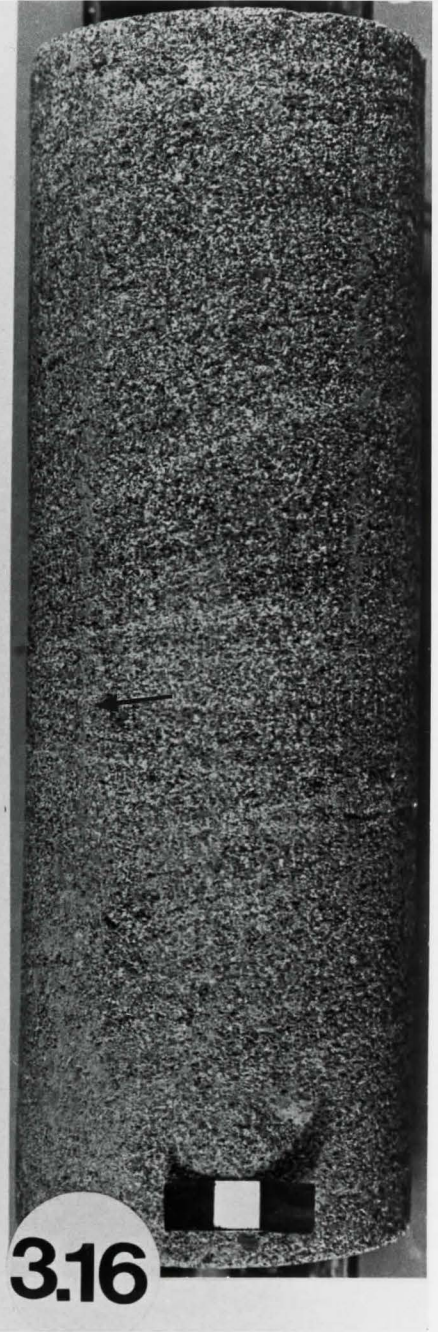
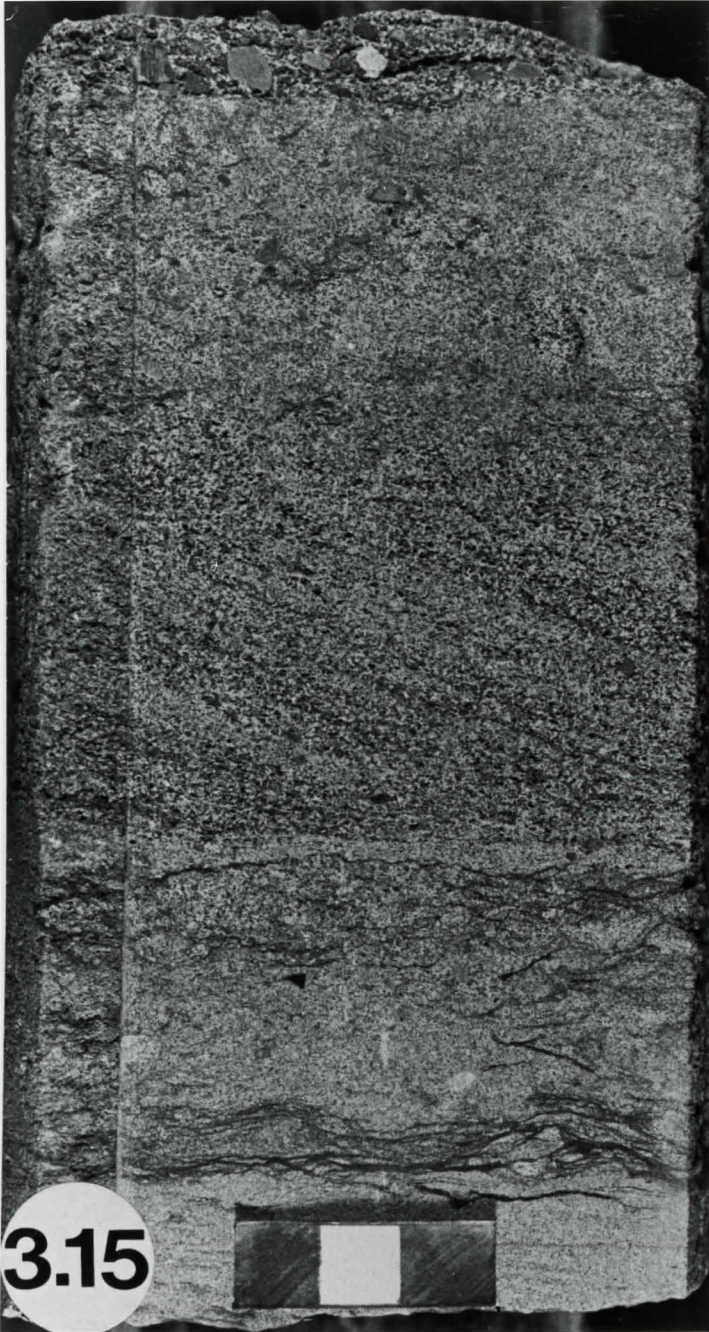
appearance, and it is characterized by a well sorted, lower to upper medium grain size. The cross-beds are inclined at an average of 15-20 degrees. These cross-beds are suggested to be trough cross-beds rather than planar tabular. The cross-beds do not approach the 34 degree angle-of-repose dip found for planar tabular cross-beds and the angle on inclination of individual foresets decreases across the core. The thick cross-bedded sandstones are commonly truncated by flat to trough-shaped beds (1-3 cm). This probably represents a cross-sectional view of the lowermost portion of the trough cross-bed. The individual laminations of the cross-beds have a fair to good textural differentiation where slightly coarser grains accumulate along the base of the foresets. The laminations also have a fair colour-grading due to larger, dark-coloured chert clasts accumulating along the base of the foresets. This helps to distinguish individual foresets.

The thin cross-bedded sandstones, have a minimum set thickness of approximately 3-5 cm, and are commonly glauconitic (Figure 3.15). The glauconite appears to accumulate preferentially along the base of the foresets.

The thick cross-bedded sandstones (Figure 3.16) have a set thickness of approximately 5-8 cm. This thickness was difficult to discern due either to the disruption in length of individual sets caused by plugging of the core for analysis or the effects of oil staining. There are scattered pebbles (2-5 mm) throughout the thick cross-bedded

Fig. 3.15. Cross Bedded Sandstone, Facies E-1. A thin cross-bedded sandstone having a set thickness of 4 cm and bounded at the base and top by muddy bioturbated sandstone (Facies C). In core glauconite preferentially accumulated along the base of the foresets. Note that the cross-beds are inclined at about 15 degrees, 12-1-40-1W5, 5487 ft (1672.4 m). Scale in cm.

Fig. 3.16. Cross Bedded Sandstone, Facies E-2. A thick cross-bedded sandstone having a minimum set thickness of 5 and 8 cm. Note the almost flat foresets (arrow) and the increase in the inclination (20 degrees) directly above, 2-16-40-1W5, 5563 ft (1695.6 m). Scale in cm.



sandstones. A general increase in the number of these pebbles occurs stratigraphically upwards. The facies is a pebbly (cross-bedded) sandstone if the pebble content exceeds approximately 10% of the total grains. Also found associated with the thick cross-bedded sandstones were rare ripped-up siderite clasts (about 2-4 cm thick), with medium sand grains dispersed within the siderite.

The cross-bedded sandstones are interpreted to have been formed by migrating sand waves probably above fairweather wave-base.

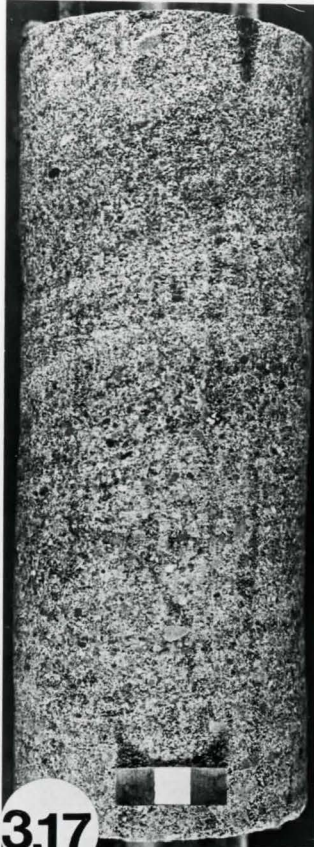
### 3.3.6 Facies F: Pebbly Cross Bedded Sandstones

Facies F (Figure 3.17) has an average thickness of 0.33 m, ranging from 0.06-0.77 m. The pebbly sandstone facies is characterized by 10-20 degree dipping cross-beds. The facies is generally matrix supported consisting of lower to upper medium grained sandstone. There also occur clast-supported examples where the number of pebbles exceeds 30% of all grains (Figure 3.19). Pebbles commonly occur concentrated in layers of 1-2 cm at the base of cross-bedded sandstones (Figure 3.18). In the finer grained beds, clasts 2-5 mm comprise 10-100% of all grains present. In the coarser grained beds, clasts greater than 5 mm comprise 10-30% of all grains present. The clasts range in size from 0.8 -20.0 mm (average of 10 largest measured clasts). The clasts are rounded to sub-rounded, polymictic, rarely imbricated and are over-all fair to poorly sorted.

**Fig. 3.17. Pebbly Cross-Bedded Sandstone, Facies F.**  
Note the similarity between this figure and Fig. 3.16 (lacking pebbles). In this photo the chert granules and pebbles are dispersed throughout. Closer inspection reveals that some of these larger grains are concentrated in thin layers at the base of the cross-beds, 10-10-40-1W5, 5520 ft (1682.5 m). Scale in cm.

**Fig. 3.18. Pebbly Cross-Bedded Sandstone, Facies F.**  
Note how pebbles are concentrated in layers of 1-2 cm at the base of cross-bedded sandstones. The beds dip at 10-15 degrees, 12-19-40-1W5, 5722 ft (1744.5 m). Scale in cm.

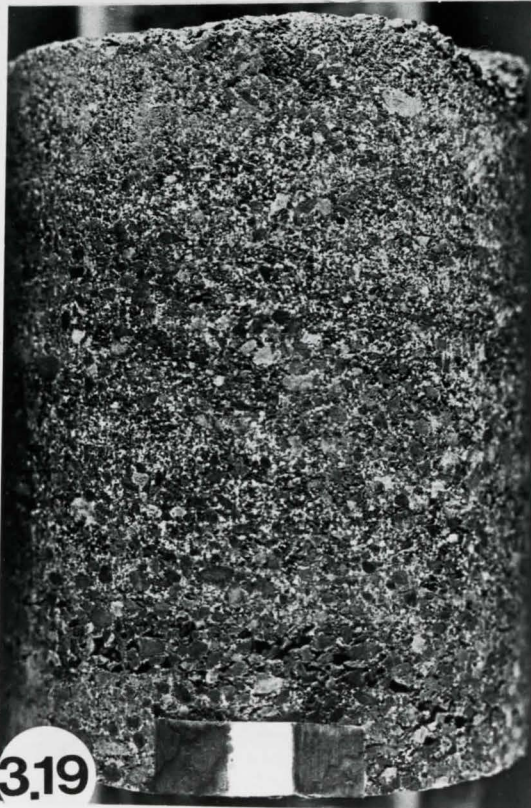
**Fig. 3.19. Pebbly Cross-Bedded Sandstone, Facies F.**  
Note how the bottom 2 cm appear to be clast supported. The cross-beds, inclined at about 15 degrees are defined by the concentration of pebbles along the base of the foresets, 16-19-40-1W5, 5848 ft (1782.9 m). Scale in cm.



3.17



3.18



3.19

The cross-beds have a minimum set thickness of 15 cm. The cross-beds are more likely to be trough cross-beds since the angle of dip on the beds is quite low (10-20 degrees) as opposed to the planar tabular type, which might be expected to be more steeply dipping. Also individual foresets show a decrease in dip across the core - a feature characteristic of trough cross stratification. Individual foresets have a poor to fair degree of color grading, due to the lack of accumulation of the darker chert pebbles in a distinct bed or laminae. They also have a fair textural differentiation, due to the normal grading along the base of the foresets (less than about 0.7 cm thick). Woody coal clasts (2-4 cm in length), ripped-up mud clasts and rounded, sideritized pebbles (both about 2-20 mm in length) are found throughout the facies.

The pebbly cross-bedded sandstones are interpreted to have been deposited above fairweather wave base.

### 3.3.7 FACIES G: Laminated Mudstone-Pebbly Sandstones

Facies G (Figure 3.20) has a measured average thickness of 0.48 m, ranging from 0.09-1.27 m. This facies resembles Facies D in appearance, although it normally occurs stratigraphically above it, only infrequently contains layers of bioturbated muddy sandstone and contains pebbly sandstone beds with pebbles dispersed throughout the mudstone. These pebbles give the mud a "gritty" appearance. The facies is characterized by mudstone laminations inter-

bedded with lower fine to coarse sand size beds. The coarse sand beds commonly contain pebbles (2-6 mm).

The mudstone laminations (less than 1 mm) and thicker mudstone beds (1-3 cm) have a sharp base. They are relatively flat to undulating with some burrowing, giving them an irregular shape.

The fine to coarse sand size beds (ranging from 1-5 cm), commonly have sharp, loaded bases (Figure 3.21). Examples of the sharp, erosive emplacement of the sands into the mud were more commonly found towards the top of the facies (Figure 3.22). There is evidence of grading within the sandstone beds where the lighter-coloured coarse sediment grades upward into the darker-coloured, fine sediment (Figure 3.21). The graded sandstone ranges up to an upper medium and lower coarse sand. The stratification within the beds is normally parallel and flat for the finer sand sizes and appears massive for the pebbly sandstone beds. The tops of the beds are sharp to graded. Small granules to 2 mm sized pebbles are often found chaotically dispersed in mudstone beds.

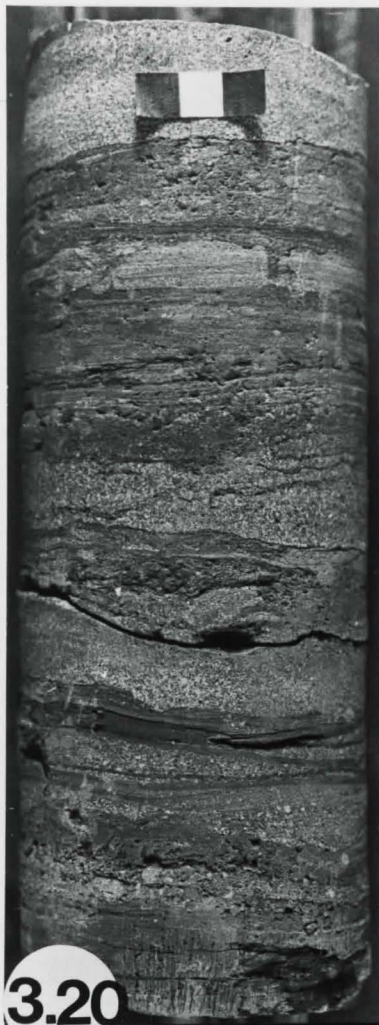
There is some evidence of burrowing through this facies, but the only recognizable burrows found were Skolithos (3-6 cm in length). These Skolithos burrows have fairly sharp, well defined walls.

Sideritized mudstone (3-5 cm thick) is commonly found within the facies. The siderite has a dark brown colour with an inner dirty white coloured portion, similar to that

Fig. 3.20. Laminated Mudstone-Pebbly Sandstone, Facies G. Note the sharp to bioturbated base and top of the mudstone laminations (less than 1 mm) and mudstone beds (1-3 cm) which are interbedded with fine sand beds (0.5-4.0). The sand beds have sharp to slightly bioturbated bases and tops. The stratification in the two upper sand beds is parallel and flat, 12-19-40-1W5, 5719 ft (1743.6 m). Scale in cm.

Fig. 3.21. Laminated Mudstone-Pebbly Sandstone, Facies G. Note the the coarse sand beds (1-5 cm) contain pebbles (2-6 mm). The base and tops of the sandstone beds are sharp to bioturbated with the bases loaded(L). The mudstone laminae (0.5-1.0 mm) and beds (1-3 cm) have sharp to bioturbated base and tops with small grains and granules dispersed throughout. Note the Skolithos burrow (S) (5 cm) which cross-cuts the mudstone and sandstone beds, 4-20-40-1W5, 4741 ft (1445.4 m). Scale in cm.

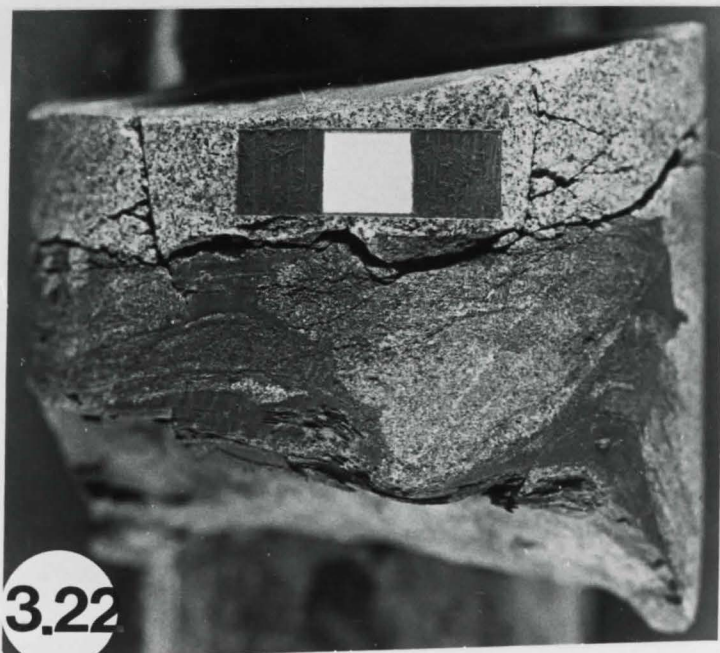
Fig. 3.22. Laminated Mudstone-Pebbly Sandstone, Facies G. Note the V-shaped base of the sandstone bed and the sharp contact it has with the mudstone laminae, 4-11-40-1W5, 5505 ft (1678.4 m). Scale in cm.



3.20



3.21



3.22

described in Facies B.

Facies G is interpreted to have been episodically emplaced. The mud laminations and beds represent periods of quiet deposition. The sharp bases of the sandstone beds imply that they were erosively emplaced possibly during periods of storm deposition. The loading of these sands into the muds also implies sudden emplacement. The grading is caused by waning flows as the storms energy dissipates. The stratification (ripple cross-lamination) within the finer sandstone beds may suggest reworking of the deposits between fairweather and storm wave base.

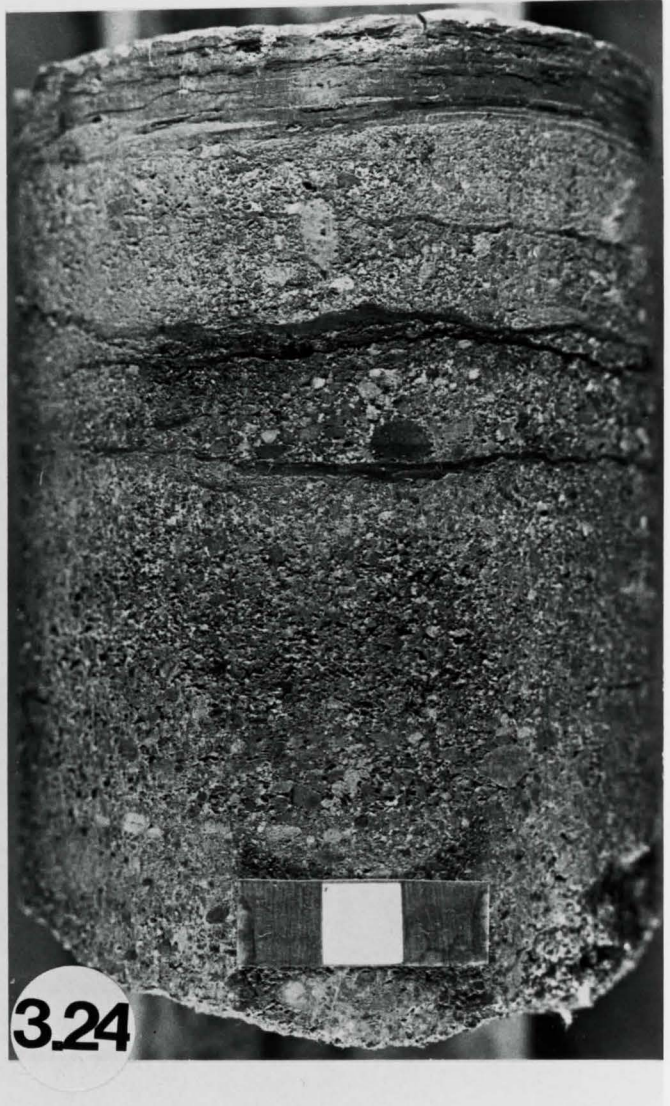
### 3.3.8 Facies H: Massive Pebbly Sandstones

Facies H (Figure 3.23) has an average thickness of 0.23 m, ranging from 0.04-0.83 m. The massive pebbly sandstones are characterized by their lack of visible stratification. The sandstone of the matrix ranges from a lower to upper medium sand. Clasts which are granule to 5 mm in size represent 10-100% of all grains present. Larger clasts which are greater than 5 mm represent 10-30% of all grains present. The pebbles are rounded to sub-rounded, polyimictic and were poorly to moderately sorted.

There are fine irregular and slightly undulating mud drapes (about 1-4 cm thick), usually found toward the bottom or top of the facies (Figure 3.24). Some examples of inverse grading also exist within this facies, there is no

Fig. 3.23. Massive Pebbly Sandstone, Facies H. The pebbly sandstone shows no evidence of stratification. The small patches of very fine matrix are identified in thin section (see Chapter 4, Figure 4.14) as kaolinite, 4-11-40-1W5, 5509 ft (1679.6 m). Scale in cm.

Fig. 3.24. Massive Pebbly Sandstone, Facies H. Note the fine irregular and slightly undulating mud drapes (1-4 cm thick) in the upper half of the core, 12-16-40-1W5, 5638 ft (1718.9 m). Scale in cm.



evidence of bioturbation.

The massive pebbly sandstones are interpreted to have been deposited suddenly with no subsequent reworking by currents.

### 3.3.9 FACIES I: LAMINATED MUDSTONES AND CONGLOMERATES

In core, Facies I (Figure 3.25) has a measured average thickness of 0.37 m, ranging from 0.07-0.50 m. The facies is characterized by mudstone laminations and rip-up clasts interbedded with beds of conglomerate.

The mudstone laminations (1-4 mm thick) are normally irregular and have bioturbated to sharp contacts with the coarse sediment. These mudstone laminations often rest at high angles with the coarse sediment (Figure 3.26). Also occurring are large ripped-up mud clasts (1 x 5 cm). The clasts have both sharp and rounded edges and are sometimes bent. Some of these clasts are sideritized.

The conglomerates (Figure 3.25) generally contain more pebbles towards the top of the facies. The matrix is a medium sand sized, salt and pepper sandstone. The pebbles (5 x 15 cm) are well rounded and oblong in shape. They are chaotically orientated and have no imbrication. The top of the facies had pebbles protruding up at an angle into the commonly overlying black mudstone (Facies K). The unit commonly appears to represent a pebbly sandstone because of the low percentage (10%) of large pebbles. However, as discussed above, this unit contains laminated mudstone,

Fig. 3.25. Laminated Mudstone and Conglomerate, Facies I. Mudstone laminations are interbedded with a pebbly sandstone to conglomerate towards the top of the core. The irregular mudstone laminations, have irregular and bioturbated to sharp contacts with the coarse sediment. Vertical burrows (B) (2 cm long) cross-cut the mudstone laminations. A sideritized mudstone clast (C) and larger pebbles occur towards the top of the photo. The black mudstone (Facies K) drapes over the uppermost pebbles of Facies I, 4-11-40-1W5, 5507 ft (1679 m). Scale in cm.

Fig. 3.26. Laminated Mudstone and Conglomerate, Facies I. Note that the mudstone laminations are inclined at high angles (20 degrees) with the coarse sediment. The coarse sediment approaches a clast supported conglomerate towards the top of the photo, 6-8-41-2W5, 5933 ft (1809 m). Scale in cm.

some inclined up to 30 degrees, which help distinguish this facies from Facies H (massive pebbly sandstone).

The burrow forms recognized include vertical Skolithos and a circular burrow seen in cross-section. The Skolithos burrows (2-4 cm) have poorly defined walls. The circular burrows have the same diameter as the Skolithos burrows (less than 1 cm) and may represent the Skolithos occurring at a different angle. These burrows cut through the mud laminations and are filled with the same sand size as the matrix.

The laminated mudstones and conglomerates are interpreted to represent a rapid period of coarse sediment deposition, followed by quiet periods of mud deposition. The ripped-up mud clasts and the chaotic nature of the pebbles may suggest deposition during a storm event. The fine mud laminations implies deposition in deeper, quiet waters. The commonly dipping mud laminae could represent deposition onto an inclined surface. Skolithos burrows are commonly associated with higher energy environments and their development may be associated with the periods of coarse sediment accumulation.

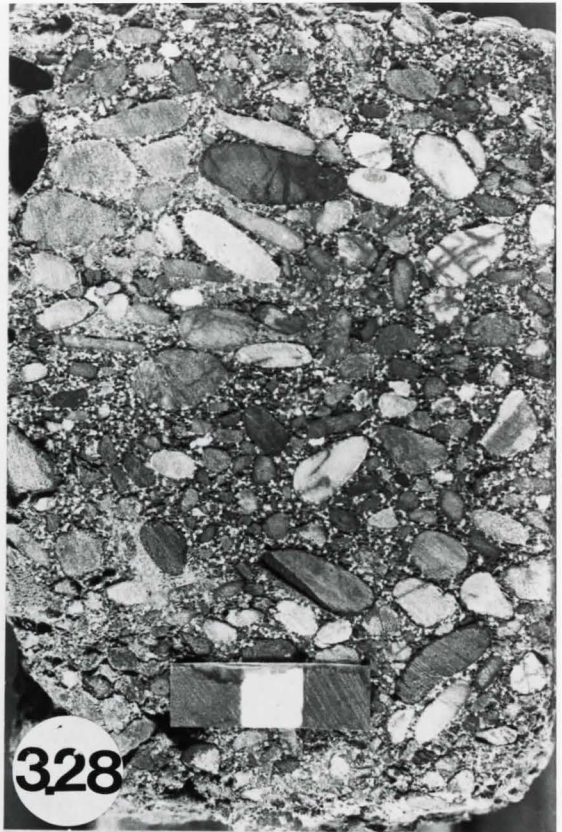
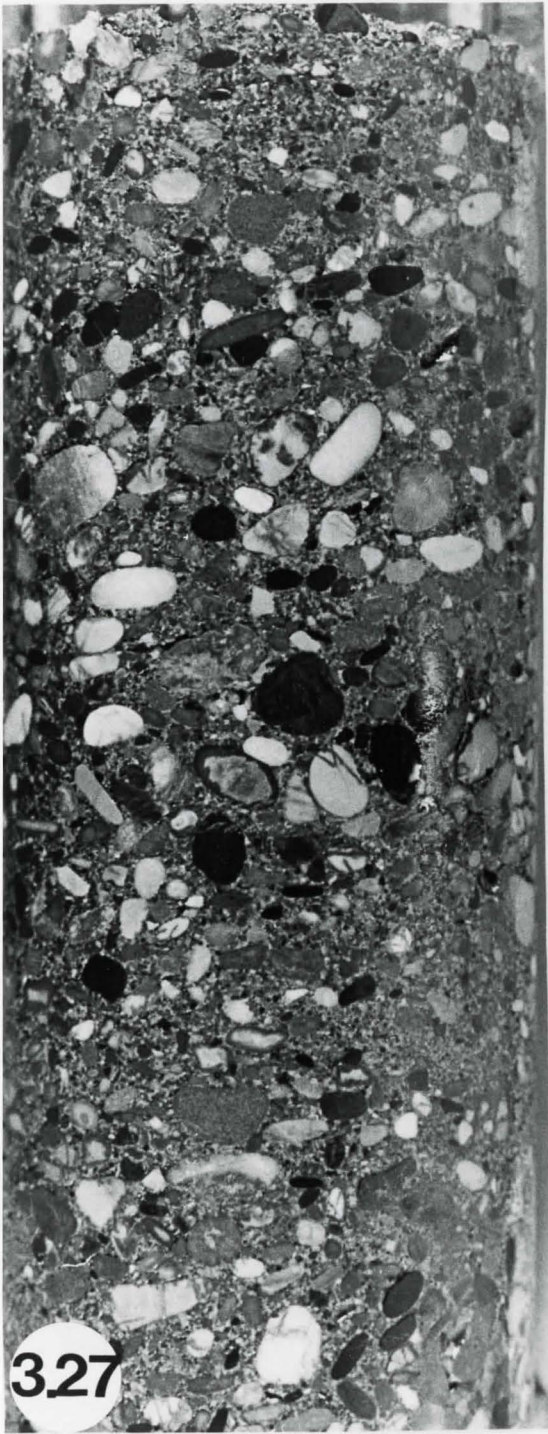
### 3.3.10 FACIES J: CONGLOMERATES

Facies J (Figure 3.27) has an average thickness of 1.16 m, ranging from 0.08-3.34 m. The conglomerate facies is characterized by a medium sand size matrix containing greater than 30% chert clasts (greater than 5 mm).

Fig. 3.27. Conglomerate, Facies J. Note the salt and pepper appearance of the sandstone matrix (see facies E, Fig. 3.28) and abundant chert pebbles (greater than 5 mm). The clasts are well-rounded to oblong in shape. There is no definite imbrication or visible stratification, 12-3-41-3W5, 6255 ft (1906.5 m). Core is 3.5 in (8.9 cm) wide.

Fig. 3.28. Conglomerate, Facies J. Note the oblong shape of many of the larger chert pebbles. The pebbles are chaotically scattered throughout, 12-2-41-3W5, 6455 ft (1968 m). Scale in cm.

Fig. 3.29. Conglomerate, Facies J. Note how the chert pebbles are in contact with one another and the absence of sandstone matrix in the central portion of the photo, 2-30-40-1W5, 5816 ft (1773 m). Scale in cm.



The conglomerates are mainly polymictic, clast supported and poorly sorted. The matrix is a lower to upper medium sand size, having a salt and pepper appearance similar to that in Facies E (Figure 3.28). There is no imbrication, nor any visible stratification. The pebbles lie both vertically and inclined. The clasts range in color from dirty-yellow, bluish-grey to black. The clasts are well-rounded and the larger ones (generally larger than 10 mm) are oblong in shape (Figure 3.29).

There are a few examples of sideritization (2-4 cm thick) within the facies. Commonly, a few pebbles at the top of the facies will protrude above the top of the bed into the overlying black mudstone. Some conglomerates lack matrix and may have good porosity.

The conglomerates are interpreted to have been emplaced rapidly since the pebbles are poorly sorted and chaotically dispersed. There is no evidence for bioturbation which might have disturbed any original stratification.

### 3.3.11 Facies K: BLACK MUDSTONES

The black mudstone facies (Figure 3.30) represents the Upper Viking Formation (Koldijk, 1976; p.64). It overlies all of the coarse facies. This facies is characterized by its very black colour and fissility which causes the "poker-chip" shape of the mudstone in core. The black mudstones frequently contain greyish-white silt beds (each

2-6 cm thick). In core the silt beds can be both continuous or lenticular in shape. These silt beds, where found, tend to make the black mudstone less fissile in core. The silt beds have sharp bases and contain silt laminae. These beds are colour graded, due to the grain size differences between the black laminae representing the finer clay sediment and the greyish-white laminae representing the silt sized sediment. They are composed of flat parallel laminations and ripple cross-laminations (both approximately 0.5 mm thick, see Fig. 3.30). The ripple cross-laminations were most likely formed by both unidirectional currents and waves. The current formed ripple cross-laminations are identified where the ripples appear to fade and die by the delicate interfingering of mudstone laminae in the silt (Figure 3.30). The wave formed ripple cross-laminations appear to flatten out and fade at a lower angle than the current formed ripples. The laminations often show evidence of soft sediment deformation (Figure 3.31). The silt beds have sharp top contacts with the black mudstone.

Also occurring randomly through the facies are coarse granular to pebbly medium-grained sandstone beds (Figure 3.32). These beds (less than 2 cm in width) are either lenticular or continuous in core.

The black mudstone facies lacks visible bioturbators, but there are disrupted laminae which have been disturbed by horizontal burrowers. Examples of small (1 cm x 2 cm) fishscales (Figure 3.33) were found within the facies.

Fig. 3.30. Black Mudstone, Facies J. Note the fissile appearance of the black mudstone and the numerous silt laminae (less than 0.5 mm) and silt beds (less than 6 cm thick). Some of the silt beds are colour graded and are composed of flat parallel laminations (P) and ripple cross-laminations (R). Note the interfingering of mudstone laminae in the siltstone ripple cross-laminations. There is also some evidence for bioturbation (arrow) of the silt beds.

Fig. 3.31. Black Mudstone, Facies J. Note the flat to parallel orientation of the ripple cross-lamination formed by wave influence. The curl in the laminations (arrow) are formed by soft sediment deformation. Scale in cm.

Fig. 3.32. Black Mudstone, Facies J. Note the lenticular pebbly medium-grained sandstone bed (less than 1 cm in width). Both the top and base of this bed is sharp with the black mudstone. The base of the pebbly sandstone bed is slightly loaded into the mudstone below and the top of the bed is draped over by the mudstone. Scale in cm.

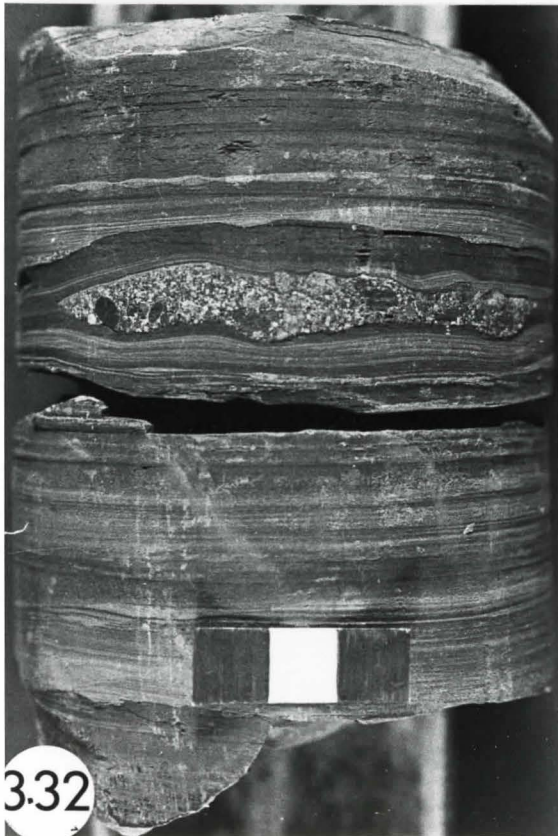
Fig. 3.33. Black Mudstone, Facies J. Portion of a fishscale (1 cm x 2 cm) preserved in the black mudstone. Scale in cm.



3.30



3.31



3.32



3.33

The black mudstones are interpreted to have been deposited in a deep, muddy basin. The sharply based silt beds were storm emplaced. The colour grading is due to an episodic, waning flow. The ripple cross-laminations formed by wave and unidirectional current influence.

### 3.4 Generalized Facies Sequence

#### 3.4.1 Introduction to Facies Sequence

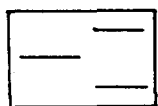
Study of cores within the Gilby A and B field allows the delineation of four general facies sequences, each representing a different area within the fields (see Figure 3.35). Vertical and lateral facies sequences are presented and discussed, with 5 core cross-sections (their locations shown in Figure 3.35) and where possible Markov Chain analysis. The Markov sequences were calculated separately for each area.

Facies are referred to by letters which correspond to the Facies names shown in Figure 3.34 (p.<sup>77</sup>68). The discussion emphasizes the coarser Viking sediments (Facies B through J), referred to subsequently as the "coarse sediment package". Throughout the study area the coarse sediment package abruptly overlies Facies A and is abruptly overlain by Facies K.

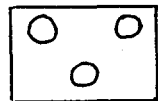
All core cross-sections show that with respect to the upper marker (A) taken to be horizontal, the base of the

SYMBOLS ON LITHOLOGS

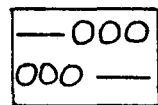
FACIES



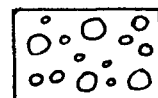
K BLACK MUDSTONES



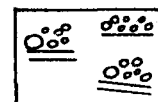
J CONGLOMERATES



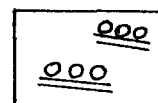
I LAMINATED-MUDSTONES AND CONGLOMERATES



H MASSIVE PEBBLY SANDSTONES



G LAMINATED MUDSTONE-PEBBLY SANDSTONES



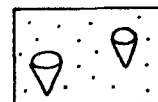
F PEBBLY CROSS BEDDED SANDSTONES



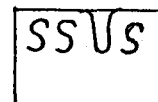
E CROSS BEDDED SANDSTONES



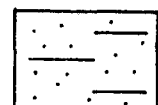
D BURROWED-LAMINATED MUDSTONES-SANDSTONES



C PERVASIVELY BIOTURBATED MUDDY SANDSTONES



B SIDERITIZED MUDDY SILTSTONES (WITH SKOLITHOS)



A HOMOGENEOUS MUDDY SILTSTONE

OTHER SYMBOLS

VVV Bentonite

▽ Bioturbation

≈ Cross-lamination

∩ Fishscales

99 Glauconite

SSS Siderite

Fig. 3.35. Location map for core and log cross-sections used in the study area. The Gilby A and B fields are outlined with a solid black line where the larger of the two fields is Gilby A. The lightly hatched outline on the map represents a portion of the Willesden Green field. The core and litholog cross-sections are numbered 1 through 5. The log cross-sections include all cored wells used in the litholog cross-sections, these are shown encircled, wells within squares are included in the log cross-sections only. Heavily hatched lines separate the Gilby A and B field into specific areas (labelled A-1, A-2, A-3 and B-1) which represent different vertical facies sequences as discussed in text.

R 5W5

R 4W5

R 3W5

R 2W5

# GILBY A & B

## LOCATION MAP FOR CORE & LOG CROSS-SECTIONS

INTERPRETATION BY : H.K.R. DATE : MAY, 1985  
SCALE : 1:63,360 CONTOUR INTERVAL :

WILLEDEN GREEN FIELD  
 CORE CROSS-SECTION  
 LOG CROSS-SECTION



T 42

T 41

T 40

T 39

T 41

T 40

T 39

R 5W5

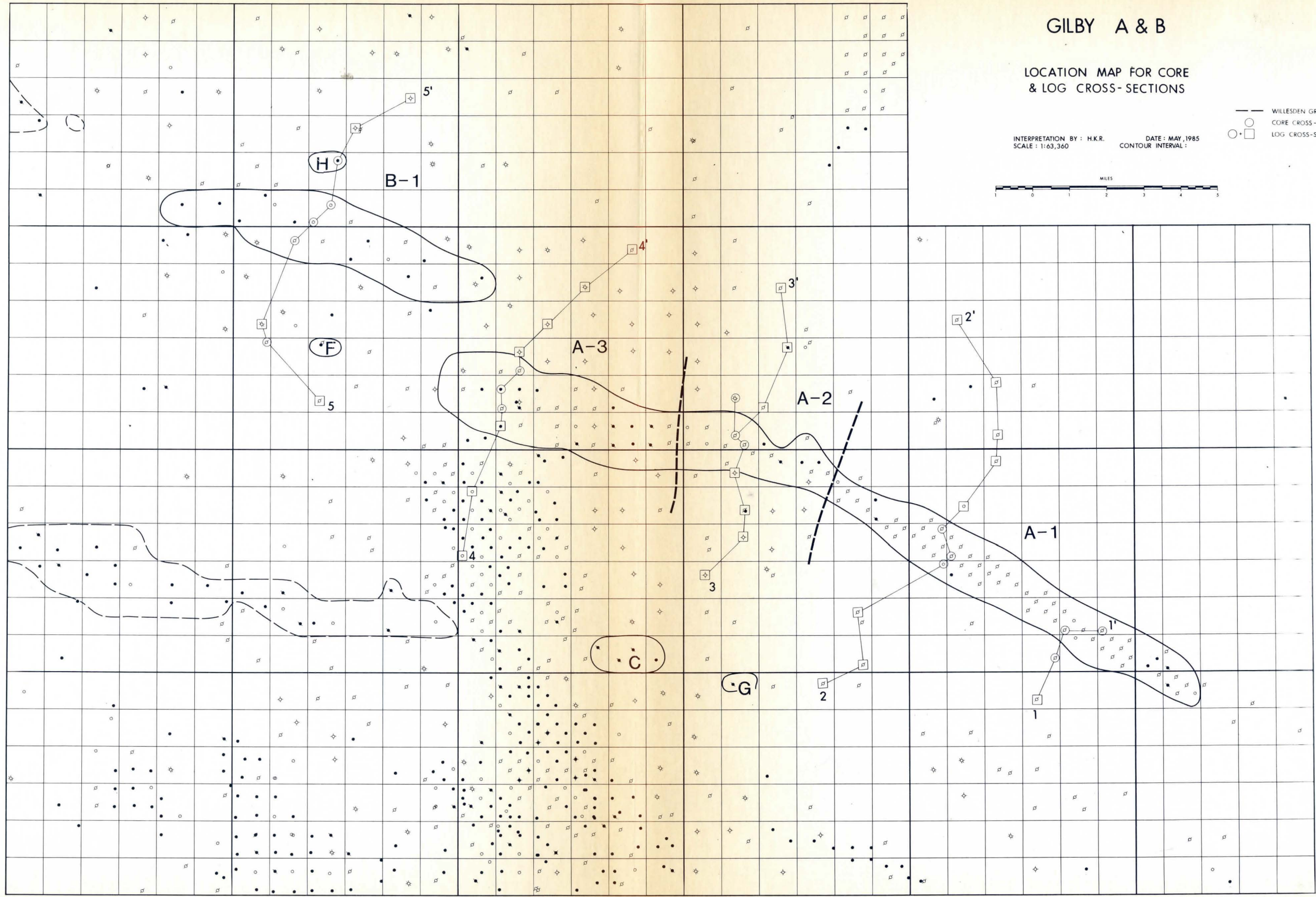
R 4W5

R 3W5

R 2W5

R 1W5

R 28W4



coarse sediment package is irregular, with up to 19 ft of relief. Within the field boundaries, the base of this package is stratigraphically lower in the northeast than the southwest. The geometry of this surface will be discussed in more detail over the study area in Chapter 5.

### 3.4.2 Discussion

Examination of cores of the Viking coarse sediment package in the Gilby A field suggests two distinct vertical facies sequences (A-1, A-3; Fig. 3.35), aerially separated by a third transitional facies sequence (A-2; Fig. 3.35). The Gilby B field has one sequence (B-1; Fig. 3.35), which with minor modifications is similar to that of A-3.

The facies sequences for each area of the Gilby A and B fields are discussed with a representative core cross-section (see Figs. 3.36, 3.37, 3.9, 3.41 and 3.42) oriented southwest to northeast (perpendicular to the strike of the field). Each section is drawn with the upper datum (marker A, see Chapter 2) horizontal. This datum is regionally very reliable over the study area. Refer to Chapter 5 for further discussion on this datum and its structure over the study area. In each section the heavy solid line correlates the base of the coarse sediment package. The slope of this surface with respect to the horizontal datum is given adjacent to the solid correlation line. Dashed lines correlate similar facies (lettered) within each core cross-section.

Alongside each core, individual coarsening-upward sequences are emphasized with upwardly curving arrows. The base of an individual coarsening-up sequence is recognized by Facies C, D, E or G while the top of an individual coarsening-up sequence is recognized by Facies F, H, I or J. In general the base of an individual coarsening-up sequence has a finer matrix, containing more mudstone and fewer pebbles than the top of an individual coarsening-upward sequence. Numbers 1 through 3, beside the arrows refer to lower, middle and upper individual coarsening-upward sequences respectively. Equivalently labelled individual coarsening-upward sequences in different core cross-sections may not necessarily be correlative. Recognition of these individual coarsening-up sequences within the coarser sediment package was a relatively easy procedure using core. However, matching core with electric log responses was difficult and where no core was available recognition of individual coarsening-up sequences was not possible.

The top of the coarse sediment package in each cross-section is correlated with a heavily dashed line. This surface may not necessarily be synchronous in adjacent wells.

To examine whether there was any preferred sequence of facies, Markov Chain analysis was performed separately with data from each area (A-1, A-2, A-3 and B-1). The computer program BMDP 4F (Brown, 1981) was used in computing the Markov analysis.

The Markov analysis involves testing vertical facies sequence against a null hypothesis of a random succession of facies (Carr, 1982; p.905). Rejection of the null hypothesis implies a non-random or preferred facies sequence. The presence of a Markov process indicates cyclicity of facies deposition, implying geological significance. The Markov analysis performed is a first-order process, dependent upon the preceding facies.

Techniques for Markov Chain analysis are discussed by Powers and Easterling (1982) and their method is used here. The analysis involves a comparison of the observed and expected transition frequencies. Powers and Easterling (1982, p.114) test the null hypothesis by a statistic which determines the value of chi-squared. The probabilities for the chi-squared values are determined and if they are less than the set level of significance (0.2) then the null hypothesis is rejected and there is a preferred facies sequence. A level of significance of 0.2 or 2% means rejecting the null hypothesis when it is correct two times out of 100 trials (Davis, 1973; p.91). As the value of the probabilities approach 0.2 the particular facies sequence is regarded as being more random.

#### 3.4.3 Gilby A-1-Facies Sequence (Cross-Section 1, Fig. 3.36)

The Gilby A-1 area contains the thickest sandstone accumulation in the study area. Within Gilby A-1 the

Fig. 3.36. Litholog cross-section 1 from cored wells 8-3-40-1-W5, 4-11-40-1W5 and 4-12-40-1W5 located on Figure 3.36. Core measurements are in metres and grain size measurements are found at the bottom of the litholog. The scale at the bottom of each litholog represents the grain size of the distinguishing sediments used in naming the facies. Beginning with the fine size fractions the "c" stands for clay, the "s" for silt, the "vf", "f" and "m" for very fine, fine and medium sandstone respectively and the coarser size fractions "C", "G", "P" and "Cgl" stand for coarse, granular, pebbly and conglomeratic respectively. The heavy solid line correlates the base of the coarse sediment package. The slope of this surface with respect to the horizontal datum (marker A) is shown adjacent to the solid correlation line. Dashed lines correlate similar facies (lettered). The upwardly curving arrows emphasize the individual coarsening-upward sequences numbered as 1 through 3, which refer to the lower, middle and upper facies sequence. The top of the coarse sediment package is correlated between wells by the dashed-dotted line. See text for discussion.

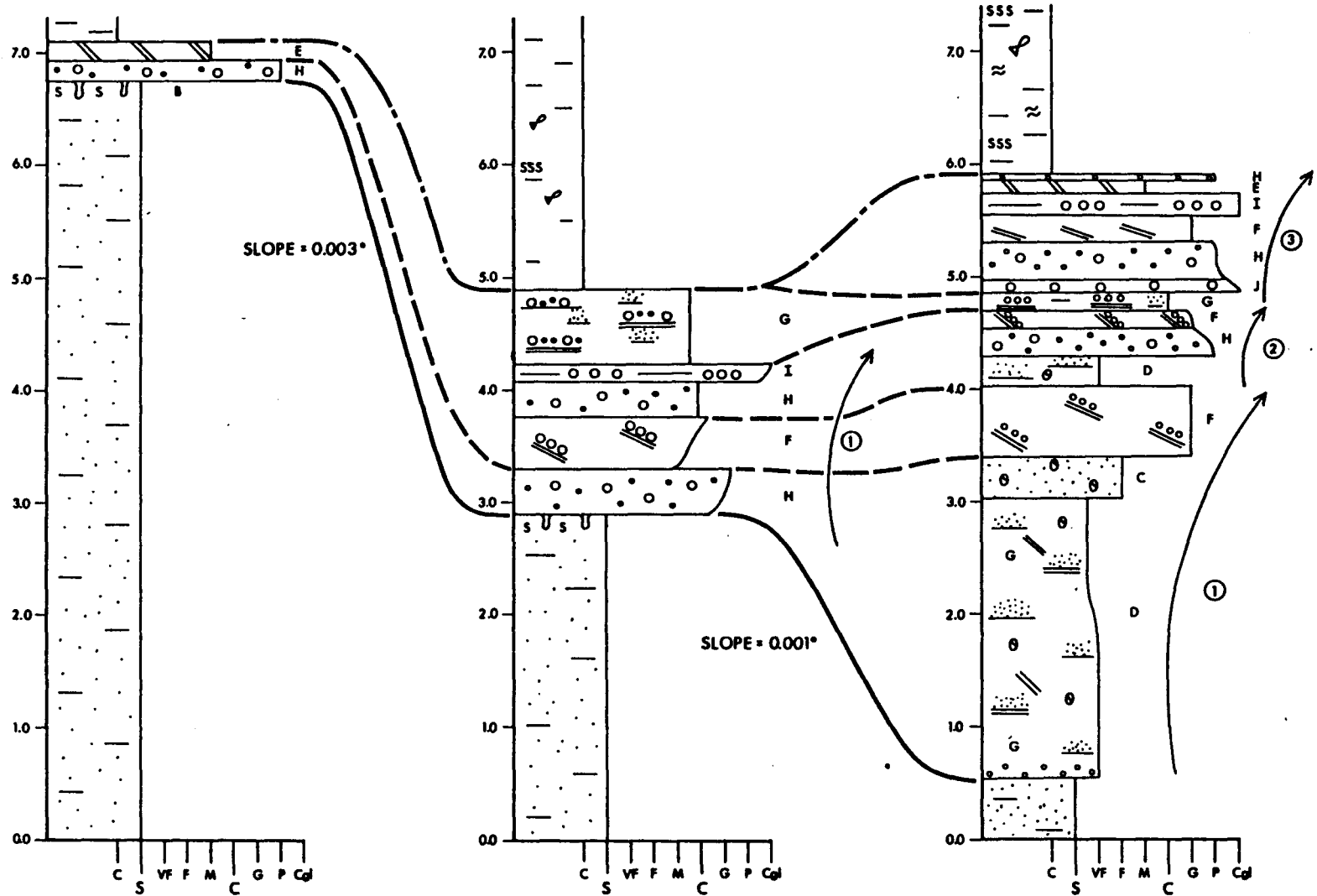
SW  
1

NE

8-3-40-1 W5  
5479' - 5504'

4-11-40-1 W5  
5499' - 5523'

4-12-40-1 W5  
5475' - 5499'



sandstones thicken towards the northeast. Vertical and lateral facies sequence are demonstrated with core cross-sections 1 and 2 (Fig. 3.35 and 3.36 respectively).

In cross-section 1 well 8-3 is situated approximately three-quarters of a mile southwest of the Gilby A field boundaries as designated by the ERCB. The coarse sediment package in 8-3 is thin and consists of only one sequence beginning with Facies B. The basal contact of Facies B with Facies A is erosive and abrupt. Facies H overlies the firmground and is in turn abruptly overlain by a thin unit of Facies E. Facies E caps the coarse sediment package. Well 4-11 is located close to the southwest margin of the field, and contains a single coarsening-up sequence. The sequence begins with Facies B (see also cross-section 2, Fig. 3.37, well 16-18), which has an erosive and abrupt contact with Facies A. Facies H overlies the firmground in 4-11. Above here, facies contacts into F, H and I are gradational. Facies I caps the single coarsening-up sequence and is gradationally overlain by Facies G, which completes the coarse sediment package.

Well 4-12 lies furthest to the northeast in cross-section 1 (Fig. 3.36) in about the middle of the field. The coarse sediment package contains three coarsening-up sequences. The lowermost sequence begins with a thick accumulation of Facies D. A few chert pebbles are scattered in the lower 10 cm of this unit. The percentage of laminated mudstone in Facies D increases toward the top

of the unit. Above here, Facies contacts into C and Facies F are gradational. Facies F caps the first coarsening-up sequence.

The second coarsening-up sequence also begins with Facies D, which is abruptly overlain by Facies H. Facies F gradationally overlies Facies H and caps the second coarsening-upward sequence.

The third coarsening-up sequence begins abruptly with Facies G, which is gradationally overlain by Facies J. Contacts up into facies H, F, I are all gradational (Figure 3.36). Above here, facies contacts into E and H, which caps the sequence, are gradational.

Gilby A-1 - Facies Sequence (Cross-Section 2, Figure 3.37):

Cross-section 2 (Fig. 3.37) begins with well 16-18, located on the southwest margin of area A-1. This well has a single coarsening-up sequence. Facies B begins the coarsening-up sequence (see also 8-3 and 4-11 in cross-section 1, Fig. 3.36), which has an erosive and abrupt contact with Facies A below. Facies H overlies Facies B and is abruptly overlain by Facies E. Facies E envelopes a thin unit of Facies C. Facies H abruptly overlies Facies E and caps the coarsening-up sequence.

The facies sequence at 16-18 (cross-section 2) is very similar to that at 8-3 (cross-section 1), in that both have a thin coarse sediment package. The differences include the addition of Facies C, E and H in 16-18.

Fig. 3.37. Litholog cross-section 2 from cored wells 16-18-40-1W5, 4-20-40-1W5 and 16-19-40-1W5 located on Fig. 3.35. See Fig 3.36 caption (p.83) for full description of diagram labels. See text for discussion.

SW  
2

16 - 18 - 40 - 1 W 5

5670' - 5688'

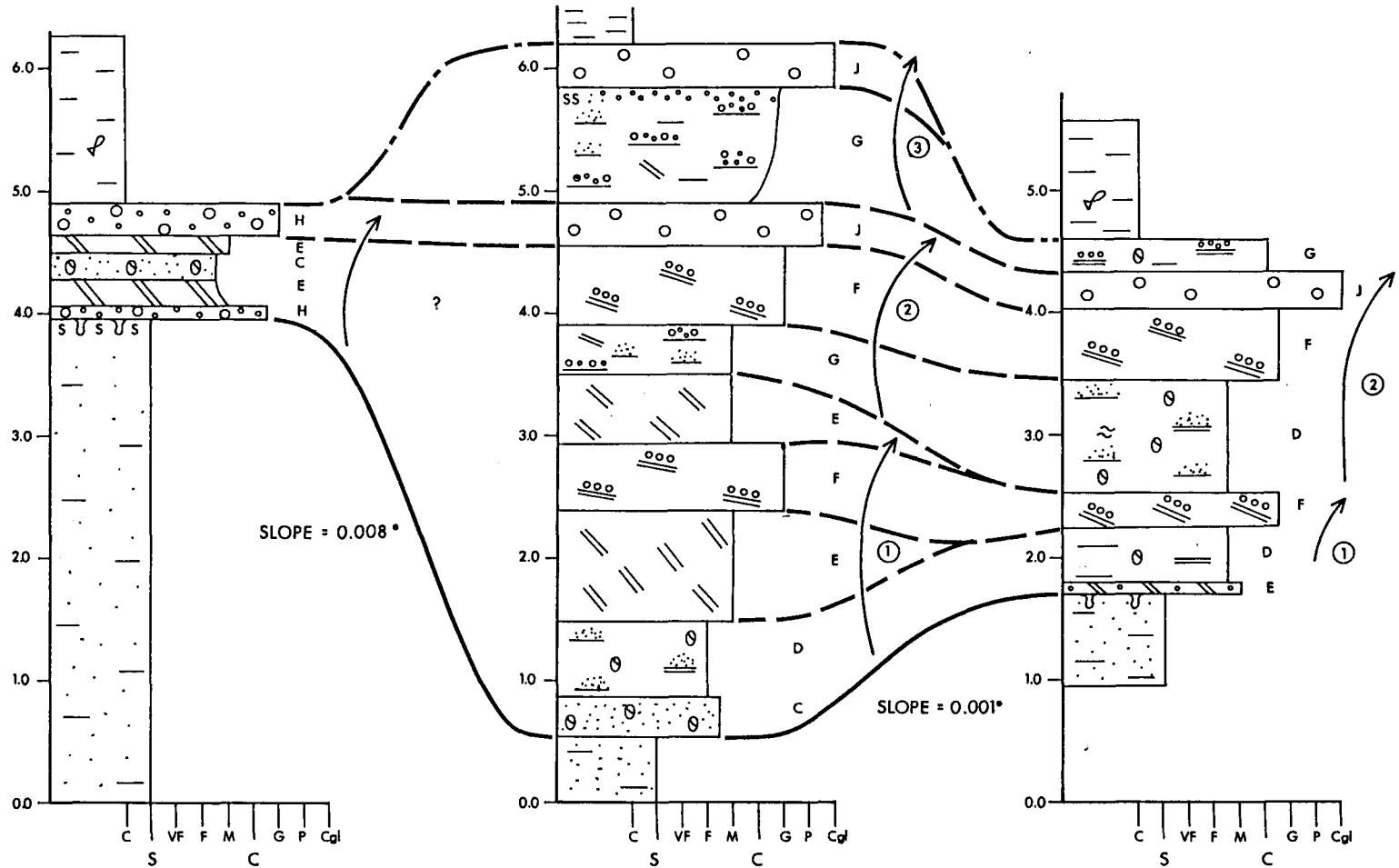
4 - 20 - 40 - 1 W 5

5734' - 5756'

NE

16 - 19 - 40 - 1 W 5

5839' - 5856'



Well 4-20 in cross-section 2 (Fig. 3.36) has three coarsening-up sequences. This well is typical of core from the central area of A-1. The first coarsening-up sequence begins with Facies C which is gradationally overlain by Facies D. Facies E abruptly overlies Facies D. Above this point Facies contacts into F and E are gradational. Facies E caps the first coarsening-up sequence.

The second coarsening-up sequence begins with Facies G which abruptly overlies Facies E. Above here, Facies contacts into F and J are gradational. Facies F caps the second coarsening-up sequence.

The third coarsening-up sequence begins with a thick unit of Facies G which abruptly overlies Facies F. Facies G is gradationally overlain by Facies J which caps the third coarsening-up sequence.

A consistent facies sequence pattern within individual coarsening-up sequences occur in 4-20. An interbedded laminated mudstone-sandstone (Facies D or G) occurs at the base of the sequences, while the pebbly cross-bedded sandstones or conglomerates (Facies F and J respectively) cap the coarsening-up sequence. Within each coarsening-up sequence in 4-20 gradational facies contacts were noted, the only exception being that Facies contacts at the lower and upper surface of Facies D and G were usually abrupt.

Well 16-19 is situated furthest to the northeast in cross-section 2 (see Fig. 3.37). This core is typical of the northeast margin of Gilby A-1. The coarse sediment

package in 16-19 contains two coarsening-up sequences. These sequences are similar to those observed in 4-20.

The first coarsening-up sequence begins with a thin Facies E, containing a few scattered chert pebbles near the base. Above here, facies contacts into D and F are abrupt. Facies F caps the first coarsening-up sequence.

The second coarsening-up sequence begins with a thick unit of Facies D. Above here, facies contacts into F and J are gradational. Facies J caps the second coarsening-up sequence. Facies D abruptly overlies Facies J and caps the coarse sediment package.

#### Gilby A-1 - Markov Chain Analysis:

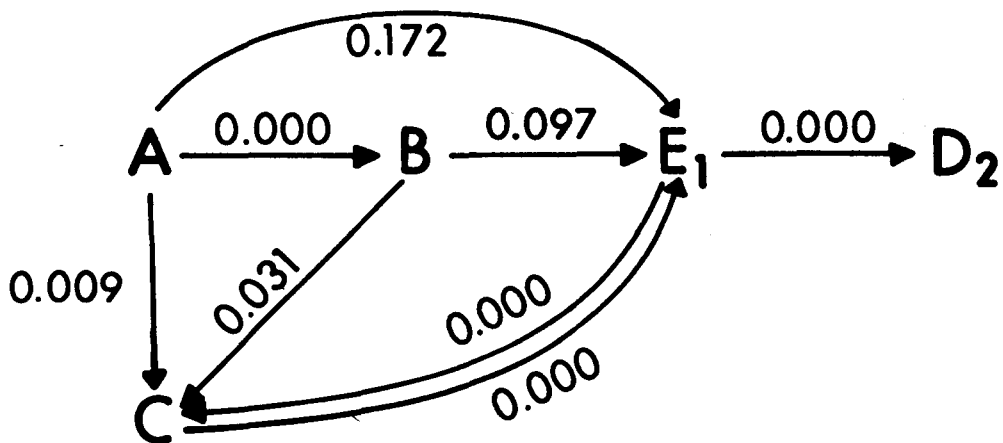
Markov Chain analysis was performed using all facies transitions from cores in the A-1 area. See Appendix 1 (p. 213) for the observed and expected frequency tables and the calculated probabilities used in determining the preferred facies sequence. The results were interpreted from core data to represent a sandstone coarsening-up sequence and a conglomerate coarsening-up sequence referred to as the "S-1" and "C-2" sequences respectively (Fig. 3.38). Numbers above the arrows on Figure 5 refer to the probability of that particular transition. The closer the probability is to the set level of significance (0.2) then the more random the particular facies transition.

The S-1 and C-2 sequences can be interpreted as simplified versions of the first, second or third

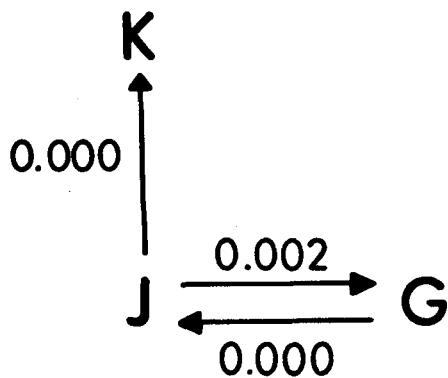
Fig. 3.38 Facies relationship diagram determined from Markov chain analysis for the Gilby A-1 area. The numbers above the arrows refer to the probability of that particular facies transition. The closer the numbers are to 0.2 (the set level of significance used in the Markov analysis) the more random and the less cyclicity represented by the facies transition. Refer to Figure 3.34 (p.77) for the Facies legend. The stratigraphically higher Facies in each diagram is shown in the direction of the arrow. For example in the S-1 sequence Facies B is underlain by Facies A. See text for discussion.

# GILBY A-1 MARKOV CHAIN ANALYSIS

S-1 (SANDSTONE COARSENING - UP SEQUENCE)



C-2 (CONGLOMERATE COARSENING - UP SEQUENCE)



coarsening-upward sequences (see Fig. 3.36 and 3.37, cross-sections 1 and 2 respectively). For example the S-1 sequence is found as a simplified version of the lowermost (first) coarsening-up sequence where the coarse sediment package is thick. The C-2 sequence is found as a simplified version of the middle and upper (second and third) coarsening-upward sequences. The coarse sediment package is thick within the central and northeast margin of the Gilby A-1 area.

Sequence S-1 or the sandstone coarsening-up sequence begins with Facies A (Fig. 3.38). Facies A is overlain in order of increasing randomness (the larger the probability) by Facies B, C or directly overlain by E-1. Facies E-1 is overlain by Facies C or D-2. Facies C and E-1 have a closed loop between them and hence always occur in association with each other. Therefore Facies C and E-1 could be considered together as a single facies. Facies D-2 is defined as the base of the coarsening-upward sequence. From Markov analysis for the S-1 sequence no more facies having a determined probability of less than 0.2 are present. This implies that facies sequence above Facies D-2 occur in a random manner and have no geological significance.

Sequence C-2, the conglomerate coarsening-upward sequence begins with Facies J and G (Fig. 3.38). These two facies have a closed loop between them and hence always occur in association with each other. Therefore Facies J and G could be considered together as a single facies.

Facies J can be overlain by Facies G and K and underlain by Facies G. The C-2 sequence is suggested to represent the middle and upper (labelled 2 and 3 respectively on Fig. 2 and 3) coarsening-upward sequences where the coarse sediment package is thick. The coarse sediment generally begins with Facies G and is capped with Facies J.

Summary - Gilby A-1:

The lower, middle and upper coarsening-upward sequences (labelled as 1, 2 and 3 respectively on the cross-sections, Fig. 3.36, 3.37) occur in the coarse sediment package of the Gilby A-1 area. From Markov Chain analysis these sequences can be interpreted to represent two generalized coarsening-up sequences, a sandstone (S-1 sequence) and conglomerate (C-2) sequence. Within the A-1 area the coarse sediment thickness increases in a northeasterly direction. Minimum sandstone development occurs along the southwest margin of A-1 where Facies B is observed (1 coarsening-up sequence). Maximum sandstone development occurs in the central area of A-1 (2 to 3 coarsening-up sequences).

Also observed within the field boundaries is the consistent stratigraphic drop of the lower surface of the coarse sediment package, with respect to a horizontal upper datum (marker A), towards the northeast. The coarse sediment package is thicker where its lower surface is stratigraphically lower.

3.4.4 Gilby A-3 - Facies Sequence (Cross-Section 4, Figure 3.39)

The thickest conglomerate accumulation within the study area occurs in the central region of the Gilby A-3 area. From the central region of A-3 conglomerates thin outwards in a radial pattern. Vertical and lateral facies sequences within Gilby A-3 are demonstrated with core cross-section 4 (Fig. 3.39). Marker A is horizontal in all cross-sections.

In 4-8 a single coarsening-up sequence occurs within the coarse sediment package (see also 8-3 and 4-11 in cross-section 1, Fig. 3.36). The coarse sediment package begins with Facies J gradationally overlain by Facies F. Another conglomerate, Facies J, gradationally overlies Facies F, capping the coarsening-upward sequence.

The centrally located well 12-8 in cross-section 4 is typical of a well from the center of the A-3 area. The single coarsening-up sequence consists of a thin unit of Facies H, gradationally overlain by a thick unit of Facies J which caps the coarse sediment package. Pebble size tends to increase upwards within Facies J.

Well 2-17 located furthest to the northeast contains two coarsening-upward sequences. The first and lowermost coarsening-upward sequence in 2-17 begins abruptly with Facies H. Above here, facies contacts into C and F are gradational. Facies F caps this lowermost sequence.

The middle or second coarsening-up sequence begins abruptly with Facies G. This unit also begins the middle

Fig. 3.39. Litholog cross-section 4 from cored wells 4-8-41-3W5, 12-8-41-3W5 and 2-17-41-3W5 located on Fig. 3.35. See Fig. 3.36 caption (p.83) for full description of labels. See text for discussion.

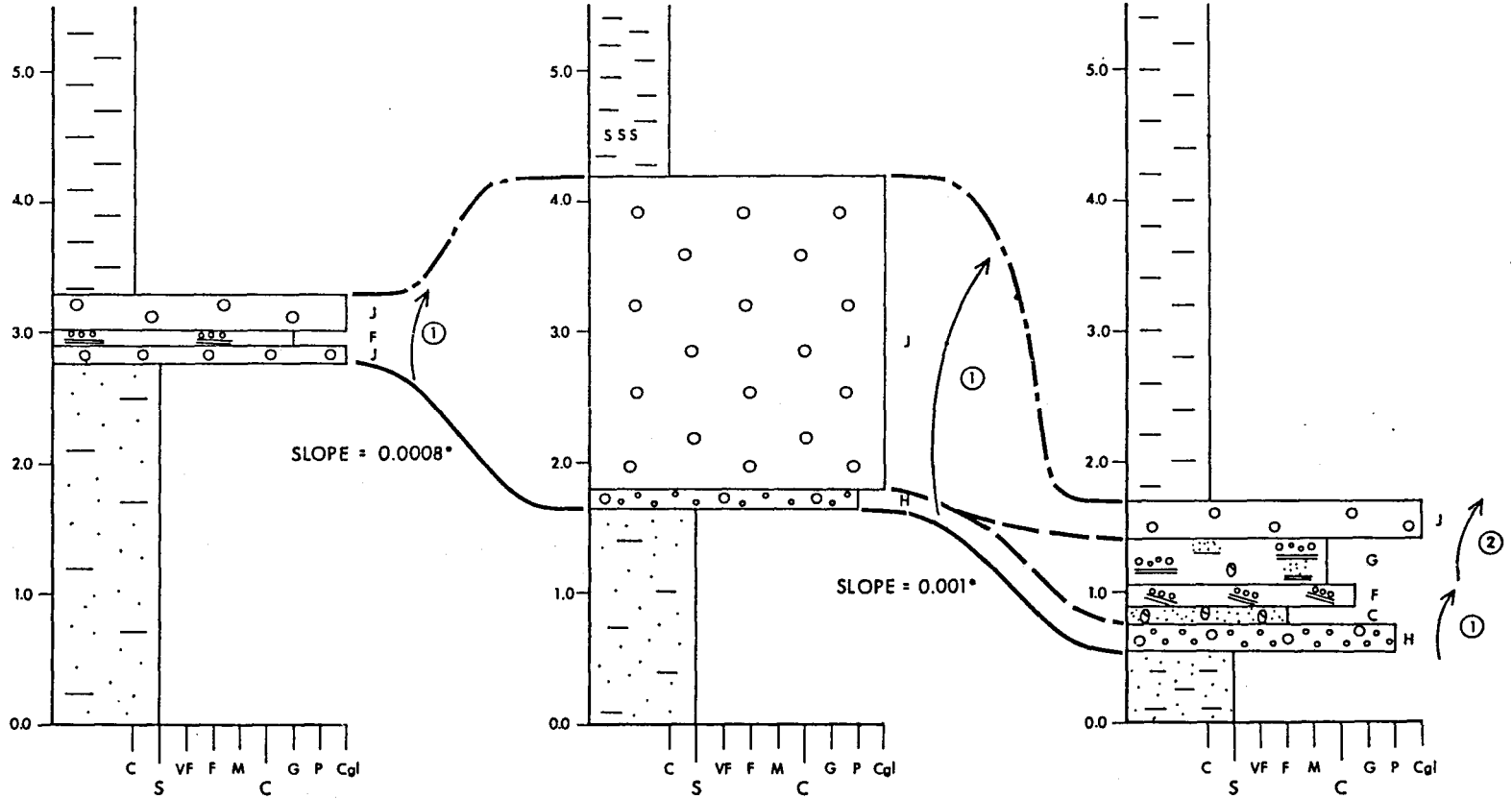
SW  
4

NE

4-8-41-3 W5  
6284' - 6302'

12-8-41-3 W5  
6292' - 6310'

2-17-41-3 W5  
6300' - 6318'



coarsening-upward sequence in wells 4-20 and 16-19 (both in cross-section 3.37). Facies J abruptly overlies Facies G and caps the middle coarsening-upward sequence.

#### Gilby A-3 - Markov Chain Analysis

Markov Chain analysis resulted in two facies sequences (Fig. 3.40). See appendix 1 (p.215) for the observed and expected frequency tables and the calculated probabilities used in determining the preferred facies sequences. In one sequence Facies A is overlain by Facies B. In the A-3 and A-1 area of Gilby A, Facies B was observed to occur only along the southwest margin. See Chapter 5 for further discussion on the distribution of Facies B over the study area. The other facies sequence consists of Facies J overlain by Facies K.

#### Summary Gilby A-3:

Within the center of Gilby A-3 the Viking coarse sediment package consists entirely of conglomerates (Facies J) within a single coarsening-upward sequence. The conglomerates thin and the sequence separates into two coarsening-upward sequences in a radial pattern away from the center of A-3. These coarsening-up sequences consist of thin conglomerates and thin sandstone units.

Also observed in the A-3 area is the consistent stratigraphic drop to the northeast, of the lower surface of the coarse sediment package (again with respect to a

Fig. 3.40. Facies relationship diagram determined from Markov analysis for the Gilby A-3 area. Refer to Figure 3.38 caption (p.92) for the explanation of labels used. Note that there are only two facies transitions determined for the Gilby A-3 area which can be referred to as non-random or having cyclicity. Sideritized muddy siltstones (Facies B) overlie the homogeneous muddy siltstones and black mudstones (Facies K) overlie conglomerates (Facies J) with the former transition representing the more non-random transition since it has the smaller probability (0.00016). See text for discussion.

# GILBY A-3 MARKOV CHAIN ANALYSIS

$$A \xrightarrow{0.00016} B$$

$$J \xrightarrow{0.50816} K$$

horizontal upper datum (marker A).

3.4.5 Gilby A-2 - Facies Sequence (Cross-Section 3, Figure, 3.41)

The facies sequence within Gilby A-2 is best described as transitional since it includes portions of the general sequence from both Gilby A-1 and A-3. The core in cross-section 3 (see Fig. 3.41) are representative of the general facies sequence observed in A-2.

Within 2-5 two coarsening-up sequences within the coarse sediment occur. The first and lowermost coarsening-up sequence begins with Facies D which has numerous chert pebbles scattered within 10 cm of the base. This facies is overlain by Facies G separated gradationally from the lower facies (D) by a thin unit of Facies H. Facies F abruptly overlies Facies G. Facies F gradationally coarsens upward in to Facies H which caps the lowermost coarsening-upward sequence.

This lowermost coarsening-upward sequence in 2-5 (cross-section 3) is very similar to the second and third coarsening-upward sequences in both 4-20 and 16-19 (cross-section 2).

The second coarsening-upward sequence in well 2-5 (cross-section 3) begins abruptly with Facies D. Abruptly overlying this unit and capping the second coarsening-up sequence is Facies J.

The second coarsening-up sequence in 2-5 (cross-section

Fig. 3.41. Litholog cross-section 3 from cored wells 2-5-41-2W5, 6-5-41-5W5 and 6-8-41-2W5 located on Fig. 3.35. See Fig. 3.36 (p.83) for full description of labels. See text for discussion.

SW  
3

NE

2 - 5 - 41 - 2 W5

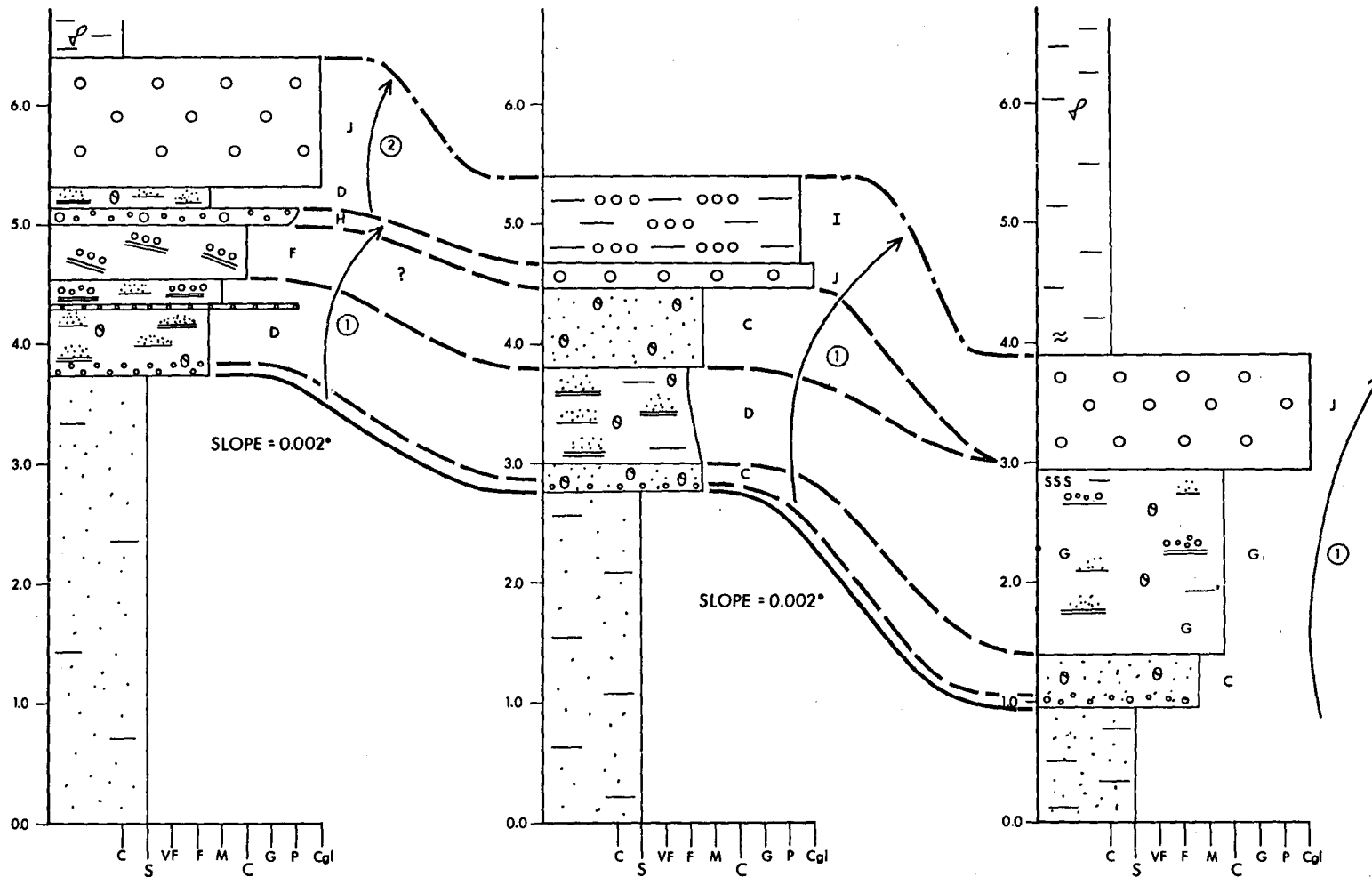
5934' - 5956'

6 - 5 - 41 - 2 W5

5946' - 5964'

6 - 8 - 41 - 2 W5

5921' - 5943'



3) is very similar to the third coarsening-upward sequence in 4-20 (cross-section 2). Important differences between these sequences in 2-5 and 4-20 include the change in facies thickness. Burrowed-laminated mudstone-sandstone (Facies D) in well 2-5 is five times thinner than the similar facies, the laminated mudstone-pebbly sandstone (Facies G) in 4-20. The conglomerate (Facies J) within the second coarsening-upward sequence in well 2-5 is approximately three times as thick as the conglomerate within the third coarsening-upward sequence in 4-20. In 12-8 (cross-section 4, Fig. 3.39) the single coarsening-upward sequence is similar to the second coarsening-upward sequence in 2-5 (cross-section 3). The main difference between 12-8 and 2-5 is the increased conglomerate thickness and the absence of sandstone facies in 12-8.

Well 6-5 in the central portion of cross-section 3 has a single coarsening-upward sequence. This sequence is generally similar to the coarse sediment package in 2-5 (cross-section 3). Both wells begin with Facies D, where chert pebbles are scattered near the coarse sediment base and are capped by Facies J.

Well 6-8 in cross-section 3 has a single coarsening-upward sequence which is very similar to that of well 6-5 (cross-section 3). The sequence in 6-8 begins with Facies C with a few scattered chert pebbles within the first few cm. Above here, facies contacts into G and J are abrupt. Facies J caps the single coarsening-upward sequence.

### Gilby A-2 - Markov Chain Analysis

Markov Chain analysis for the A-2 area was not possible because too few cored wells were available. (App. 1, p.214).

#### Summary A-2 area:

The generalized facies sequence found in the A-2 area is represented by a single coarsening-upward sequence. This sequence begins abruptly with a thin unit of bioturbated muddy sandstone (Facies C). Scattered chert pebbles are found within the lower few cm of this unit. The bioturbated muddy sandstone (Facies C) is abruptly overlain by either the burrowed-laminated mudstone-sandstone (Facies D) or the laminated mudstone-pebbly sandstone (Facies G). These laminated Facies (D and G) are abruptly overlain by conglomerate (Facies J). Pebbly cross-bedded sandstones (Facies F) and bioturbated muddy sandstone (Facies C) may occur between the conglomerate and laminated facies.

Major differences in facies sequence between area A-1 and A-2 include the fact that fewer sandstone facies (Facies E, F, and H) but thicker accumulations of conglomerate (Facies J) are found in A-2. Differences in facies sequence between area A-2 and A-3 include an increase in conglomerate thickness and both the thinning and disappearance of sandstones (Facies C, E and F) and interbedded mudstones (Facies D and G) in A-3.

Also observed within the field boundaries is the consistent stratigraphic drop of the lower surface of the

coarse sediment package with respect to a horizontal marker A. This lower surface begins to drop stratigraphically at the southwest margin of the A-2 area. The coarse sediment package is generally thickest where its lower surface is stratigraphically lowest.

#### 3.4.6 Gilby B-1 - Facies Sequence (Cross-Section 5, Figure 3.42)

The Gilby B field, designated area B-1 on Figure 1, has a similar facies sequence to the Gilby A-3 area. Within the Viking coarse sediment package in B-1, one or two coarsening-up sequences occur. The coarse sediment package is generally thickest in the central part of the B-1 area. Core cross-section 5 (Fig. 3.42) is representative of the vertical and lateral facies sequences observed in the B-1 area.

Well 16-18 occurs furthest southwest in cross-section 5, situated approximately 2 mi (3.2 km) outside the Gilby B field boundaries (as designated by the ERCB). Within 16-18 the coarse sediment package consists of a thin unit of Facies I.

The first on-field well, 10-32, is located approximately 2.75 mi (4.4 km) to the northeast of 16-18. It contains one coarsening-upward sequence which is markedly thicker than that encountered in 16-18. The sequence begins abruptly with Facies B. Above here, facies contacts into Facies C, D and J are abrupt. Facies J caps the single

Fig. 3.42. Litholog cross-section 5 from cored wells 16-18-41-4W5, 10-32-41-4W5, 4-4-42-4W5, 10-4-42-4W5 and 16-9-42-4W5 located on Fig. 3.35. See Fig. 3.36 caption (p.83) for description of labels. See text for discussion.

SW

NE

16 - 18 - 41 - 4 W5

6578' - 6596'

10 - 32 - 41 - 4 W5

6428' - 6451'

4 - 4 - 42 - 4 W5

6397' - 6415'

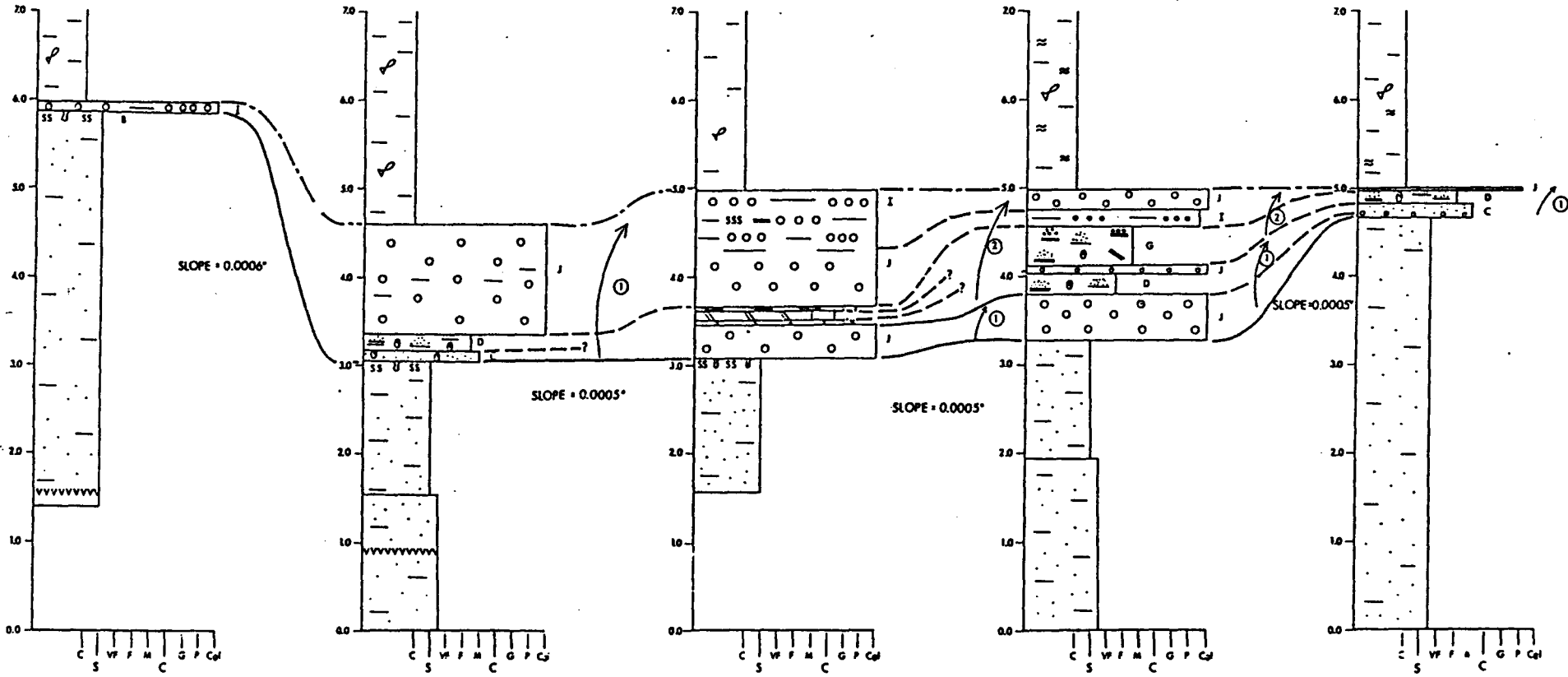
10 - 4 - 42 - 4 W5

6354' - 6377'

16 - 9 - 42 - 4 W5

6284' - 6307'

5



coarsening-upward sequence.

The sequence at 10-32 (cross-section 5, Figure 3.42) is similar to the sequence at 12-8 (cross-section 4, Figure 3.39). Differences between 10-32 and 12-8 include the absence of Facies C and D and a two-fold increase in conglomerate thickness in 12-8. The sequence at 10-32 is also similar to the sequence in 6-8 (cross-section 3, Figure 3.41). The difference here is the occurrence of thicker sandstone units (Facies C and D) in 6-8. The two adjacent wells, 4-4 and 10-4 in cross-section 5 (Figure 3.42), have 2 coarsening-up sequences. Within these wells the coarsening-up sequences begin with a very similar thickness of Facies J. Facies B occurs below Facies J in 4-4. Facies J caps the first coarsening-up sequence in both 4-4 and 10-4.

The second coarsening-upward sequence in 4-4 begins with Facies E which is gradationally overlain by a thin unit of Facies F. The second coarsening-up sequence in 10-4 is different from 4-4 in that the base begins with Facies D in 4-4 and Facies E in 10-4. Facies J caps the coarsening-up sequence abruptly in both 4-4 and 10-4. Well 2-17 (cross-section 4, Fig. 3.39) has a similar coarse sediment sequence to that in 4-4 and 10-4. Coarsening-up sequences in 4-4, 10-4 and 2-17 begin with and are capped by conglomerates (Facies J and H). Internally, the sequences include Facies G in both 10-4 (cross-section 5, Fig. 3.42) and 2-17 (cross-section 4) and Facies E in 4-4 (cross-section 5) and 2-17.

Well 16-9, located furthest northeast in cross-section 5, has a single coarsening-up sequence. This single sequence begins with Facies C. Facies D abruptly overlies Facies C. A thin band of pebbles cap the sequence abruptly. The single coarsening-up sequence in 16-9 is generally similar to that in 16-18 (cross-section 5), but the former includes thin sandstone units (Facies C and D).

#### Gilby B-1 - Markov Chain Analysis

Markov Chain analysis suggests only one facies sequence (Fig. 3.43). See appendix 1 (p.216) for the observed and expected frequency tables and the calculated probabilities used in determining the preferred facies sequence. The transition of Facies A overlain by Facies B is the only transition which occurs as a non-random sequence in the Gilby B-1 area.

#### Summary Gilby B-1:

The facies sequence in Gilby B-1, interpreted from core, consists of two types of coarsening-upward sequences. However, around the margins of Gilby B a single coarsening-upward sequence is likely to occur (for example 16-9). Two coarsening-upward sequences are more likely to occur in the central area of Gilby B (for example 4-4).

The single coarsening-upward sequence or lower of the two individual coarsening-up sequences begins with Facies B only along the southwest margin of the B-1 area (Facies B is

Fig. 3.43. Facies relationship diagram determined from Markov analysis for the Gilby B-1 area. Refer to Figure 3.38 caption (p.92) for a description of the labels used. For the Gilby B-1 area there is a single facies transition (Facies A overlain by Facies B) which represents a non-random sequence. See text for discussion.

# GILBY B-1 MARKOV CHAIN ANALYSIS

$$A \xrightarrow{0.08762} B$$

eroded to the northeast) and is capped abruptly with Facies J. The second coarsening-up sequence begins abruptly with Facies C or D and Facies J caps the sequence.

Important facies sequence similarities between B-1 and A-3 include thick conglomerate (Facies J) accumulations and thin to absent sandstone (Facies C, E and F) accumulations in both. Differences between B-1 and A-3 include the fact that two coarsening-upward sequences occur in the region of B-1 where as only a single coarsening-up sequence occurs in A-3.

Also observed is the consistent stratigraphic drop of the lower surface of the coarse sediment package with respect to a horizontal upper datum (marker A). This surface begins to drop stratigraphically toward the northeast along the southwest margin of the field. It differs from the same surface in Gilby A in that it rises stratigraphically between 10-4 and 16-9 in Gilby B. The coarse sediment package is thicker in the central area of B-1, coinciding with the stratigraphic drop of this lower surface. Facies B is absent to the north of 4-4, which is approximately the central area of B-1.

### 3.5 Summary

1. Core examination allowed sub-division into 11 facies; 2 of which are predominantly mudstone (Facies A and K), 2 fine to medium grained sandstone facies (Facies C and E), 2 laminated-burrowed mudstone-sandstone facies (Facies D and G), 2 pebbly sandstone facies (Facies F and H), 2 conglomeratic facies (Facies I and J) and 1 facies which represents an erosional or scoured surface (Facies B).

2. Trough cross-bedding is the dominant sedimentary structure preserved in the the sandy facies (Facies E). Low angle trough cross-bedding is observed in the pebbly sandstone facies (Facies F). The conglomeratic facies lack stratification.

3. Lateral variation of the facies sequence occur over the Gilby A and B area. The Gilby A field may be delineated into 3 specific areas (A-1, A-2, A-3) and the Gilby B field as 1 specific area (B-1). The Gilby A-1 area is composed predominantly of thick sandstones while the Gilby A-3 area is predominantly thick conglomerates. The central portion of Gilby A (A-2), where the field changes trend from northwest-southeast to east-west, is transitional having thin sandstones and conglomerates. The Gilby B-1 area closely resembles the northwestern portion of Gilby A-3 but has thinner conglomerates.

4. Vertical variation in facies sequence of the coarse sediment package is observed across the width of the Gilby A and B fields. The coarse sediment package consists of 1 to 3 individual coarsening-upward sequences. The southwestern margin of the Gilby A or B field generally contains only 1 coarsening-upward sequence, the central area of the field contains 2 to 3 individual coarsening-upward sequences and the northeastern margin contains normally 1 or 2 individual coarsening-upward sequences. The two exceptions are the Gilby A-3 area which has 2 coarsening-upward sequences along the southwest margin and only 1 coarsening-upward sequence in the central area and the Gilby A-2 area which has 1 coarsening-upward sequence in the central area.

5. The absence of Facies B - the sideritized muddy siltstone (with Skolithos) (termed a "firmground") - was observed in core where the coarse sediment package thickens, approximately in the central portion of the fields. The lower surface of the coarse sediment package (this surface is coincident with Facies B) trending southeast-northwest, drops stratigraphically to the northeast beginning approximately at the southwest field margin. This surface is stratigraphically lowest in areas where the coarse sediment package is thickest (see Chapter 5 for further discussion).

## Chapter 4: PETROGRAPHY

### 4.1 Method

Ten thin-sections were prepared from samples of Facies C, E and H from five on-field cored wells. To determine the sandstone composition point counts of 300 per section were performed. The constant distance between each point was generally larger than the largest grain size found in any particular thin section; employing this method point counts could not be performed on Facies J (conglomerate) because of the abundance of large pebbles. All sections were impregnated with blue epoxy to help estimate the percentage of porosity.

About half of the thin sections prepared were stained for potassium feldspar since the lack of feldspar twinning and cleavage make it difficult to distinguish feldspars from quartz. A sodium cobaltinitrite solution was used to stain half of the thin section as suggested by Whitlatch and Johnson (1974).

Investigations employing cathodoluminescence were performed on a number of thin sections. This analysis reveals textures in minerals and rocks which cannot be recognized in transmitted light of a petrographic microscope (Nickel, 1978). In particular, secondary quartz overgrowths are easily distinguished using this procedure.

Cathodoluminescence, as discussed by Kopp (1981), is performed by bombarding a crystallized material with electrons. This induces an emission of visible light or luminescence from the crystallized material. The particular luminescence which results is dependent upon the transition elements present in the sample (Nickel, 1978). A thorough discussion of cathodoluminescence is given by Kopp (1981), Nickel (1978) and Zinkenagel (1978).

Samples were photographed for textural and mineralogical relationships using a standard petrographic microscope and a scanning electron microscope (SEM). Long exposure-time photography was used for the cathodoluminescence analysis. Figures 4.3 to 4.14 are thin section microphotographs; in each figure the upper microphotograph was taken in plane-polarized light and the lower microphotograph (of the same field) was taken with cross-polarized light or under cathodoluminescence (specified in figure captions). In all figures the magnification is specified in the figure captions.

## 4.2 Results

The dominant detrital components of the sandstones are quartz, chert and rock fragments with minor amounts of glauconite and opaques. The percentage of porosity estimated from the blue epoxy is not a true indication of

total percent porosity in the sample. Much of the porosity present is microporosity and to get a more accurate indication of the total porosity employing impregnation, this technique would have to have been performed under higher pressures than was possible at McMaster University. Study of impregnated sections suggests authigenic clays and quartz overgrowths to be responsible for the destruction of most primary porosity.

Seven of the thin sections were point counted (modal percentages are given in Figure 4.1) and were classified as sublitharenites, with two sections plotting within the litharenite field. McBride's (1963 in Blatt, Middleton and Murray, 1972; p.311) sandstone classification was used (see Figure 4.2). The samples were found to be generally more mature and better sorted in the sandstones (Facies E) than in the bioturbated muddy sandstones (Facies C) and the massive pebbly sandstones (Facies H).

#### 4.2.1 Constituents

##### Quartz

Quartz occurs as both detrital and authigenic grains. The quartz observed was dominantly monocrystalline with undulatory extinction (greater than 5 degrees rotation). Less frequently observed were polycrystalline quartz grains. Quartz grains are fair to well sorted with the best sorting occurring in the cross-bedded sandstones (Facies E).

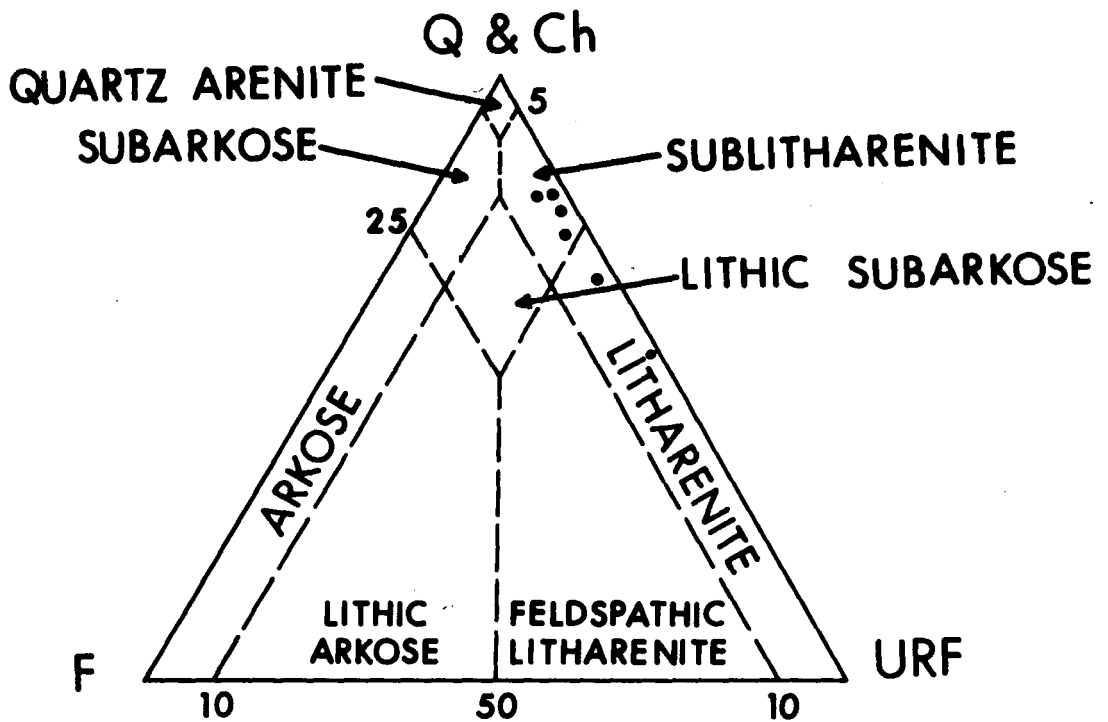
In reflecting light (plane-polarization) the quartz

Fig. 4.1 Modal percentages of constituents from point counting of seven thin sections. Point counts (300) were performed on each of the sections. Listed with the well location for each of the seven sections are the respective depth of the sample and facies as defined in Chapter 3.

CORE LOCATION (DEPTH', FACIES)	QUARTZ	ROCK FRAGMENTS	CHERT	GLAUCONITE	FELDSPAR	CLAY	POROSITY
4-12-40-1W5 (5483', Facies H)	28	43	25	01	01	01	01
12-16-40-1W5 (5638', Facies H)	32	13	44	01	02	02	06
12-16-40-1W5 (5639', Facies E)	25	16	54	01	02	00	02
12-16-40-1W5 (5643', Facies E)	56	19	14	07	02	01	01
12-16-40-1W5 (5647', Facies C)	49	11	32	04	02	00	02
6-5-41-2W5 (5945', Facies C)	41	24	32	01	02	00	00
6-5-41-2W5 (5959', Facies C)	23	33	38	02	01	01	02

Fig. 4.2 Diagram of a sandstone classification by McBride (1963, in Blatt, Middleton and Murray, 1972; p.311) showing the plot of the seven thin sections listed in Figure 4.1. Note that five of the thin sections plot within the sublitharenite field while two of the thin sections plot within the litharenite field.

# SANDSTONE CLASSIFICATION

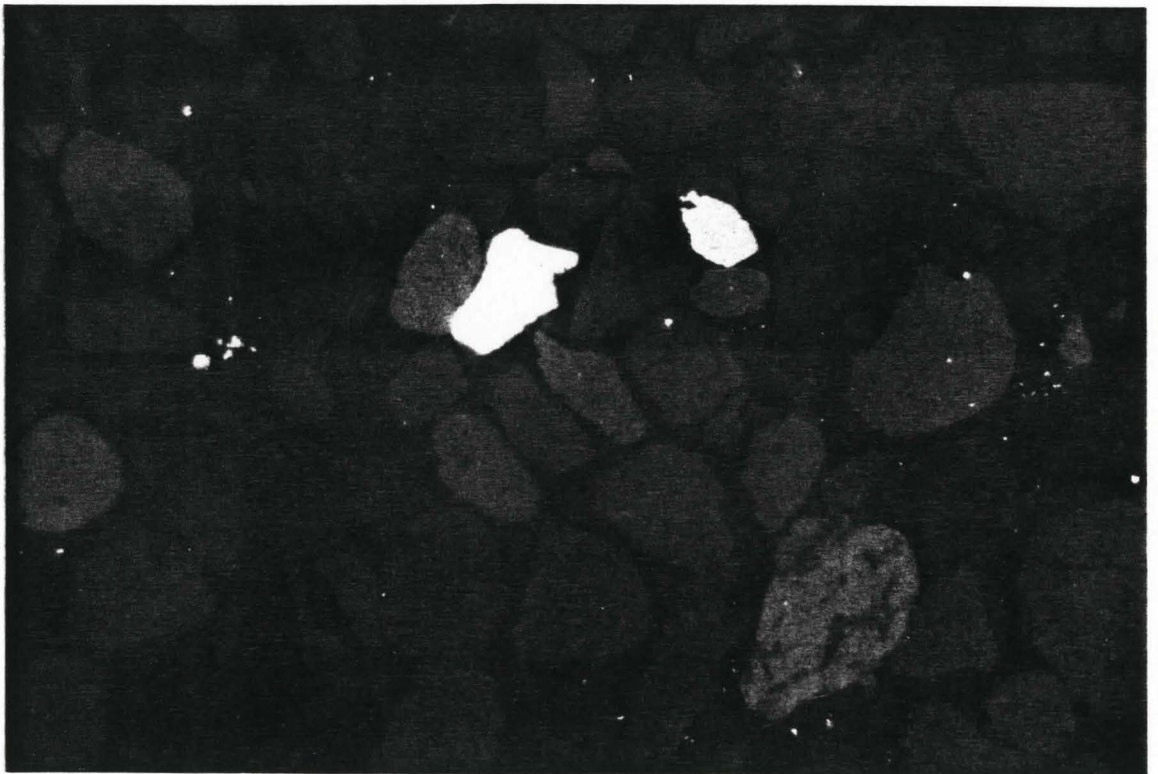
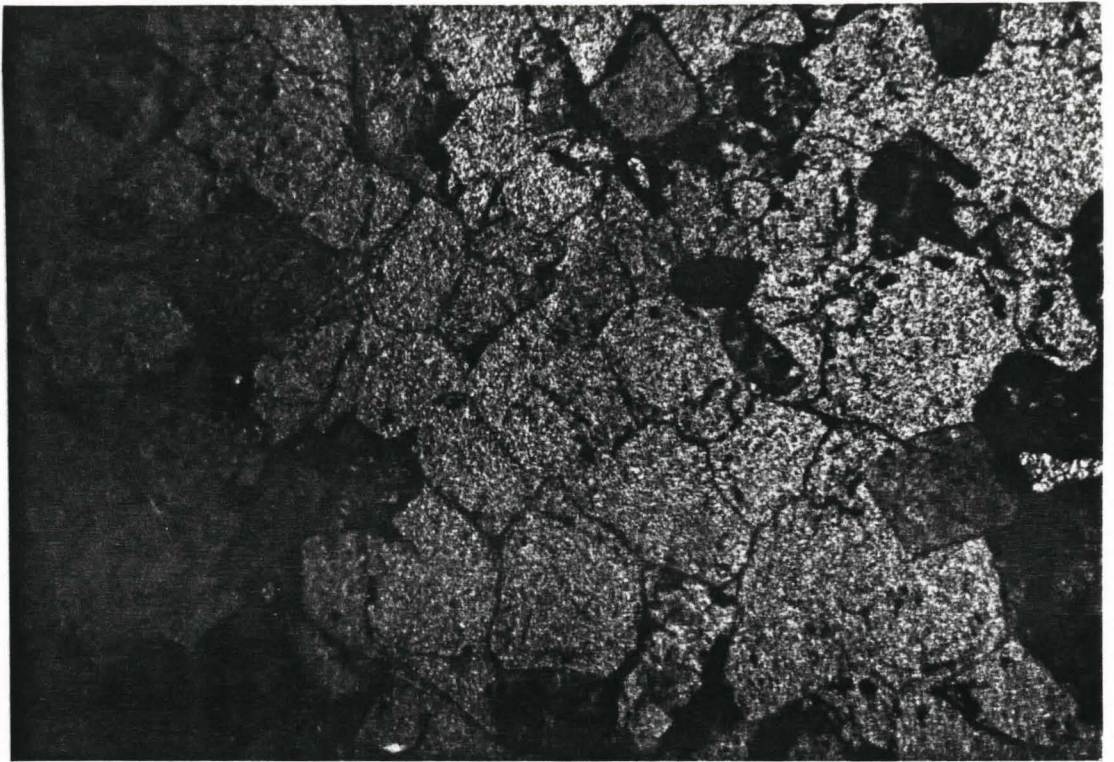


(AFTER McBRIDE, 1963)

- Q & Ch : QUARTZ PLUS CHERT
- URF : UNSTABLE ROCK FRAGMENTS
- F : FELDSPARS

Fig. 4.3. Photomicrograph of Facies E under plane-polarized light. Monocrystalline quartz is the dominant framework grain in this cross-bedded sandstone and is recognized by its low birefringence, low positive relief and lack of cleavage and twinning. The subangular quartz grains have elongate, sutured boundaries. A thin layer of inclusions can be seen just inside of the quartz boundaries in some grains. Magnification is 28X, 12-16-40-1W5, 5643 ft (1720.0 m).

Fig. 4.4. Cathodoluminescent photomicrograph of Figure 4.3. The luminescent dull blue and brown subrounded grains are detrital quartz. The non-luminescent overgrowths have infilled original pore space. The two white bright subrounded grains in the center of the photo were a more bright green color when viewed in the lab and are suggested to be feldspars. Magnification is 28X, 12-16-40-1W5, 5643 ft (1720.0 m).



grains appear subangular, with elongate, sutured boundaries (see Figure 4.3). These sutured boundaries may result from compaction. In a few grains, close inspection reveals thin layers of inclusions around the grain edge. These inclusions could represent an authigenic overgrowth or volcanic quartz zonation (Scholle, 1979; p.4). Using cathodoluminescence the same field of view is observed to contain detrital quartz grains (luminesce dull blue and brown) which are sub-rounded, touching each other only at point contacts (see Figure 4.4). The quartz overgrowths are generally non-luminescent and appear to have grown into and infilled original pore space. Quartz overgrowths are quite abundant and are found in all sections.

### Chert

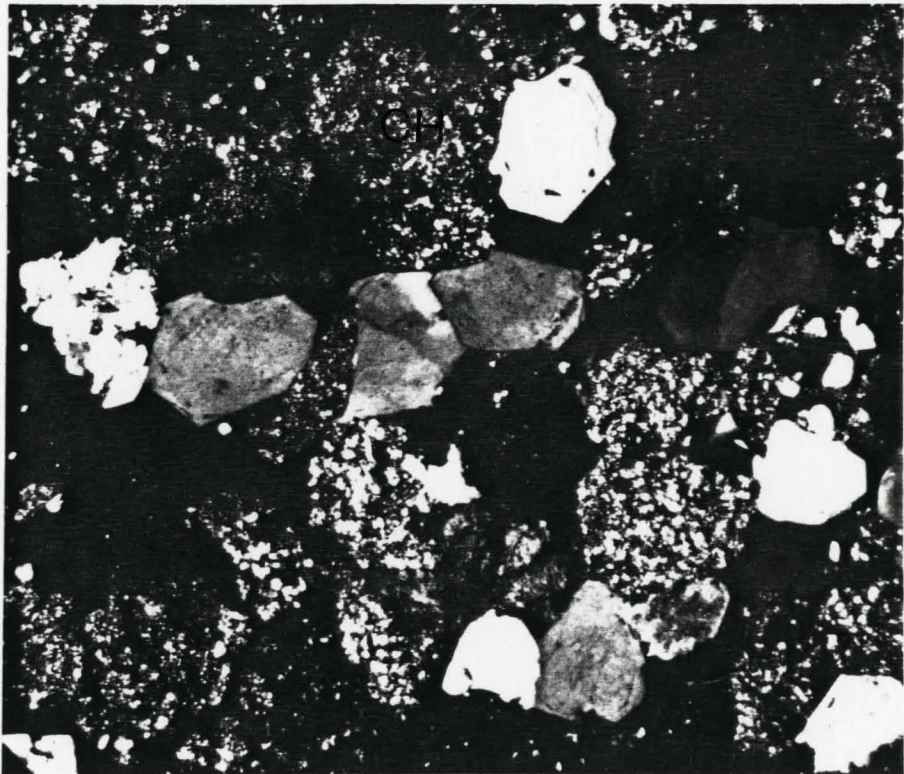
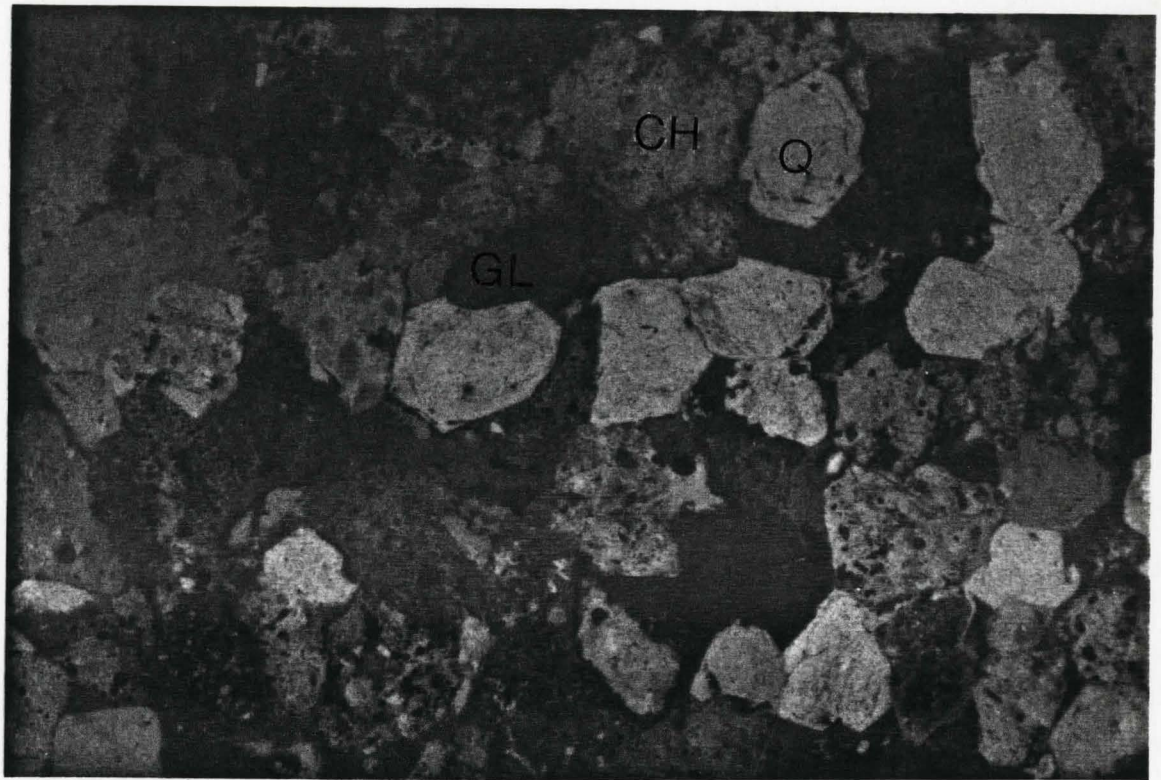
Chert is common and relatively abundant in all thin sections. The detrital chert fragments observed contain uniform microcrystalline to megaquartz crystals. The chert appears as sub-rounded grains and is best identified by its sucrosic texture under cross-polarized light (see Figure 4.6). Zebraic chalcedony (see Figure 4.12) with radiating crystal habit was infrequently observed. Chert is non-luminescent.

### Rock Fragments

Rock Fragments are common and relatively abundant in all slides. They are generally sub-rounded to sub-angular.

Fig. 4.5. Photomicrograph under plane-polarized light of cross-bedded sandstone (Facies E). The subrounded chert fragments (CH) have a darker appearance and contain many more inclusions than quartz (Q) under plane-polarized light. The darker brown, pellet shaped and subangular grains are glauconite (GL). Magnification is 25X, field of view is 4.5 mm by 2.5 mm, 12-16-40-1W5, 5639 ft (1718.8 m).

Fig. 4.6. Photomicrograph under cross-polarized light of the central field of view in Figure 4.5. Detrital chert fragments (CH) appear as speckled grains composed of microcrystalline quartz. Glauconite (GL) has a yellowish birefringence. Magnification is 25X, field of view is 4.5 mm by 2.5 mm, 12-16-40-1W5, 5639 ft (1718.8 m).



The two types frequently observed were plutonic and sedimentary rock fragments. Rarely observed were volcanic rock fragments consisting of tiny lath-like feldspars. All rock fragments observed are generally non-luminescent but sedimentary and particularly plutonic rock fragments contain bright luminescent inclusions of quartz (luminesce dull brown and blue), feldspars (luminesce bright lime green) and carbonates (luminesce bright orange) (see Figure 4.7 and 4.8).

### Feldspars

Feldspars were infrequently observed in the sections. They were best identified under cathodoluminescence as luminescent bright lime-green, sub-angular grains and had a maximum modal percentage of 2-3% per slide (see Figure 4.4 and 4.10). No twinning or cleavage of the feldspars was observed under reflecting light. Staining (staining methods discussed above) indicated that the feldspars observed are potassic. Figure 4.11 contains small, rounded, bright orange stained potassium feldspar fragments. The general absence of feldspars in all thin sections is due to the maturity of the sandstones.

### Glauconite

Glauconite was observed in a few sections as dark green, elongate rounded grains in plane-polarized light (see Figure 4.9). Other glauconite grains (see Figure 4.5)

Fig. 4.7. Photomicrograph under plane polarized light of cross-bedded sandstone (Facies E). The central angular rock fragment is a shale clast (SH) having inclusions (perhaps fine clay particles) and original horizontal banding. The orange-coloured rounded grains are collophane (CO). The dominant components are quartz grains and rock fragments which are composed of dark inclusions. Magnification is 28X, 12-16-40-1W5, 5643 ft (1720.0 m).

Fig. 4.8. Cathodoluminescent photomicrograph of Figure 4.7. Quartz is a luminescent dull brown and blue colour while the rock fragments contain many smaller luminescent quartz and other non-luminescent grains. The collophane (CO) contain small bright red and yellow inclusions within a non-luminescent background. Magnification is 28X, 12-16-40-1W5, 5643 ft (1720.0 m).

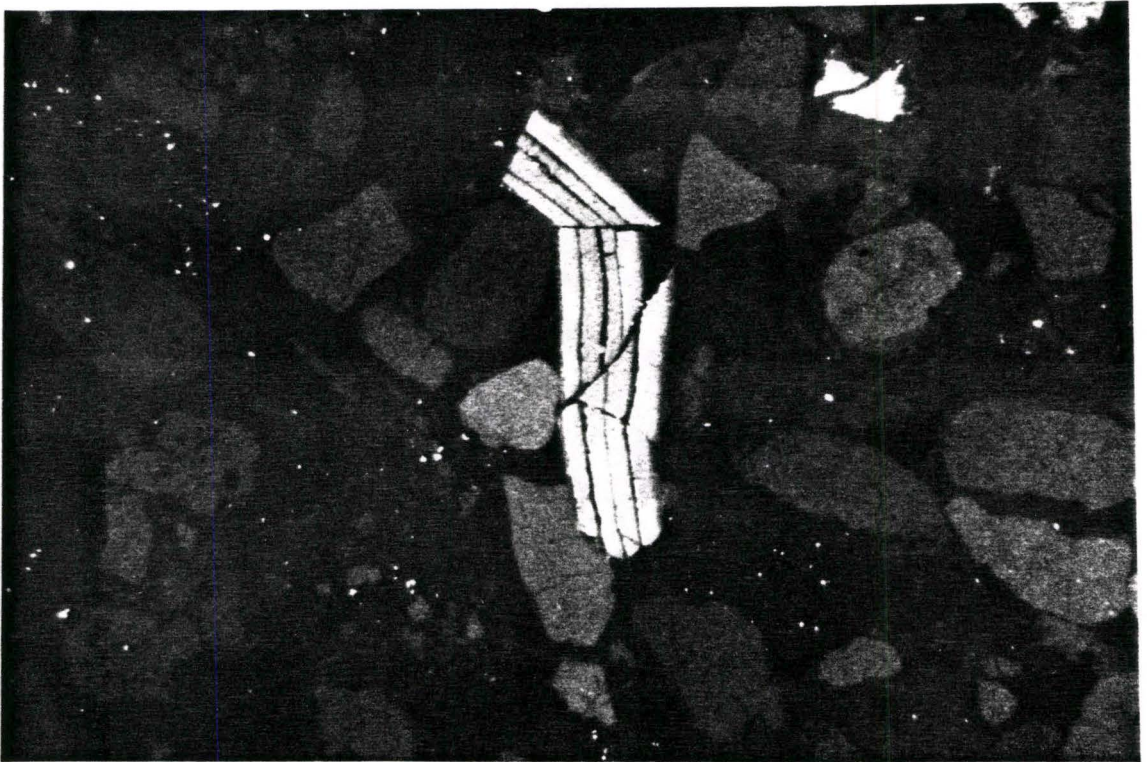
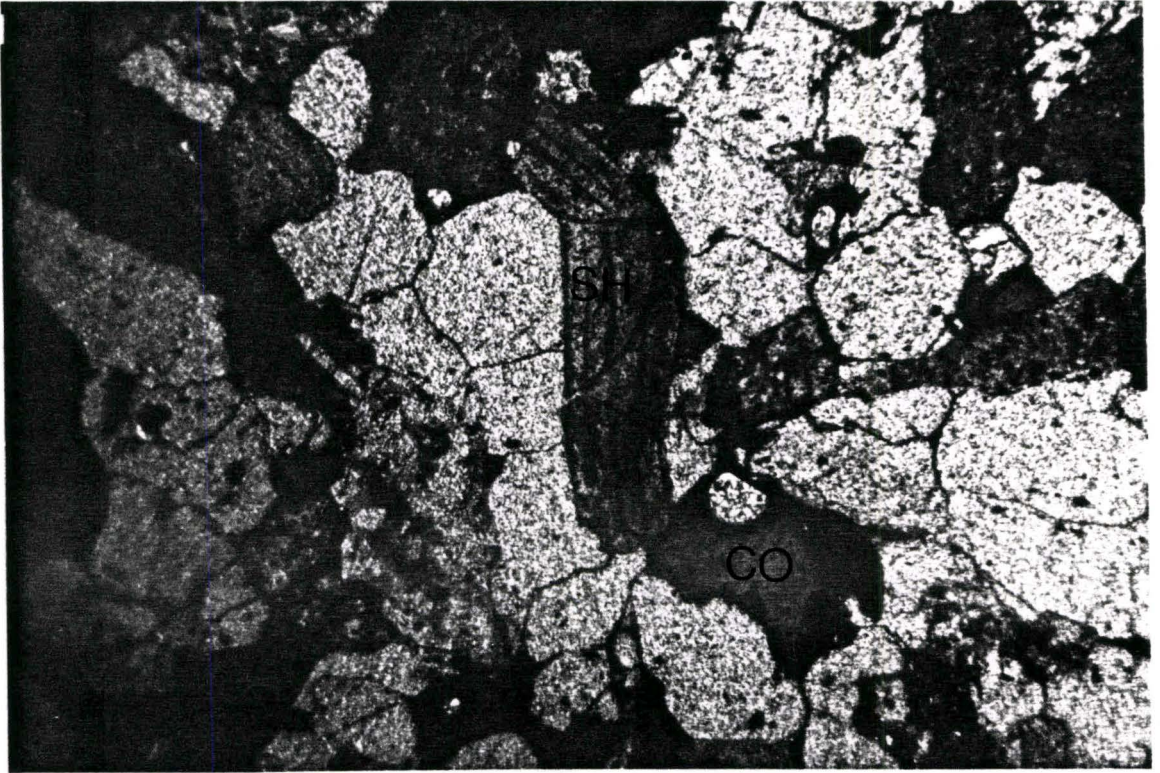


Fig. 4.9. Photomicrograph under plane-polarized light of a pervasively bioturbated muddy sandstone (Facies C). Quartz and rock fragments are dominant and appear smaller in size than those observed in Figure 4.4 and 4.8. Note the fine black material filling the pore spaces. The elongate slightly greenish grains are glauconite (GL). Magnification is 28X, 12-16-40-1W5, 5646.5 ft (1721.1 m).

Fig. 4.10. Cathodoluminescent photomicrograph of Figure 4.9. Note the lack of authigenic quartz overgrowths (non-luminescent) around the detrital quartz. The rock fragments are non-luminescent and contain red and orange luminescent inclusions. The glauconite (GL) is non-luminescent. The subrounded luminescent bright greenish-blue grains are feldspars (F). Magnification is 28X, 12-16-40-1W5, 5646.5 ft (1721.1 m).

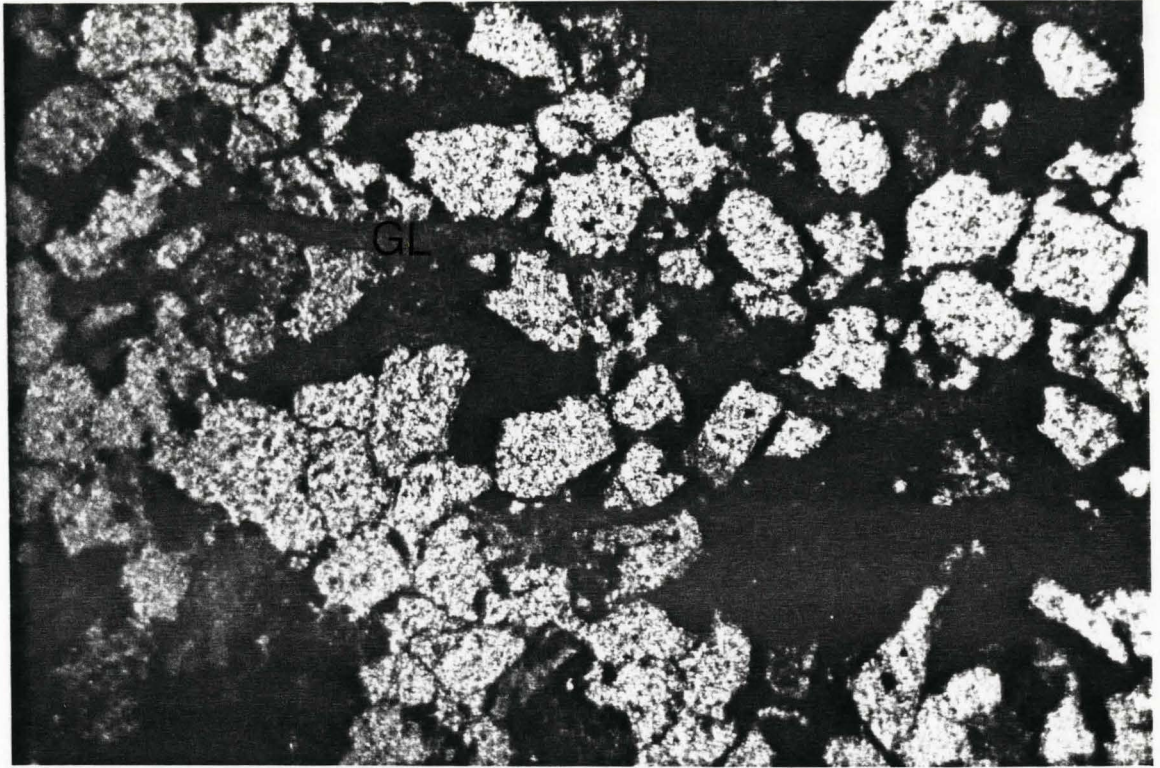


Fig. 4.11. Photomicrograph under plane-polarized light of a massive pebbly sandstone (Facies H). Note the poorly sorted detrital quartz (Q), chert (CH) and rock fragments (RF). The pore space between these detrital grains is filled with authigenic quartz and perhaps some clay. Note the sucrosic texture of these authigenic grains. The small bright orange grains are stained potassium feldspar fragments (F). The dark green staining is the blue epoxy filling pore space (E). Magnification is 28X, 4-12-40-1W5, 5483 ft (1671.2 m).

Fig. 4.12. Photomicrograph under cross-polarized light of Figure 4.11. Note the low birefringent quartz (Q) and the zebraic chalcedony (ZC) with radiating crystal habit. Magnification is 28X, 4-12-40-1W5, 5483 ft (1671.2 m).



photographed in the same section have a brownish-orange color (observed in the lab as a darkish-green color) with a rounded pellet shape. These glauconite grains may have originally been fecal pellets and are an indication of a marine depositional setting (Scholle, 1979; p.39).

### Accessory Minerals

Accessory minerals found include iron-oxides (opaques), possibly some micas, collophane (see Figure 4.7) and framboidal pyrite (viewed under the SEM). Collophane is a cryptocrystalline phosphatic material related to apatite and is a major constituent in fossil bones (Scholle, 1979). Framboids are small clusters of spherical pyrite grains which are commonly found as an authigenic replacement in sedimentary rocks (Scholle, 1979).

### Cements

The two cements observed in thin section are authigenic clay and authigenic quartz, occurring most frequently in Facies C and H. Clay cements were best recognized under cathodoluminescence where they luminesce a bright blue colour (see Figure 4.8 and 4.14). Figure 4.16 includes 2 scanning electron microphotographs under successively higher magnifications illustrating authigenic kaolinite "booklets" (c.f. Scholle, 1979; p.70) infilling pore space. Kaolinite was the only clay identified in the petrography study. Clay cements constitute less than 5% by modal analysis of a

number of thin sections (see Figure 4.1).

Authigenic quartz was also important as a cement. It commonly occurred as individual crystals infilling pore space. Figure 4.15 are two scanning electron microphotographs of euhedral shaped authigenic quartz grains with smooth crystal faces infilling pore space. The well developed crystalline habit of the quartz and clay observed in the SEM photos suggest they are probably authigenic and not detrital.

Fig. 4.13. Photomicrograph under plane-polarized light of a massive pebbly sandstone (Facies H). Note the subangular quartz and rock fragments. The dark green staining is blue epoxy filling the pore spaces. Magnification is 28X, 4-9-41-3W5, 6310 ft (1923.2 m).

Fig. 4.14. Cathodoluminescent photomicrograph of Figure 4.13. Note the rounded detrital quartz luminescing a dull blue and brown. The authigenic quartz overgrowths are non-luminescent. The rock fragment (RF) in the lower right of the field of view contains other luminescent grains. The bright dark blue pore filling may be kaolinite (KO). Magnification is 28X, 4-9-41-3W5, 6310 ft (1923.2 m).

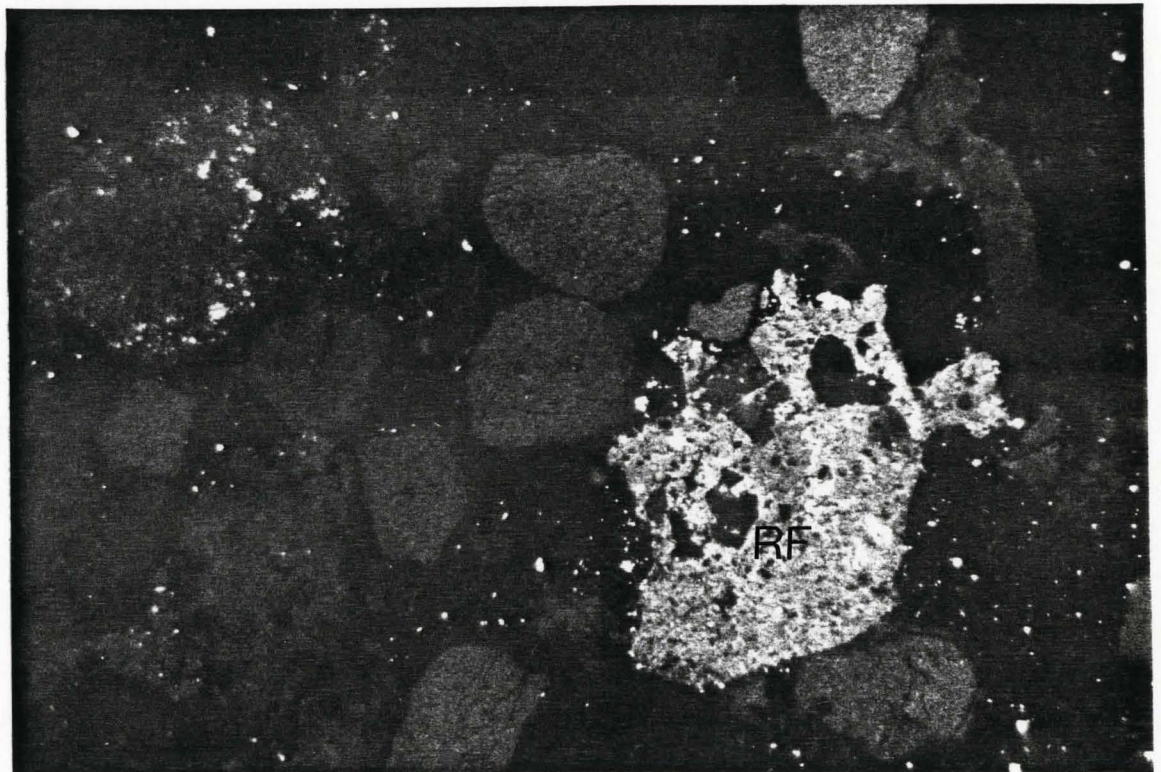
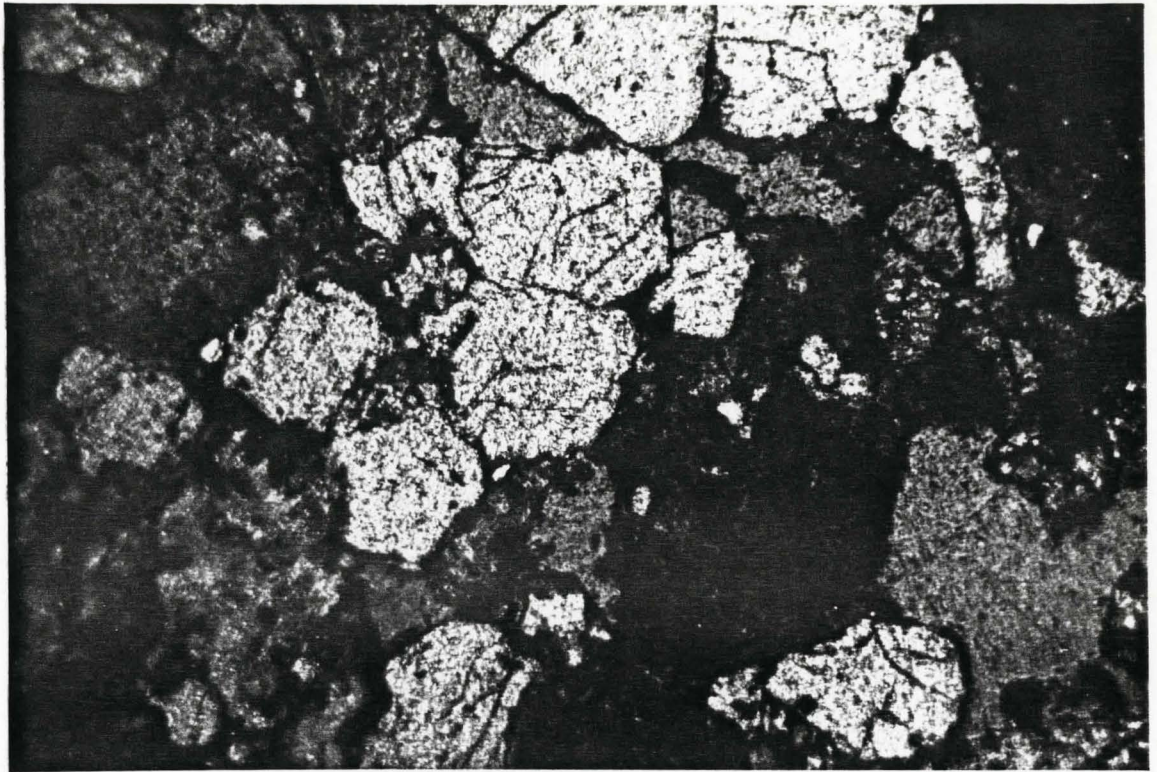


Fig. 4.15a and b. Scanning electron photomicrograph of a massive pebbly sandstone (Facies H). Note the authigenic quartz (Q) having well developed crystal faces and infilling pore space. The scale bar (micron) and magnification are located at the bottom of each photo, 12-16-40-1W5, 5643 ft (1720.0 m).

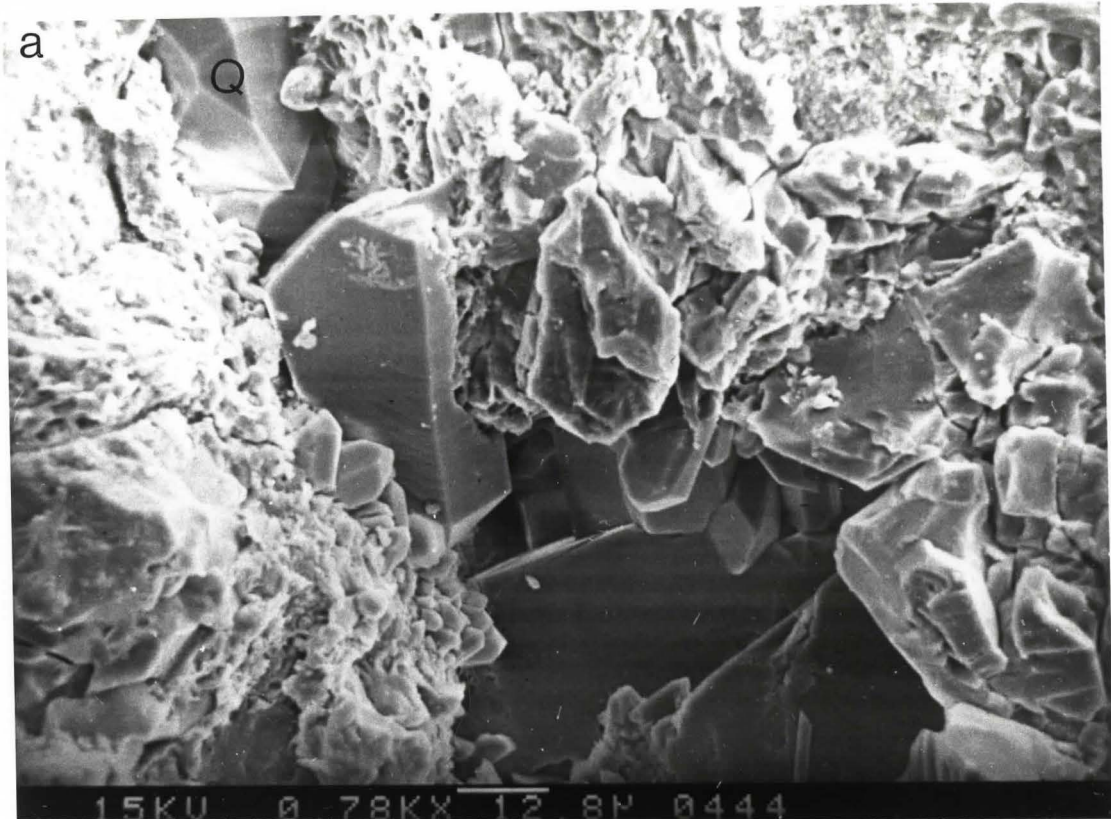
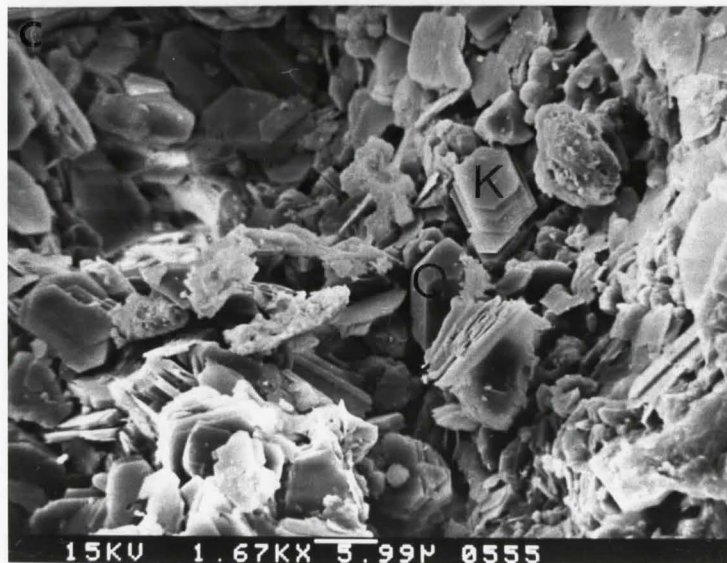
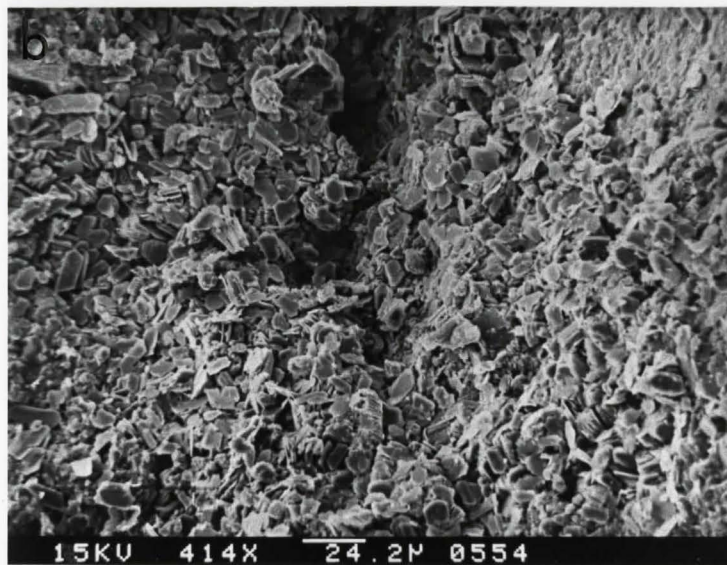
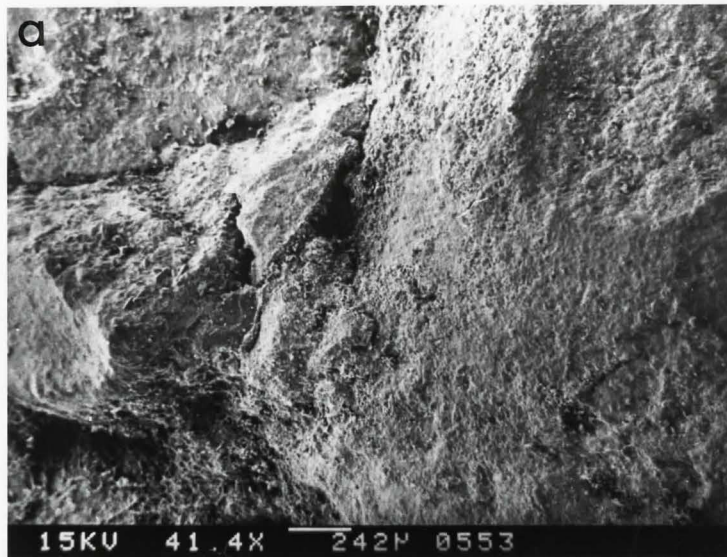


Fig. 4.16a, b and c. Scanning electron photomicrographs of progressively increased magnification (black outlined area) of a massive pebbly sandstone (Facies H). Note the authigenic quartz (Q) kaolinite booklets (K) in Figure 4.16c. Scale bar (microns) and magnification are located at the bottom of each photo, Figure 4.16c, 10-32-41-4W5, 6441 ft (1963.2 m).



## Chapter 5: FACIES DISTRIBUTION AND DETAILED FIELD GEOMETRY

### 5.1 Introduction

The first section of this chapter discusses the distribution of the capping conglomerates as measured from core along with the distribution of the maximum chert pebble sizes found in core from this unit. Also discussed is the distribution of glauconite found in cored wells within the sandstone facies.

The gross field geometry is discussed with the presentation of 5 southwest to northeast trending cross-sections. The cross-sections use marker A as an upper datum, the reliability of this datum is discussed and compared to other markers.

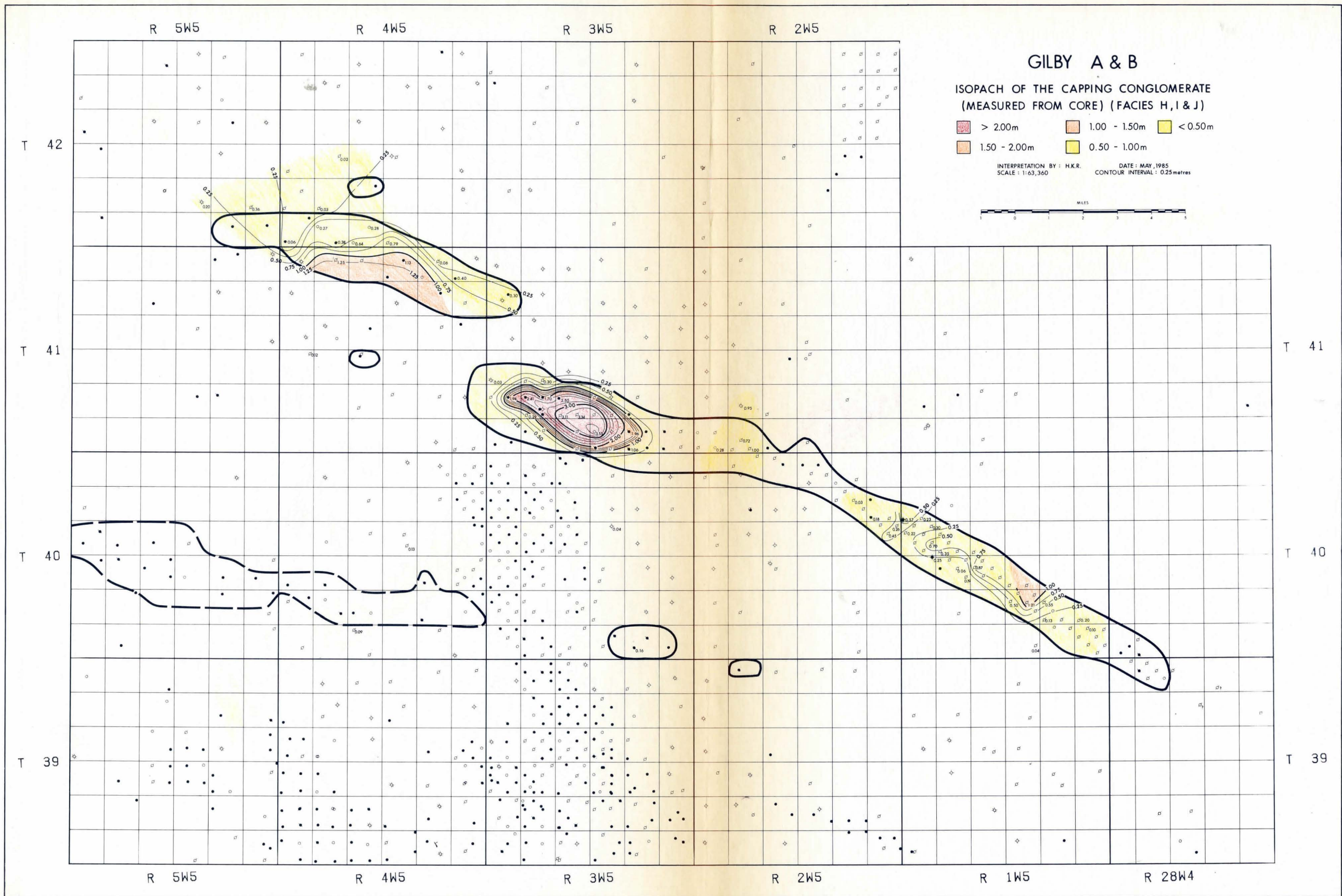
The final section of Chapter 5 extends the gross field geometry established with the log cross-sections to all examined wells in the study area (about 450 wells). This is done with an isopach map of the coarse sediment package and a representation of the paleotopography of the lower surface of the coarse sediment package throughout the study area.

### 5.2 Facies Distribution

#### 5.2.1 Capping Conglomerate Distribution (Figure 5.1)

Presented in Figure 5.1 is an isopach map (0.25 m contour interval) of the capping conglomerates (Facies H, I

Fig. 5.1. Isopach map of the Viking capping conglomerate distribution of the Gilby A and B fields. The conglomerate is measured from core and consists of Facies H, I and/or J. The contour interval is 0.25 m and conglomerate accumulations greater than 2.00 m are coloured in red, between 1.00 and 2.00 m are coloured in orange and less than 1.00 m are coloured in yellow. The outline of Gilby A and B is indicated by the heavy lines and a portion of Willesden Green is indicated by the heavy dashed lines. Note that the maximum thickness of conglomerate occurs towards the northeastern margins of Gilby A-1. In the Gilby A-3 area the maximum conglomerate thickness occurs in the center of the Gilby A-3 area and thins outward in a radial pattern from the center. The maximum thickness of conglomerate occurs in the central area of Gilby B-1 and thins towards the northeast.



**GILBY A & B**

ISOPACH OF THE CAPPING CONGLOMERATE  
(MEASURED FROM CORE) (FACIES H, I & J)

- > 2.00m
- 1.50 - 2.00m
- 1.00 - 1.50m
- 0.50 - 1.00m
- < 0.50m

INTERPRETATION BY : H.K.R.      DATE : MAY, 1985  
SCALE : 1:63,360      CONTOUR INTERVAL : 0.25metres



and J) measured from core. It is suggested that the capping conglomerates occurring in the A-1, A-2 and A-3 areas of Gilby A and in Gilby B are the same laterally adjacent units because of their similar appearance, however they may not be synchronous. The on-field wells consist mainly of Facies H (Gilby A-1 area) and Facies J (Gilby A-2, A-3, B-1 area) while off-field wells consist mainly of thinly developed Facies I. Numbers beside the cored well locations refer to the conglomerate thickness. Conglomerate thickness of greater than 2.00 m are shown in red, between 1.00 and 2.00 m are shown in orange and less than 1.00 m are shown in yellow.

The Gilby A-1 area shows conglomerate beginning at the southwest margin of the field thickening towards the northeast. The Gilby A-2 area was not contoured because of the insufficient core control. The Gilby A-3 area has the maximum conglomerate thickness found in the study area. In this area the conglomerates are arranged in a radial pattern with thicker accumulations occurring in the center, thinning outwards towards the field boundaries. The Gilby B field (B-1 area) shows conglomerate thickening towards the northeast from the southern margin of the field, this trend continues to the central area of the field where the conglomerates begin to thin towards the northeast. Core data for the southern margin of the Gilby B field was not available. There was insufficient core control to contour the conglomerates in off-field areas. Examined conglomerates occurring

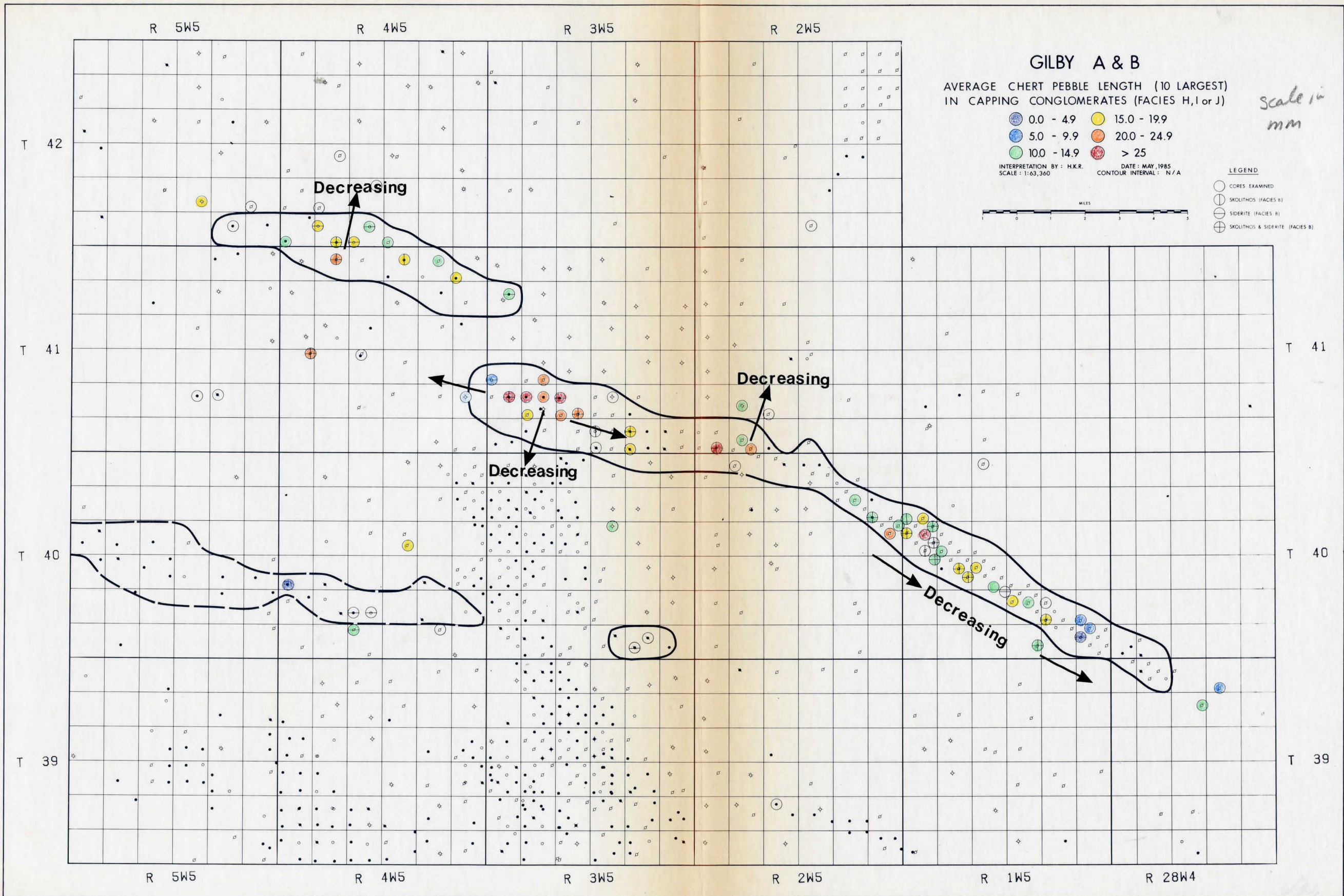
in off-field areas were thin and consisted of pebbles chaotically scattered in a black mudstone (Fig. 3.7, p.38).

#### 5.2.2 Maximum Chert Pebble Length in Capping Conglomerates (Figure 5.2)

Presented in Figure 5.2 is a plot of the average length of the 10 largest chert pebbles per core, measured in the capping conglomerates (see Figure 5.1) throughout the study area. The legend in Figure 5.2 denotes specific colours which indicate ranges of the average chert pebble lengths.

In the Gilby A-1 area there is a suggestion that the larger pebbles, greater than 20 mm (coloured orange and red) preferentially occur in the north end of A-1 and smaller pebbles, less than 9.9 mm (coloured pale blue and dark blue) occur in the south end of A-1. The central portion of the A-1 area shows a relatively constant average pebble size, ranging from 10.0 to 19.9 mm. The Gilby A-2 area has sparse core control but information from the few available cores indicates that the average pebble size is decreasing towards the north. The Gilby A-3 area shows a radial pattern where the larger average pebble size occurs in the center and decreases outward towards the field boundaries. The decreasing outward radial pattern for the average chert pebble size coincides with the thinning outward radial pattern of the capping conglomerates also in the Gilby A-3 area (Figure 5.1). Therefore, in this region the larger pebbles occur where the capping conglomerate is thickest

Fig. 5.2. Distribution of the maximum chert pebble length in the capping conglomerates of the Gilby A and B field. The average length (longest axes) of the 10 largest chert pebbles per core were measured in the capping conglomerates (see Figure 5.1). All coloured circles (see Legend on map) denote the average length in mm ranging from pebble lengths of 0.0 - 4.9 mm coloured in dark blue, 5.0 - 9.9 mm coloured in pale blue, 10.0 - 14.9 mm coloured in green, 15.0 - 19.9 mm coloured in yellow, 20.0 - 24.9 mm coloured in orange and greater than 25 mm coloured in red. The Gilby A and B fields are outlined in a heavy solid line while a portion of the Willesden Green field is outlined in a heavy hatched line. See text for further discussion.



and similarly the smaller pebbles occur where the capping conglomerates are more thinly developed. The Gilby B field (B-1 area) shows a decrease in the average pebble size towards the north margin of the field. This pattern coincides with the capping conglomerates (Figure 5.10) thinning towards the north. Again showing the relationship of larger chert pebbles occurring where the conglomerates are thick and the smaller pebbles occurring where the conglomerates are thin. Off-field core data is insufficient to suggest any pattern for chert pebble length outside of the fields.

### 5.2.3 Glauconite Distribution (Figure 5.3)

Presented in Figure 5.3 are cored well locations which contain glauconite (coloured green). The glauconite occurred most frequently in Facies C, D, or E. The majority of those wells containing glauconite occur in the A-1 area of Gilby A, especially where the sandstones were thickly developed. There was no glauconite observed in the Gilby B field or in off-field wells. The study of glauconite in thin section (chapter 4) suggests that it has formed authigenically, coating fecal pellets. Therefore the glauconite is an indication of a marine environment.

Fig. 5.3. Distribution map of cored wells which contain glauconite. Circled wells coloured in green show the distribution of glauconite. The Gilby A and B fields are outlined with a heavy solid line while the dashed outline represents the partial area of Willesden Green. The glauconite occurred most frequently in the stratigraphically lower sandstones of Facies C, D and E in the Gilby A-1 area.

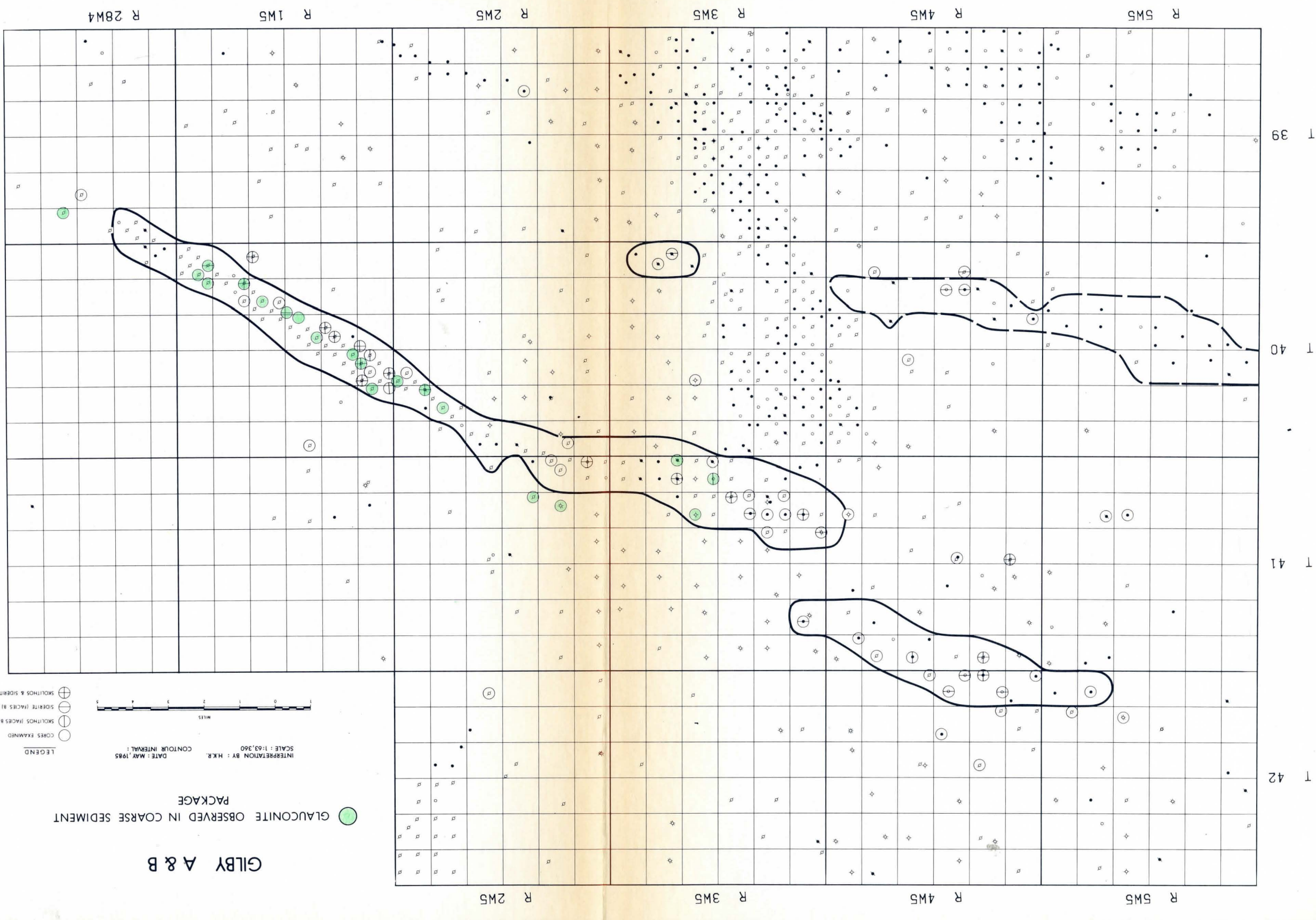
# GILBY A & B

GLAUCONITE OBSERVED IN COARSE SEDIMENT PACKAGE

- ⊕ SKOLITHOS & SIDERITE (FACIES B)
- SIDERITE (FACIES B)
- ⊕ SKOLITHOS (FACIES B)
- CORES EXAMINED



DATE: MAY, 1985  
CONTOUR INTERVAL:  
INTERPRETATION BY: H.K.R.  
SCALE: 1:63,360



### 5.3 CROSS SECTIONS

#### 5.3.1 Introduction

Five cross-sections are presented in Figures 5.4 to 5.8 orientated southwest to northeast through the Gilby A and B fields (cross-section locations are shown on Figure 3.35, p.79). Marker A is employed as the datum in all sections. The Base of Fishscale marker and markers labelled A through to H (see Figure 2.2, section 2.1.3) are correlated in all sections. Markers B and C (respectively) define the upper and lower surfaces of the coarse sediment package. In off-field wells containing little to no coarse sediment, a single marker B represents the position which is correlative with the top of the coarse sediment package in on-field wells. Marker B in off-field wells is recognized as the inflection point of the intersection of the shale-line with the resistivity log below marker A. Picking marker B is sometimes difficult, for example 6-9 and 8-19 of section 5 (Figure 5.8), without experience marker B could be incorrectly picked as the small kick on the induction log which is directly above a larger kick - this larger kick is the correct position of marker B. The resistivity at the marker B horizon is about 10 ohms and is placed at a distance approximately midway between the shale-line (5 ohms) and the silt-line (15-20 ohms) (see 4-19, Figure 5.7).

In off-field wells, particularly to the north of Gilby A and B, the base of the coarse sediment package is

gradational with the underlying siltstones (Facies A) which makes this lower surface difficult to identify in logs. To aid in the recognition of the lower surface of the coarse sediment package on resistivity logs, a cut-off of 20 ohms was used and/or the inflection point of the intersection of the maximum silt-line with the coarse sediment (see 14-9, Figure 5.5). As previously mentioned in Chapter 3 (p.81) it is difficult and most often impossible to identify on electric well logs specific facies within individual coarsening-upward sequences which were examined in core. The location of field boundaries on the sections are shown by horizontal lines terminating with vertical lines below the resistivity logs

The markers in cross-sections 5.2 to 5.5 were normalized (section 5.3.3, see Figure 5.11). This procedure is used to demonstrate that the original topography on the lower surface of the coarse sediment package, before compaction of the underlying and overlying siltstones and shales, has the same general shape as that shown in cross-sections 1 to 5.

#### 5.3.2 Section 1 (Cross-section location map, Figure 3.35)

Section 1 (Figure 5.4), the southeasternmost section, begins at 6-34 southwest of the Gilby A field. In 6-34 the coarse sediment package is only a few inches thick, northeastward into 8-3 the coarse sediment thickens to 2 ft (0.61 m). The thickness continues to increase

Fig. 5.4. Cross-section 1 with location map on Figure 3.35 (p.79). See text for discussion.

SW  
1

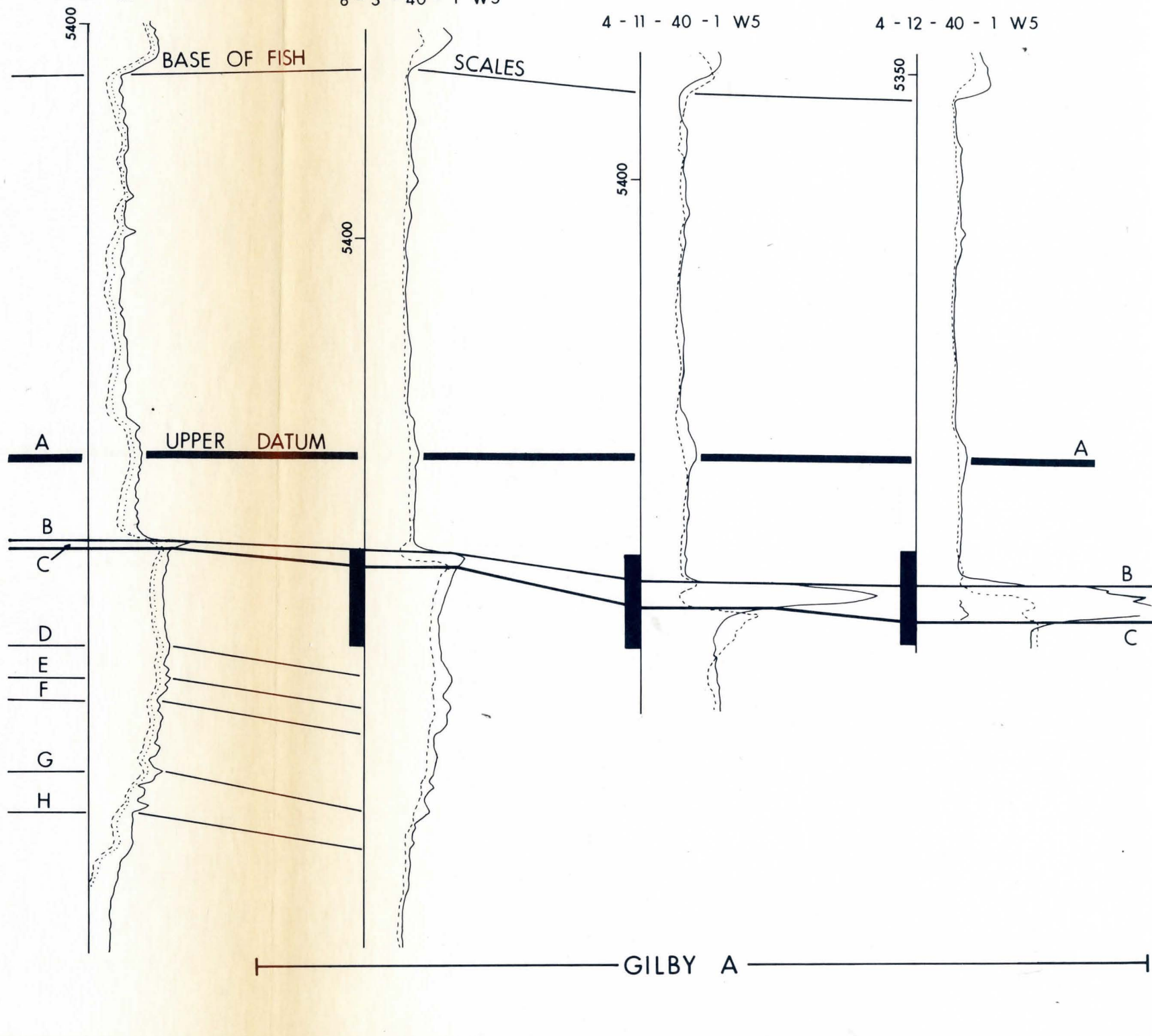
NE  
1

6-34-39-1 W5

8-3-40-1 W5

4-11-40-1 W5

4-12-40-1 W5



northeastward to 6 ft (1.8 m) in 4-11 and 12 ft in 4-12. Both 4-11 and 4-12 show a "blocky" log response, typical of on-field Viking Gilby wells in the central and northeast margin of the A-1 area. In addition to the northeastward thickening, the coarse sediment package drops stratigraphically with respect to the upper datum. The total relief on the base of the coarse sediment package, from 6-34 to 4-12, is 23 ft (7.0 m). Relief on the top of the package is 12 ft (3.7 m). Between 8-3 and 4-11, the maximum gradient on the lower surface of the coarse sediment package is 0.003 degrees. There are also thickness changes between the lower surface of the coarse sediment package (marker C) and marker E. The distance between markers C and E increases by 6 ft (1.8 m) from 6-34 to 8-3 with respect to marker A which is horizontal.

### 5.3.3 Section 2 (Cross-section location map, Figure 3.35)

Section 2 (Figure 5.5) begins at 10-34 and extends through the northern portion of the A-1 area of the Gilby A field. The first three wells 10-34, 1-2 and 10-11 have a log response typical of off-field regions south of the A-1 area of Gilby A. These wells have only a few inches of coarse sediment (see similar well 6-34, section 1, Figure 5.4). The first on-field well, 16-18, has 2 ft (0.61 m) of coarse sediment and a narrow, "v-shaped" log response typical of the southwest margin of the A-1 area. The coarse sediment package thickens to 17 ft (5.2 m) in 4-20 and thins

Fig. 5.5. Cross-section 2 with location map on Figure 3.35 (p.79). See text for discussion.

SW  
2

10 - 34 - 39 - 2 W5

1 - 2 - 40 - 2 W5

10 - 11 - 40 - 2 W5

16 - 18 - 40 - 1 W5

4 - 20 - 40 - 1 W5

16 - 19 - 40 - 1 W5

6 - 29 - 40 - 1 W5

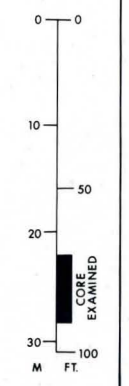
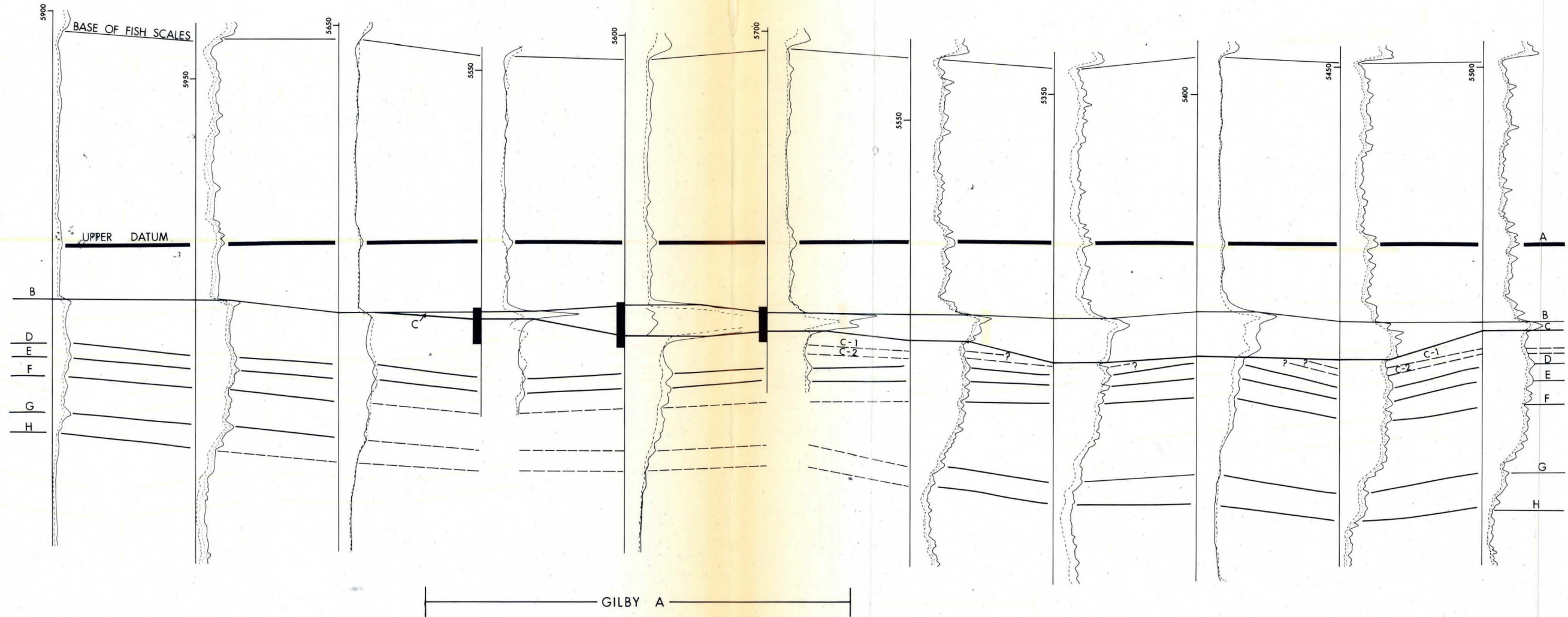
11 - 33 - 40 - 1 W5

6 - 4 - 41 - 1 W5

14 - 9 - 41 - 1 W5

6 - 20 - 41 - 1 W5

NE  
2'



to 8 ft (2.4 m) in 16-19. Both 4-20 and 16-19 have a "blocky" log response typical of on-field Viking wells in the central and northeast margin of the A-1 area. To the northeast the five off-field wells (6-29 through 6-20) have a "funnel-shaped" log response typical of wells found to the north of Gilby A. These "funnel-shaped" wells have a gradational base which makes determination of the base of the coarse sediment package difficult. As discussed in the introduction, a 20 ohm resistivity cut-off was used to position the base of the coarse sediment package in all wells with a gradational base. The coarse sediment package from 6-29 through to 6-20 attains a maximum thickness of 22 ft (6.7 m) in 11-33 and thins to 7 ft (2.1 m) at 6-20. Along with the thickening described from 10-34 through to 4-20, the base of the coarse sediment package drops stratigraphically with respect to the upper datum, marker A. The total relief on the base of the coarse sediment package between 10-34 and 4-20 is 17 ft (5.2 m). Between 4-20 and 16-19 the base of the coarse sediment rises by 4 ft (1.2 m) stratigraphically and from 16-19 to 11-33 drops 14 ft (4.3 m) stratigraphically with respect to the upper datum. From 11-33 through to 6-20 the base of the coarse sediment package rises stratigraphically, representing a total relief of 16 ft (4.9 m). The top of the coarse sediment package undulates gently throughout section 2. The maximum relief found on the upper surface of the coarse sediment package is 5.7 ft (1.7 m) between wells 6-4 and 14-9. Between 16-18

and 4-20, the maximum gradient on the lower surface of the coarse sediment package is 0.006 degrees. There are also thickness changes between the lower surface of the coarse sediment package (marker C) and marker E (with respect to marker A which is kept horizontal). The distance between markers C and E decreases by 27 ft (8.2 m) from 16-18 through to 11-33 and increases by 13.6 ft (4.1 m) from 11-33 through to 6-20.

Of particular significance between wells 6-29 through to 6-20 are two markers between C and D labelled C-1 and C-2. The C-1 marker found in 6-29 is absent in wells 11-33 and 6-4 but reappears in wells 14-9 and 6-20. The C-2 marker found in 6-29 and 11-33 is absent in 6-4 but reappears in wells 14-9 and 6-20.

#### 5.3.4 Section 3 (Cross-section location map, Figure 3.35)

Section 3 (Figure 5.6) begins at 10-18, extending through the A-2 area of Gilby A. The off-field log response typical to the south of the A-2 and A-3 area of Gilby A and to the south of Gilby B is represented in 10-18 through to 7-29. There is no log response indicative of any coarse sediment development in these first three wells. In the first on-field well, 6-32, the coarse sediment package thickens to 3 ft (0.91 m). This well has a narrow, "v-shaped" response typical to the southern margin of Gilby A (see 16-18; Figure 5.3). Northwards, the coarse sediment thickens to 8 ft (2.4 m) at 2-5, remains at 8 ft (2.4 m) in

Fig. 5.6. Cross-section 3 with location map on Figure 3.35 (p.79). See text for discussion.

SE  
3

10 - 18 - 40 - 2 W5

10 - 20 - 40 - 2 W5

7 - 29 - 40 - 2 W5

6 - 32 - 41 - 2 W5

2 - 5 - 41 - 2 W5

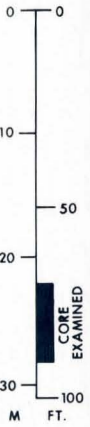
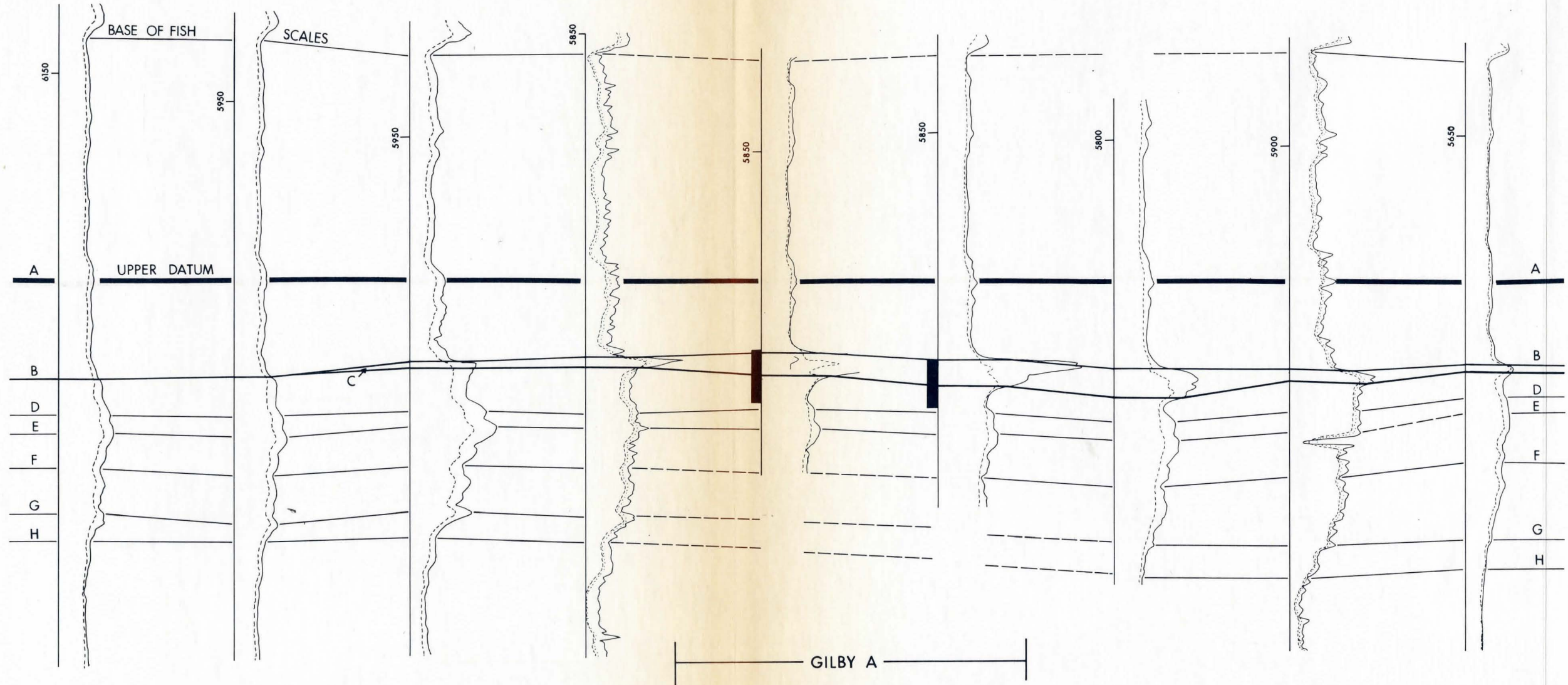
6 - 5 - 41 - 2 W5

4 - 9 - 41 - 2 W5

9 - 16 - 41 - 2 W5

7 - 28 - 41 - 2 W5

NW  
3'



6-5 and thickens to 11 ft (3.4 m) in 4-9. Both 2-5 and 6-5 have a "blocky" typical on-field log response. The first off-field well, 4-9, has a similar "blocky" response but the maximum resistivity within the coarse sediment package is reduced to approximately half the amount found in 6-5. The coarse sediment package thins to 9.8 ft (3.0 m) in 9-16 and 4 ft (1.2 m) in 7-28. Both these wells have a "funnel-shaped" log response typical of the area to the north of Gilby A. As well as the thickening described above in 7-29 through to 4-9, the lower surface of the coarse sediment package drops stratigraphically with respect to the upper datum. The total relief on the base of the coarse package is 14 ft (4.3 m). The coarse sediment package thins from 4-9 through to 7-28 and its lower surface rises stratigraphically having a total relief of 8 ft (2.4 m). The upper surface of the coarse sediment package (marker B) gently undulates throughout section 3. The maximum relief on the upper surface of the coarse sediment package is 8 ft (2.4 m) between both 10-18 to 10-20 and 4-9 to 9-16. Between 2-5 and 6-5, the maximum gradient on the lower surface of the coarse sediment package is 0.002 degrees. The distance between markers C and C increases by 4 ft (1.2 m) in the southeasternmost wells 10-18 through to 7-29. From 7-29 through to 7-28 the distance between markers C and E decreases by 8 ft (2.4 m).

#### 5.3.5 Section 4 (Cross-section location map, Figure 3.35)

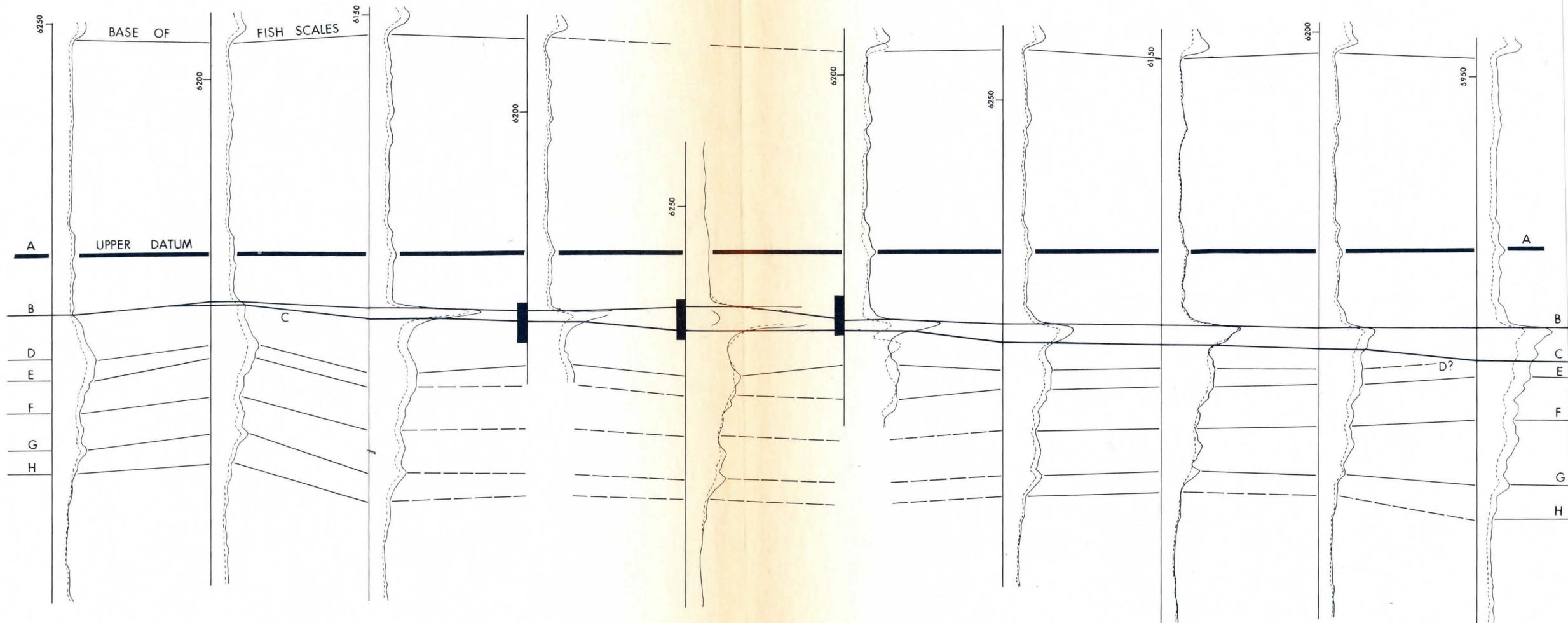
Section 4 (Figure 5.7) begins at 4-19, extending through the A-3 area of Gilby A. Both 4-19 and 14-30 to the north contain no coarse sediment and have a typical off-field log response, found south of the A-2 and A-3 area of the Gilby A and B fields. To the northeast the coarse sediment package thickens to 5 ft (1.5 m) at both on-field wells 12-5 and 4-8. The maximum on-field thickness of the coarse sediment package is 9 ft (2.7 m), reached at 12-8, but the package thins to 7 ft (2.1 m) in 2-17. The wells 12-5 through to 2-17 have a "blocky" log response typical of the centre of the Gilby A field and a "v-shaped" log response common along the margins of the field. To the northeast the coarse sediment package thickens to 9 ft (2.7 m) in 2-17 and 10 ft (3.0 m) in 6-21, thins to 8 ft (2.4 m) in 6-27 and again thickens to 17 ft (5.2 m) in 7-35. Wells 10-17 through 7-35 have a "funnel-shaped" log response typical of wells north of Gilby A. In these wells the base of the coarse sediment package is gradational, making the lower surface difficult to identify from logs. As well as the thickness changes of the coarse sediment package, the lower surface of the package drops stratigraphically while the upper surface of the package gently undulates, both surfaces with respect to the upper datum. The total relief on the lower surface is 21 ft (6.4 m) from 12-5 through to 7-35. The maximum relief on the upper surface is 6 ft (1.8 m) between 12-8 and 2-17. Between 14-30 and 12-5, the

Fig. 5.7. Cross-section 4 with location map on Figure 3.35 (p.79). See text for discussion.

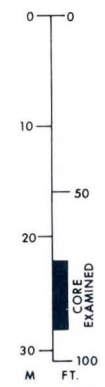
SW  
4

NE  
4'

4 - 19 - 40 - 3 W5    14 - 30 - 40 - 3 W5    12 - 5 - 41 - 3 W5    4 - 8 - 41 - 3 W5    12 - 8 - 41 - 3 W5    2 - 17 - 41 - 3 W5    10 - 17 - 41 - 3 W5    6 - 21 - 41 - 3 W5    6 - 27 - 41 - 3 W5    7 - 35 - 41 - 3 W5



GILBY A



maximum gradient on the lower surface of the coarse sediment package is 0.0007 degrees.

The distance between markers C and E increases by 10 ft (3.0 m) from 4-19 through to 12-5. The most significant increase in thickness between markers C and E is 8 ft (2.4 m) between 14-30 and 12-5. The distance between markers C and E thins by 22 ft (6.7 m) from 12-8 through to 7-35. The most significant thickness change found from 12-8 through to 7-35 is a thinning of 8 ft (2.4 m) between 2-17 and 10-17. In 7-35, the northeasternmost well, marker D is absent.

### 5.3.6 Section 5 (Cross-section location map, Figure 3.35)

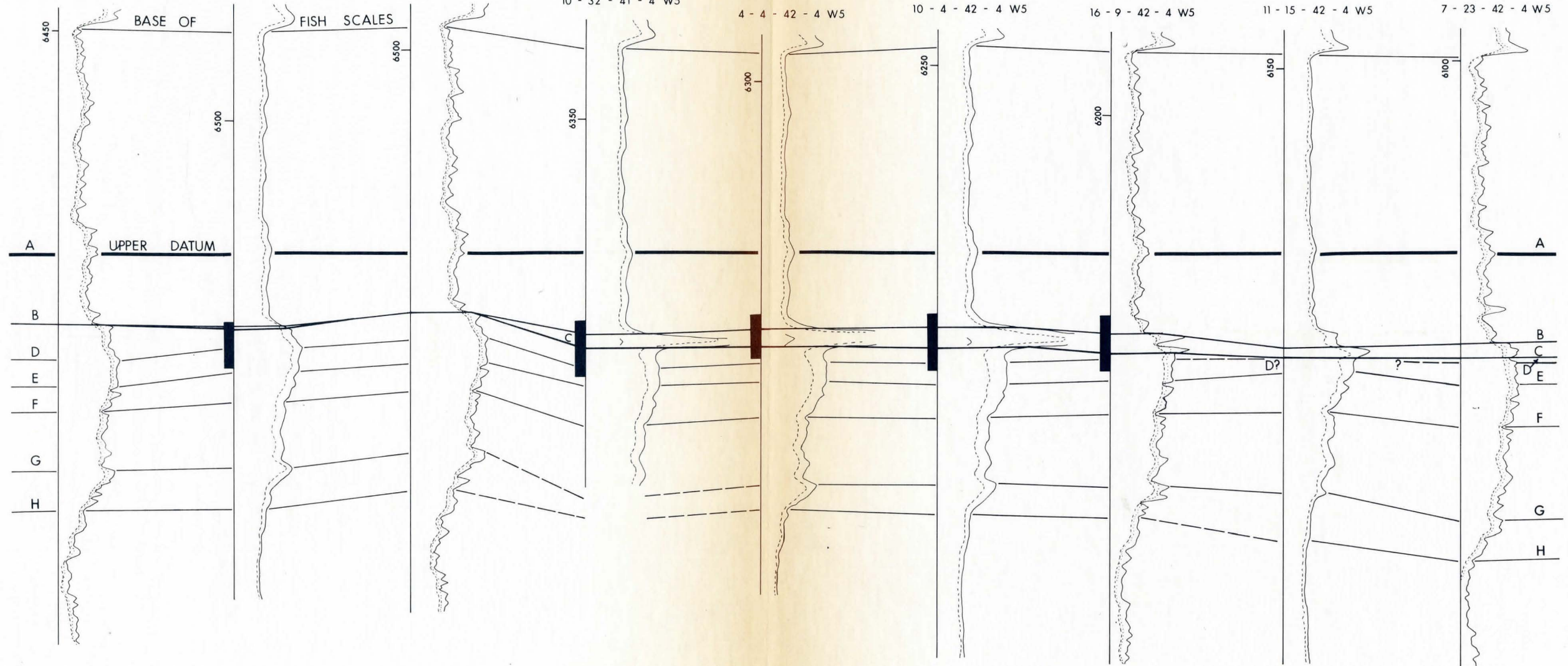
Section 5 (Figure 5.8), the only section to cross through Gilby B, begins at 6-9. The first three wells, 6-9 through to 8-19 have log responses typical of off-field wells south of both the A-2 and A-3 areas of Gilby A and Gilby B, all of which contain approximately no coarse sediment. However, at 16-18 40 cm of coarse sediment was observed in core, indicating that a thin development of coarse sediment (pebble veneer) may occur in other wells which have this log response. The coarse sediment thickens to 4 ft (1.2 m) at 10-32, 6 ft (1.8 m) at 4-4 and thins to 5 ft (1.5 m) at 10-4. All of these on-field wells have a "blocky" log response. The coarse sediment package thickens to 8 ft (2.4 m) at 16-9 in the Gilby Viking H field at 16-9 in the Gilby Viking H field (see Chapter 1, p.5). Northeast the coarse sediment package

Fig. 5.8. Cross-section 5 with location map on Figure 3.35 (p.79). See text for discussion.

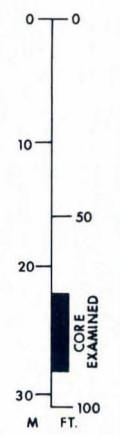
SW  
5

NE  
5'

6 - 9 - 41 - 4 W5      16 - 18 - 41 - 4 W5      8 - 19 - 41 - 4 W5      10 - 32 - 41 - 4 W5      4 - 4 - 42 - 4 W5      10 - 4 - 42 - 4 W5      16 - 9 - 42 - 4 W5      11 - 15 - 42 - 4 W5      7 - 23 - 42 - 4 W5



————— GILBY B ————— ||————— GILBY H —————



thins to 4 ft (1.2 m) in 11-15 and to less than 1 ft (0.3 m) in 7-23. Both these wells have a "funnel-shaped" log response typical of the area to the north of Gilby A and B where recognition of the lower surface of the coarse sediment is difficult. Along with the thickness changes of the coarse sediment package through Section 5, the lower surface of the package drops stratigraphically with respect to the upper datum from 8-19 through to 11-15. The total relief on the lower surface is 14 ft (4.3 m). The upper surface of the coarse sediment package with respect to the upper datum gently undulates through the section. The maximum relief on the upper surface of the coarse sediment package is 7.2 ft (2.2 m) between 16-9 and 11-15. Between 8-19 and 10-32, the maximum gradient on the lower surface of the coarse sediment package is 0.0006 degrees. The distance between marker C and E thins by 7.3 ft (2.2 m) between the southernmost well 6-9 through to 16-18 and thickens by 2.3 ft (0.7 m) from 16-18 to 8-19. There is again thinning, between markers C and E, of 15.9 ft (4.8 m) from 8-19 through to 10-4, and thickening of 6.1 ft (1.9 m) from 10-4 to 16-9. From 16-9 to 11-15 a 1 ft (0.3 m) thinning between markers C and E occurs, followed by a thickening of 9.3 ft (2.8 m) in the northeasternmost wells 11-15 to 7-23. Marker D is absent in wells 10-32 and 11-15 which coincides with the stratigraphic drop of the lower surface of the coarse sediment package.

### 5.3.7 Datum Investigation and Normalization

To confirm that the upper datum, marker A, may be used to investigate the Viking Formation at Gilby A and B the lower surface of the coarse sediment package was normalized relative to upper marker A and lower marker E. As discussed earlier, sections using marker A as a datum show the lower surface of the coarse sediment package to drop stratigraphically at the southwest margin of the Gilby A and B fields towards the northeast. However, identical sections using lower marker E as a datum show the lower surface of the coarse sediment package to have a flat base and dome or bar-like shape beginning at the southwest margin of the fields and continuing to the northeast. As discussed previously (Chapter 3), the sedimentology of the coarse sediment package does not exemplify the geometry of a positive bar feature. For example the contact of the lower surface of the coarse sediment package is erosive and abrupt with the lower siltstone (Facies A) whereas a barrier bar feature would have a gradational coarsening-up sequence. The conglomerates found capping the coarse sediment package are unsorted and show a chaotic fabric whereas in a barrier bar system reworking and sorting of the conglomerates might be expected. As discussed previously (Chapter 3) Facies B (sideritized-Skolithos) is found only southwest of the initial stratigraphic drop of the lower surface of the coarse sediment package and is absent to the northeast of this boundary. Figure 5.9 shows the estimated boundary of

Fig. 5.9. Location map of the Sideritized muddy siltstone (with Skolithos) Facies (B) boundary. The solid line is the estimated northeasternmost extent of Facies B as determined from core. The hatched line represents the position of the initial stratigraphic drop of the lower surface of the coarse sediment package determined from both core and well logs. See text for further discussion.

R 5W5

R 4W5

R 3W5

R 2W5

# GILBY A & B

— BOUNDRY OF OBSERVED FACIES B (FROM CORE)  
 - - - POSITION OF INITIAL STRATIGRAPHIC DROP AT BASE OF COARSE SEDIMENT

INTERPRETATION BY : H.K.R. DATE : MAY, 1985  
 SCALE : 1:63,360 CONTOUR INTERVAL : N/A

- LEGEND
- CORES EXAMINED
  - SKOLITHOS (FACIES B)
  - SIDERITE (FACIES B)
  - ⊕ SKOLITHOS & SIDERITE (FACIES B)



T 42

T 41

T 40

T 39

T 41

T 40

T 39

R 5W5

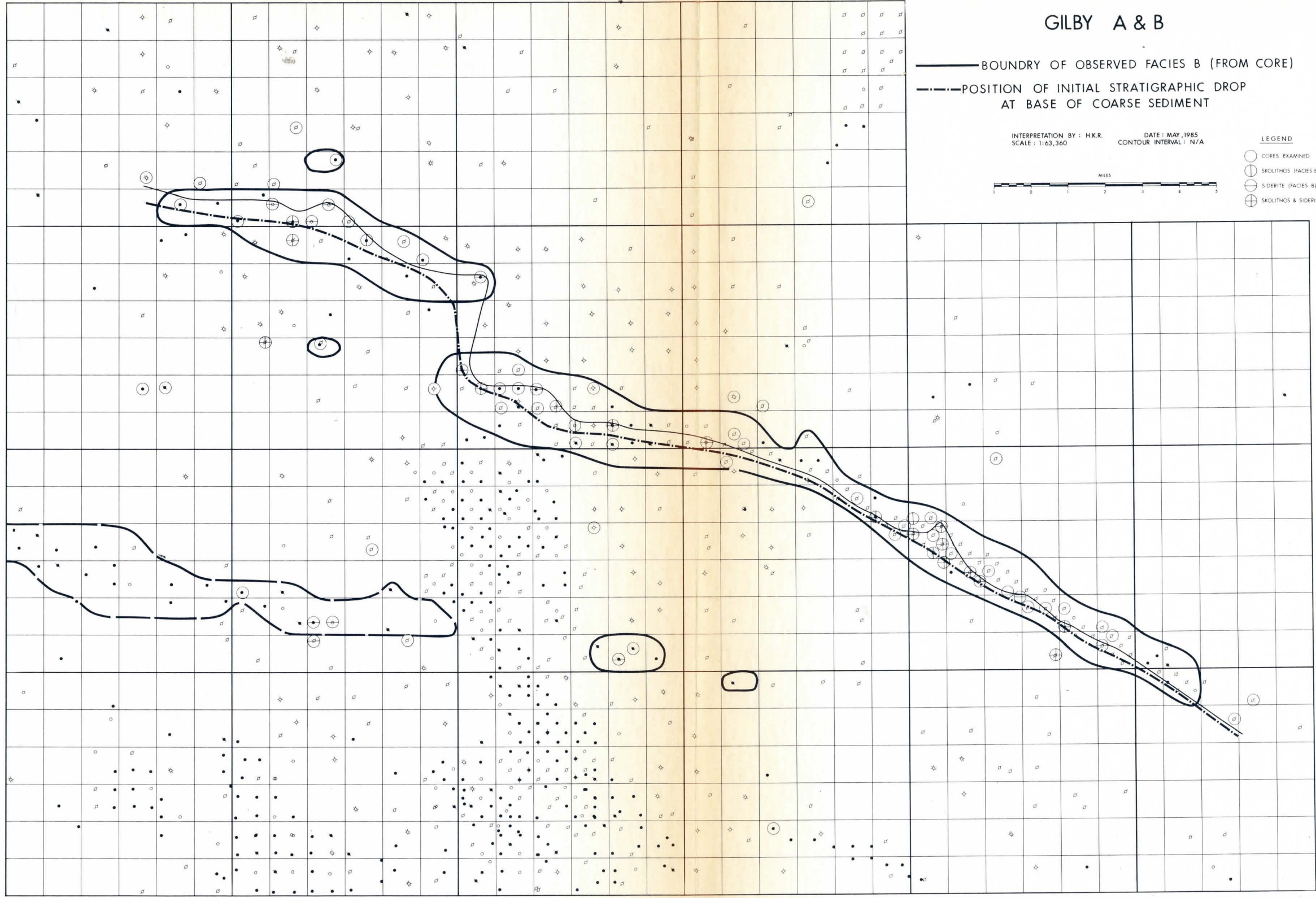
R 4W5

R 3W5

R 2W5

R 1W5

R 28W4



Facies B distribution - Facies B was not observed in core to the north of this boundary. The position of the initial stratigraphic drop of the lower surface of the coarse sediment package is shown in Figure 5.9 as a hatched line. From the relationship between the initial stratigraphic drop and the northern limit of Facies B it can be inferred that the Facies B was eroded at approximately the position of the initial stratigraphic drop of the lower surface of the coarse sediment package, towards the northeast. Other suggestions of erosion include the truncation of markers (C-1, C-2 and D) below the coarse sediment package in cross-sections 2 (Figure 5.5), 4 (Figure 5.7) and 5 (Figure 5.8). Also evident in all cross-sections is the change in thickness between the lower surface of the coarse sediment package and marker E. The separation between these markers tends to thin on-field and gradually thicken off-field towards the northeast (see cross-section 2, Figure 5.5 and cross-section 5, Figure 5.8) or gradually thin off-field towards the northeast (see cross-section 3, Figure 5.6 and cross-section 4, Figure 5.7). The loss of sediment thickness between markers C and E is suggested to represent erosion. Such examples of erosion would be difficult to explain in a barrier bar system.

Since the sedimentology of the coarse sediment does not support a bar-like geometry, it is reasonable to suggest that the upper datum (marker A) was relatively flat when deposited. To confirm this, a structure map of marker A

Fig. 5.10. Structure map in the Gilby A and B field of the upper datum (marker A) calculated from a sea level datum. All depths beside well symbols have a negative sign representing feet below sea level. The hatched lines outline the Gilby A and B field. Refer to text for further discussion.

R.5

R.4

R.3

R.2 W5M

# GILBY A & B

## STRUCTURE ON UPPER DATUM (MARKER A)

INTERPRETATION BY : H.K.R. DATE : MAY, 1985  
SCALE : 1:63,360 CONTOUR INTERVAL : 20'



T. 42

T. 41

T. 40

T. 39

T. 41

T. 40

T. 39

R.5

R.4

R.3

R.2

R.1 W5M

R. 28 W4M

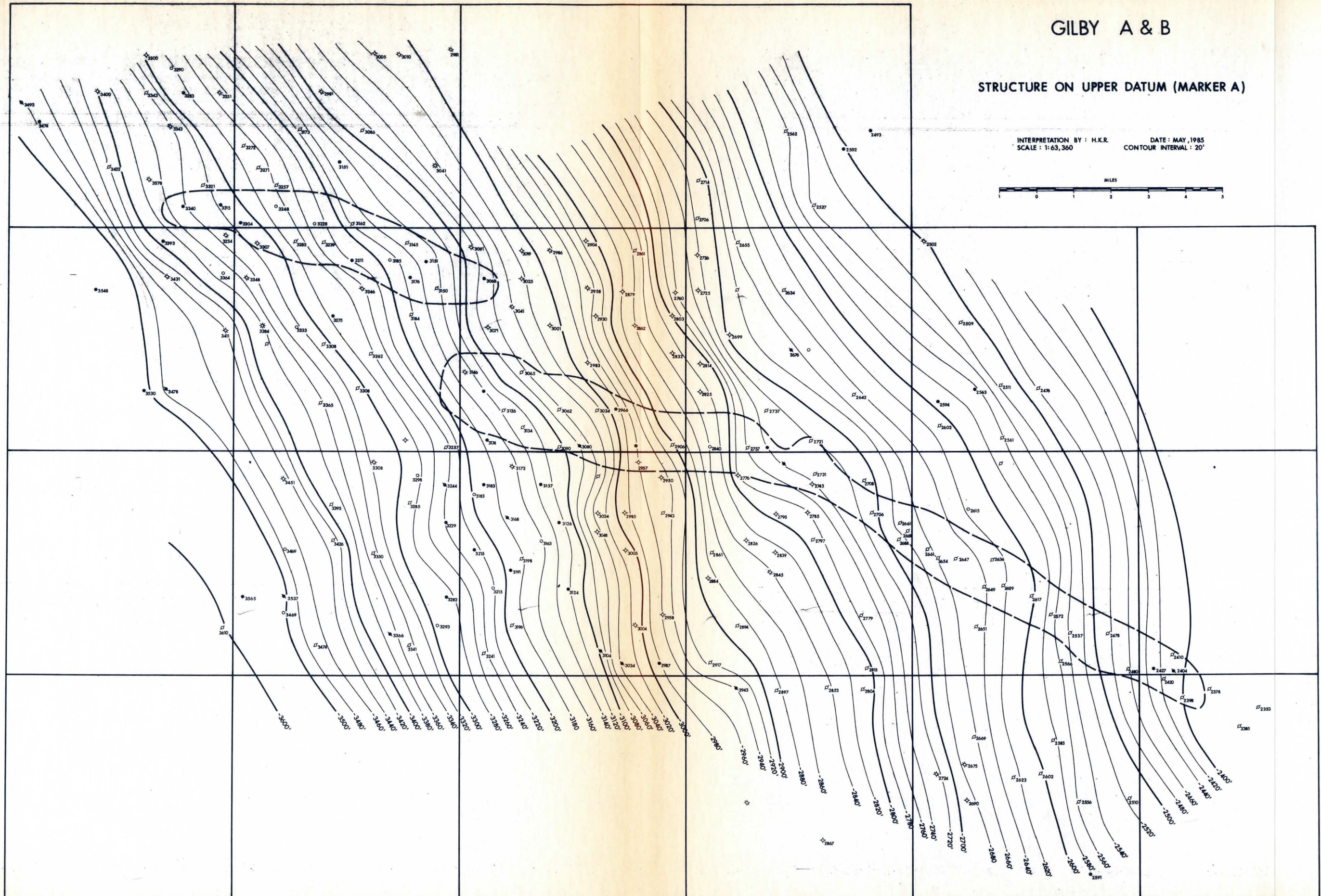


(Figure 5.10) was constructed (Gilby field boundaries are shown on the figure with hatched lines). The structure map shows the regional southwest dip (40 ft per mi) and little topography developed on this surface. Markers D to H approximately parallel each other and the lower surface of the coarse sediment package. This is probably due to compactional effects of the siltstones (Facies A). If this is the case then markers A and markers D to H were probably originally deposited horizontally. The lower surface of the coarse sediment package, before compaction effects, can be approximated by making marker A and E, for example, parallel to each other. This procedure is referred to as "normalization" and was used to determine the position of the lower surface of the coarse sediment package as a percentage of the distance between markers A and E.

Calculations were performed on all wells in the section having markers A, B or C and E. All letters in the following equations refer to the depth of the particular marker. The compaction of siltstone and shale is taken to be twice that of sandstone. Therefore, all siltstone/shale thicknesses (such as those measured between markers A to B, B to E and C to E) were multiplied by two to compensate for compaction. If the well contained no coarse sediment the equation,

$$\frac{[(A-B) \times 2]}{[(A - B) \times 2] + [(B - E) \times 2]} \times 100$$

determined the percentage of the distance that the lower

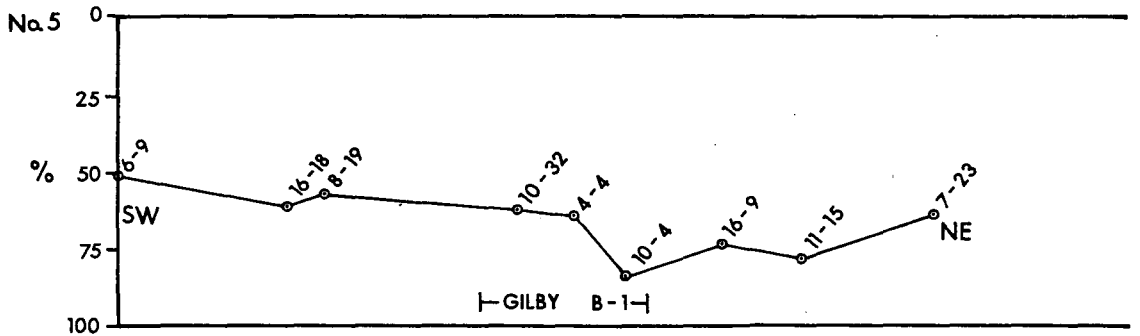
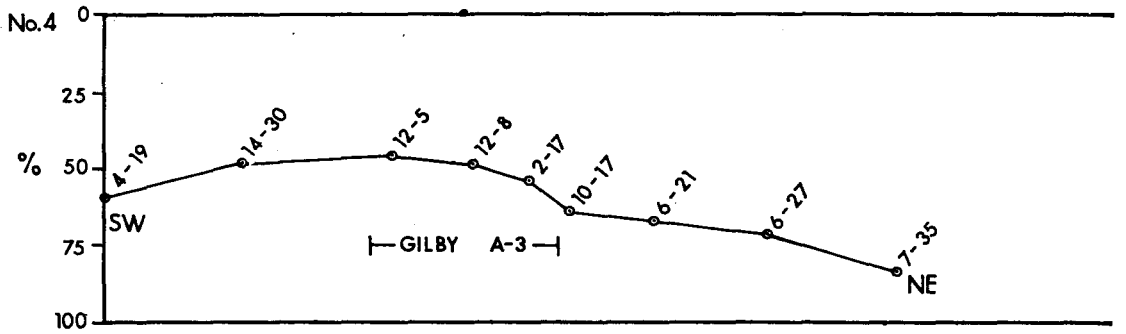
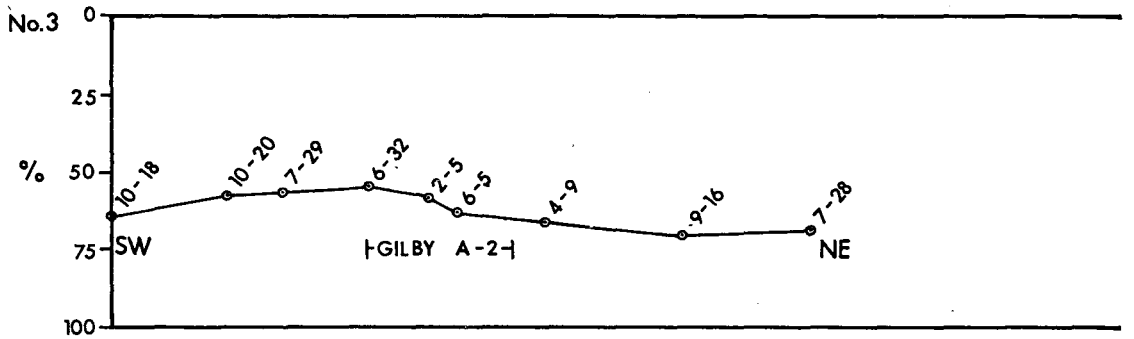
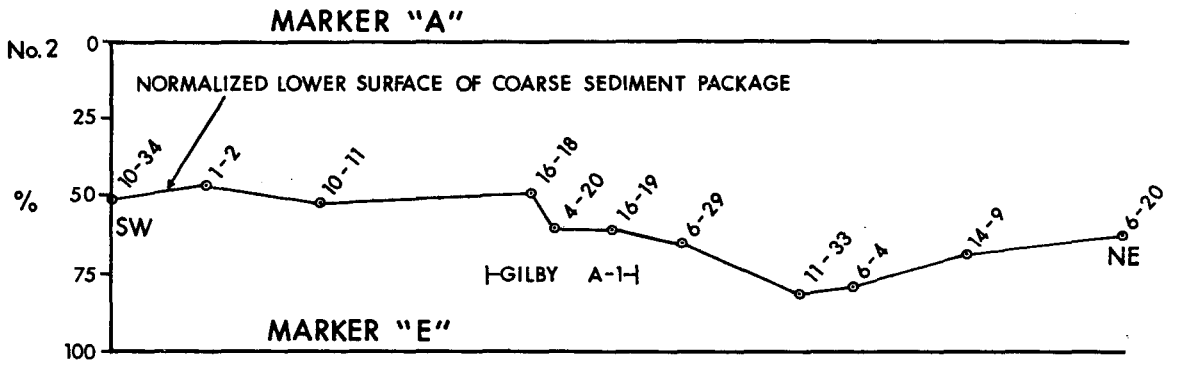
surface (in this case marker B) occurs between markers A and E. If the well contains coarse sediment the equation,

$$\frac{[(A-B) \times 2] + [(B-C)]}{[(A - B) \times 2] + [(B - C) + (C - E) \times 2]} \times 100$$

determines the percentage of the distance that the lower surface of the coarse sediment package (marker C) is found between markers A and E.

The lower surface of the coarse sediment package was normalized for sections 2 through to 4 (Figure 5.11). All of these sections demonstrate that the lower surface of the coarse sediment package drops stratigraphically to the north east, beginning approximately at the southwest margin of the Gilby A and B fields. Normalized sections 2 (Fig. 5.11) and 5 (Fig. 5.11) are similar in that they have the initial stratigraphic drop at the southwest margin of the field and have a second stratigraphic drop found northeast of the field boundaries. In normalized section 2 (Figure 5.11) the second stratigraphic drop is shallower than its first. In normalized section 2 the lower surface of the coarse sediment package at 6-20, the northeasternmost well, is at the same stratigraphic position as the first stratigraphic drop, while in normalized section 5 the lower surface at 7-23, the northeasternmost well, is at the same stratigraphic position with the area to the southwest of the field. Normalized sections 3 and 4 (Figure 5.11) are similar in that they have only one main stratigraphic drop which begins at the southwest margin of the field. The

Fig. 5.11. Normalized cross-sections 2, 3, 4 and 5 investigate whether or not marker A is a reasonably flat datum. This was accomplished by normalizing the lower surface of the coarse sediment package (marker B or C) relative to markers A and E. The upper horizontal line on each of the four cross-sections represents marker A and the lower horizontal line represents marker E (see Figure 2.2, p.19). The vertical scale represents the percentage of the distance that marker B or C occurs between markers A and E. The Gilby A and B field boundaries are located on each of the sections. The well locations are identical to those locations on log cross-sections located on Figure 3.35 (p.79). See text for detailed discussion.



## NORMALIZATION OF MARKER C

lower surface of the coarse sediment package begins to rise stratigraphically at 7-28 in normalized section 3.

#### 5.3.8 Summary

From examination of a number of cross-sections through the Gilby A and B fields, five of which were presented and discussed previously (5.3.2), the following conclusions can be drawn regarding the geometry of the fields:

1. The upper surface of the coarse sediment package (marker B) undulates gently over the study area.
2. The lower surface of the coarse sediment package (marker C) stratigraphically drops at the southwest margin of the fields towards the northeast and may rise stratigraphically at some distance (about 3-4 mi, 4.8-6.4 km) beyond the northern margin of the field boundaries.
3. Erosion of the muddy siltstones (Facies A) below the coarse sediment package is evident northeastwards of the southwest margin of the fields because: 1) the absence of Facies B at the lower contact with the coarse sediment package and; 2) the thinning of Facies A between markers C and E which includes the disappearance of log markers (C-1, C-2 and D).

Fig. 5.12. Isopach map of the Viking coarse sediment package (distance between marker B and C) of the Gilby A and B field. The contour interval is 2 ft (0.61 m). Areas with coarse sediment thickness greater than 15 ft (3.7 m) are coloured red, between 5 (1.2 m) and 15 ft (3.7 m) are uncoloured and less than 5 ft (1.2 m) are coloured yellow. The outline of the Gilby A and B field is indicated by the heavy dashed lines. Note that the thickest accumulations are located in the central part of the A-1, A-2 and A-3 areas of Gilby A and in the northwest corner of Gilby B. North of the field boundaries in both Gilby A and B are specific areas of thick coarse sediment accumulation.

R 5W5

R 4W5

R 3W5

R 2W5

# GILBY A & B

ISOPACH COARSE SEDIMENT  
--- FIELD BOUNDARY

INTERPRETATION BY : H.K.R.      DATE : MAY, 1985  
SCALE : 1:63,360      CONTOUR INTERVAL : 2'



T 42

T 41

T 40

T 39

T 41

T 40

T 39

R 5W5

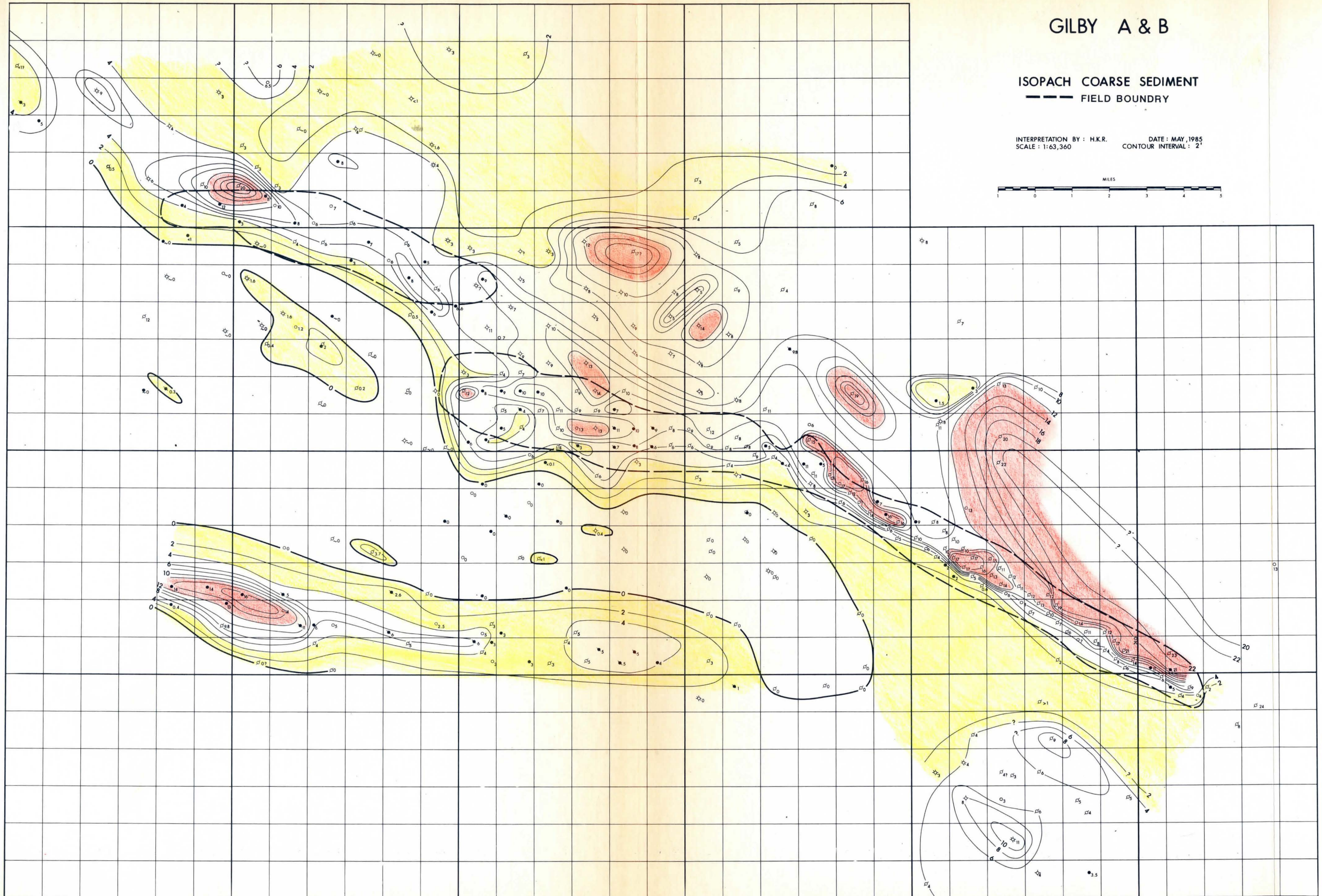
R 4W5

R 3W5

R 2W5

R 1W5

R 28W4



## 5.4 Isopach Maps

### 5.4.1 Isopach of the Viking Coarse Sediment Package

Shown in Figure 5.12 is an isopach map of the Viking coarse sediment package (between marker B and C, see Figure 2.2, p.19) measured from resistivity logs (see section 5.3.1 for discussion of marker cut-offs). The contour interval is 2 ft (0.61 m). Areas with coarse sediment thickness greater than 15 ft (4.6 m) are coloured red, between 5 (1.5 m) and 15 ft (4.6 m) are uncoloured and less than 5 ft (1.5 m) are coloured yellow.

As determined from the log cross-sections (Figures 5.5 to 5.8) in section 5.3.2 and mapping of the maximum pebble size (Figure 5.2), the coarse sediment in the off-field wells is not as coarse as that found in on-field wells. There is essentially no coarse sediment development to the south of Gilby A and B and to the north of Willesden Green (partially mapped). There are a few scattered wells which contain thin accumulations of coarse sediment, previously referred to as a "pebble lag" (chapter 3 and this chapter, 5.2). The coarse sediment gradually thickens along the southern margin of the Gilby A and B fields towards the northeast. The coarsest and thickest accumulations occur in the central part of the A-1, A-2 and A-3 of Gilby A and in the northwest corner of Gilby B. To the north of the field boundaries in both fields the coarse sediment locally thickens but generally gradually thins towards the

Fig. 5.13. Isopach map of the upper datum (marker A) to the lower surface of the coarse sediment package (marker B or C) in the Gibly A and B fields. This map represents the topography on the lower surface of marker B or C with regional tilt removed. Separations of 20-30 ft (6.1-9.1 m) are coloured red (denoting highest stratigraphic area), separations of 30-50 ft (9.1-15.2 m) are uncoloured and separations of 50-60 ft (15.2-18.3 m) are coloured yellow (denoting lowest stratigraphic area). Note that the highest stratigraphic areas occur south of the Gilby A and B fields and to the north of the Willesden Green field and the lowest stratigraphic areas occur over the fields and to the north of Gilby A and B.

R. 5

R. 4

R. 3

R. 2 W5M

# GILBY A & B

## ISOPACH UPPER DATUM TO BASE OF COARSE SEDIMENT

INTERPRETATION BY : H.K.R.      DATE : MAY, 1985  
SCALE : 1:63,360      CONTOUR INTERVAL : 2'



T. 42

T. 41

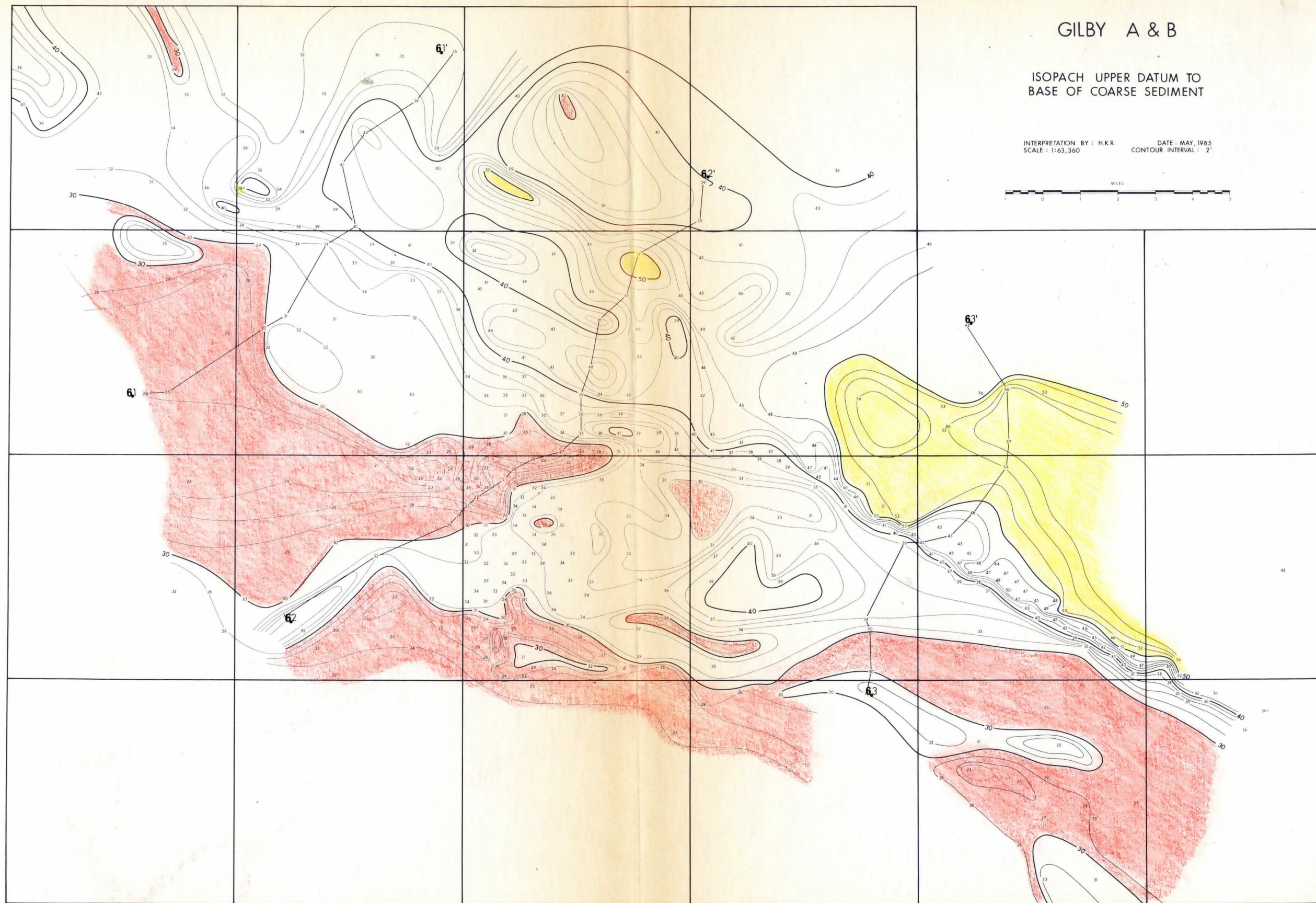
T. 40

T. 39

T. 41

T. 40

T. 39



northeast.

#### 5.4.2 Isopach of Upper Datum to Lower Surface of Coarse Sediment Package

Shown in Figure 5.13 is the isopach of the upper datum (marker A) to the base of the coarse sediment package (marker B or C). Refer to 5.3.3 for the discussion of the reliability of the upper datum (marker A). Since it has been shown that the upper datum is horizontal, this isopach map is essentially illustrating (removing the regional dip to the southwest) the topography on this lower surface over the study area. As discussed previously in chapters 3 (section 3.3) and 5 (section 5.2.2) this lower surface of the coarse sediment package represents a period of erosion - a depositional hiatus. The three solid lines numbered 1, 2 and 3 refer to cross-sections which are presented in Chapter 6.

The thinnest separation (20 to 30 ft, 6.1 to 9.1 m) between marker A and the lower surface of the coarse sediment package denotes the highest stratigraphic area, which is coloured in red (Figure 5.13). Conversely, the thickest separation (50 to 60 ft, 15.2 to 18.3 m) between marker A and the lower surface of the coarse sediment package denotes the lowest stratigraphic area, which is coloured in yellow. The areas having separations between 30 and 50 ft (9.1 to 15.2 m) are uncoloured.

In general the separation between markers A and B or C

is thickest over the Gilby A and B fields and to the north of these fields. The thinnest separation occurs to the south of the Gilby A and B fields and to the north of the Willesden Green field (see location map, Figure 3.35, p.79). Therefore the lowest stratigraphic areas generally occur where the coarse sediment is thick.

### 5.5 Summary

Mapping of the facies distribution and study of the detailed field geometry through the use of core and log data allows a number of generalizations to be made about the Viking sediments in the study area:

1. The capping conglomerates are thickest in the Gilby A-3 area and are thinnest in the Gilby A-1 and Gilby B-1 areas. A thin, discontinuous "pebble lag" (or pebble veneer) is suggested to occur off-field south of the Gilby A and B and to the north of the Willesden Green field.

2. The largest chert pebbles within the capping conglomerates occur within the thickest accumulations of that unit.

3. Glauconite is generally found in the A-1 and A-2 area of Gilby A but is absent in the A-3 area of Gilby A and in all of Gilby B.

4. The lower surface of the coarse sediment package is stratigraphically lowest in areas where the coarse sediment package is thickest. This relationship is shown with a horizontal marker A.

5. Evidence for erosion below the lower surface of the coarse sediment package is shown through: 1) the thinning and absence of markers (C-1, C-2 and D) between markers C and E; and 2) the absence of Facies B north of the central part of the Gilby A and B fields.

6. The coarse sediment package extends to the north beyond the field boundaries, where the lower surface of the coarse sediment drops to its lowest stratigraphic position about 3-4 mi (4.8-6.4 km) northeast of the field and thereafter very gradually rises stratigraphically.

## Chapter 6: CONCLUSIONS

### 6.1 Introduction

The Viking Gilby A and B fields may have been deposited either as a shoreface attached sandbody or an offshore developed sandbody (see Chapter 1). Through discussion and interpretation of the facies and field geometry (Chapters 3 and 5) it will be shown that the Gilby fields were more likely deposited as a shoreface attached sandbody.

### 6.2 Gilby A and B Scour

Detailed study of log markers and facies variations throughout the study region has revealed a linear scour which begins along the southwestern margin of the Gilby A and B fields. This scour surface is coincident with the lower surface of the Viking coarse sediment package (defined in Chapter 2) and is represented by a chert pebble-lag (pebble-veneer) to the southeast of the fields. Important to the recognition of the scour surface was determining that this surface is coincident with Facies B (sideritized muddy siltstone with Skolithos) in the areas where Facies B occurs. As has been discussed previously (Chapters 3 and 5), Facies B immediately underlies the chert pebble lag and occurs only along and to the south of the southwest margins of the fields - it has been eroded to the northwest where

the scour surface has been shown (Chapter 5) to drop stratigraphically. Additional evidence of scour and erosion was observed in the thinning of muddy siltstones (Facies A) between markers C and E which include the disappearance of log markers (C-1, C-2 and D) (see Chapter 5). The scour surface has been shown to drop stratigraphically towards the northeast margin of the fields and gently rises stratigraphically approximately 3-4 mi (4.8-6.4 km) beyond the northeastern margin of the fields. The maximum thickness of the coarse sediment package "infill" occurs along the central portion of the fields. Before discussing and suggesting a possible mechanism of development of the scour and its subsequent infill a number of cross-sections showing the relationship between the scour and the Viking coarse sediment package will be discussed.

### 6.3 Review of the Gilby A and B Coarse Sediment Distribution and Scour

#### 6.3.1 Introduction of Figures 6.1, 6.2 and 6.3

To summarize and emphasize the geometry and thickness changes of the Viking coarse sediment package with respect to the scour throughout the study area Figures 6.1, 6.2 and 6.3 are included. Figures 6.1, 6.2 and 6.3 each contain two cross-sections from the southwest-northeast oriented lines of section labelled 6.1, 6.2 and 6.3 in Figure 5.13. Cross-sections in each figure show the

Fig. 6.1. Cross sections 6.1a and 6.1b, location shown on Figure 5.13. See text for discussion.

FIGURE 6-1

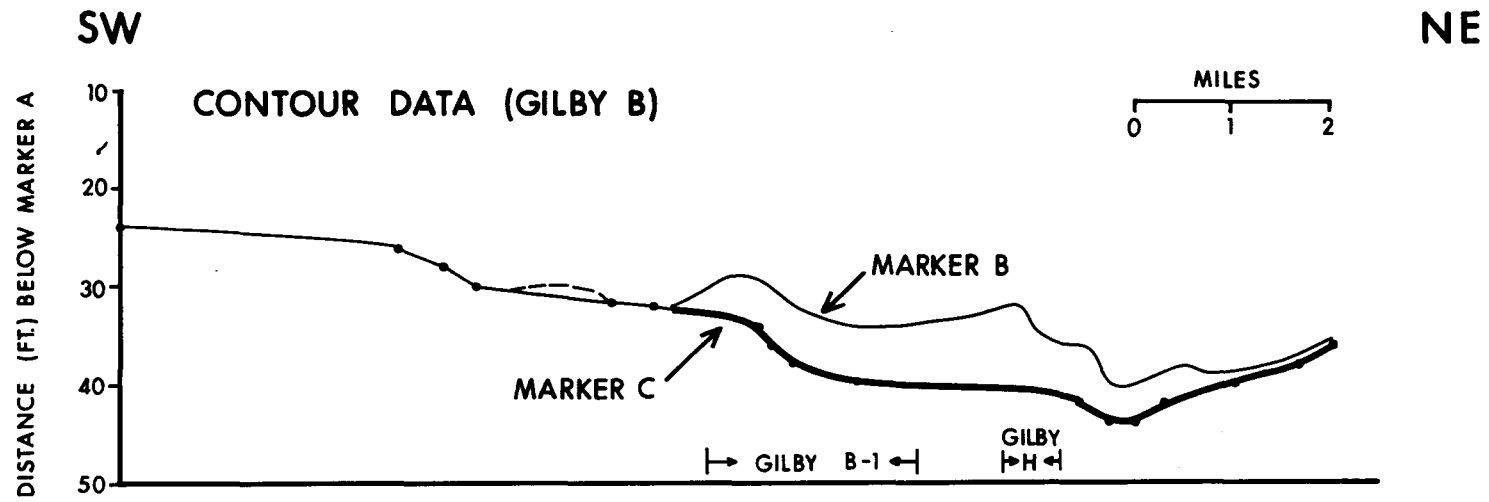
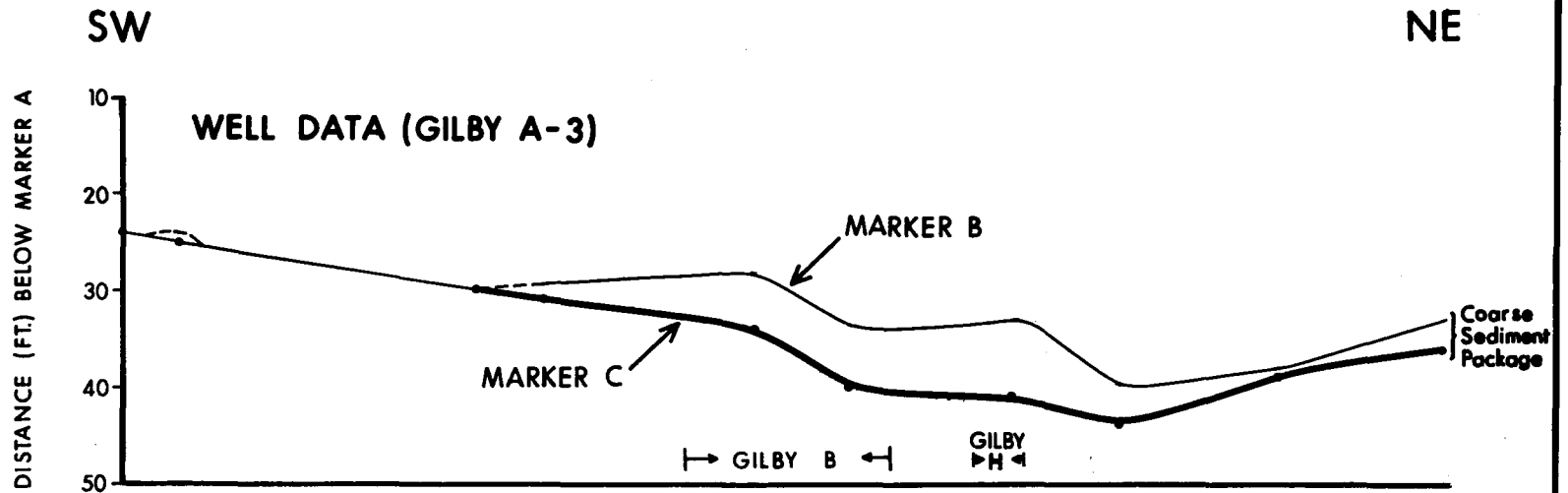


Fig. 6.2. Cross sections 6.2a and 6.2b, location shown on Figure 5.13. See text for discussion.

FIGURE 6-2

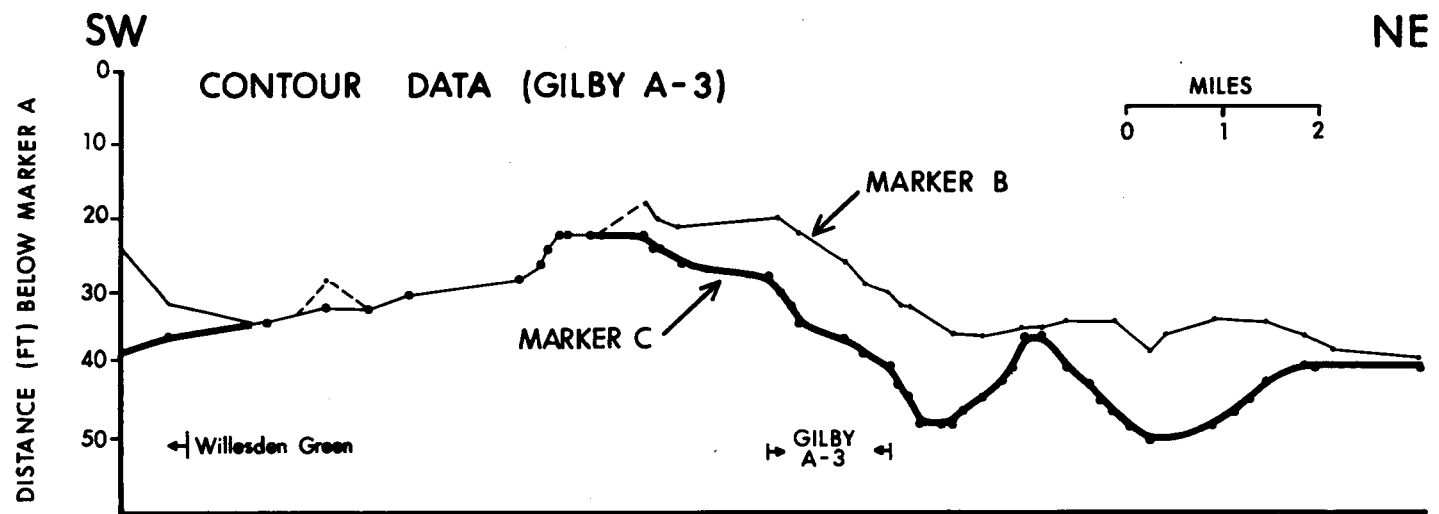
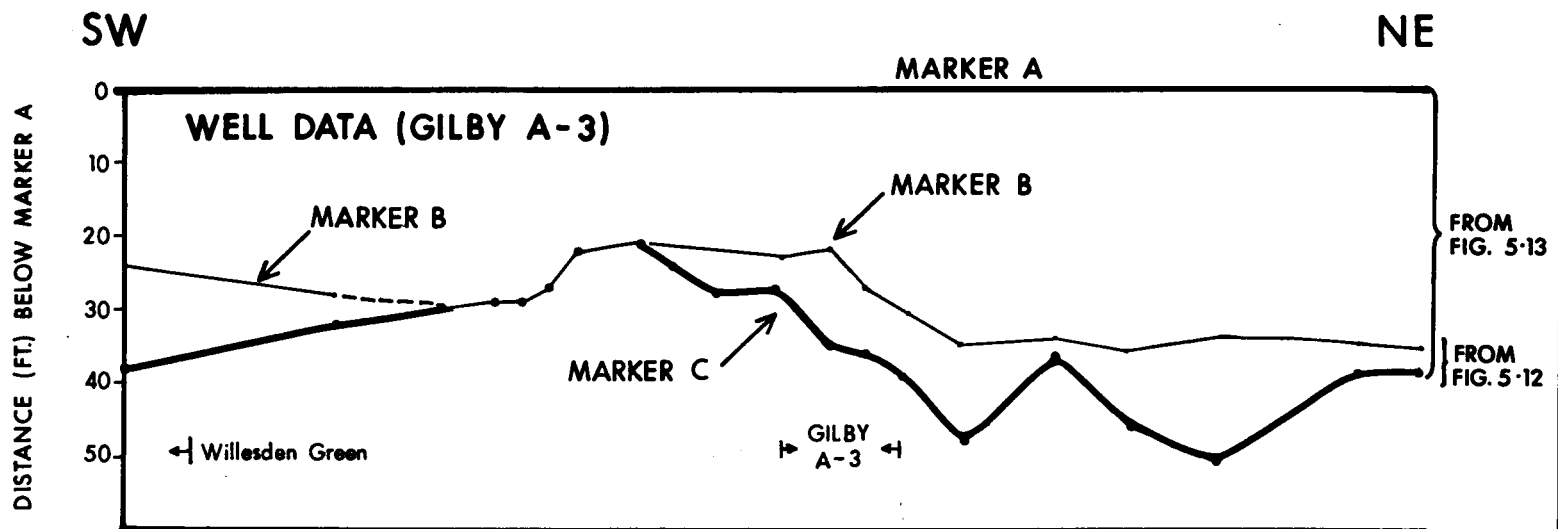
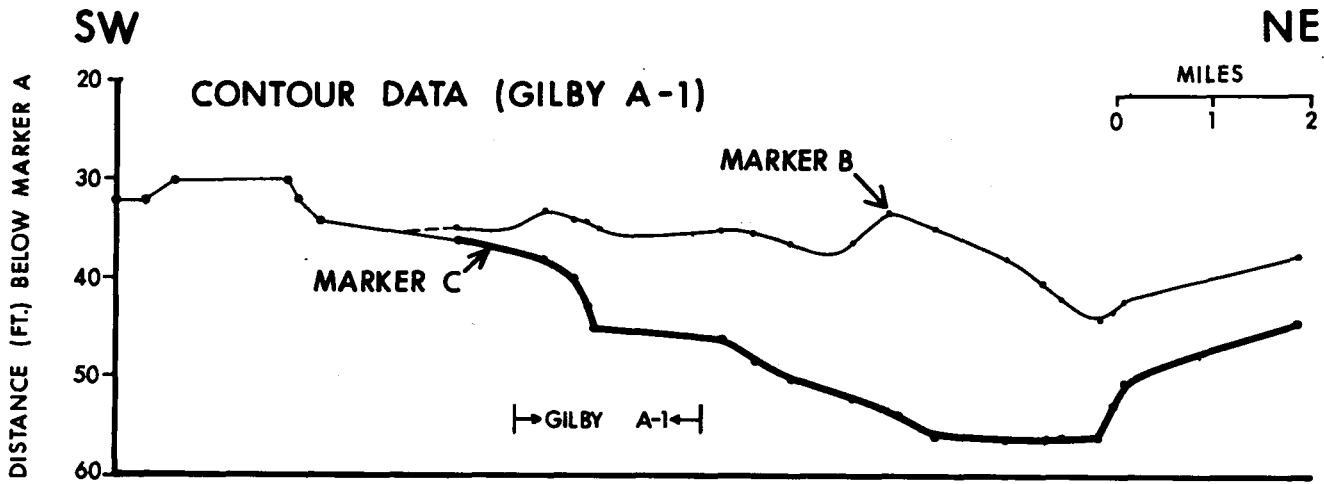
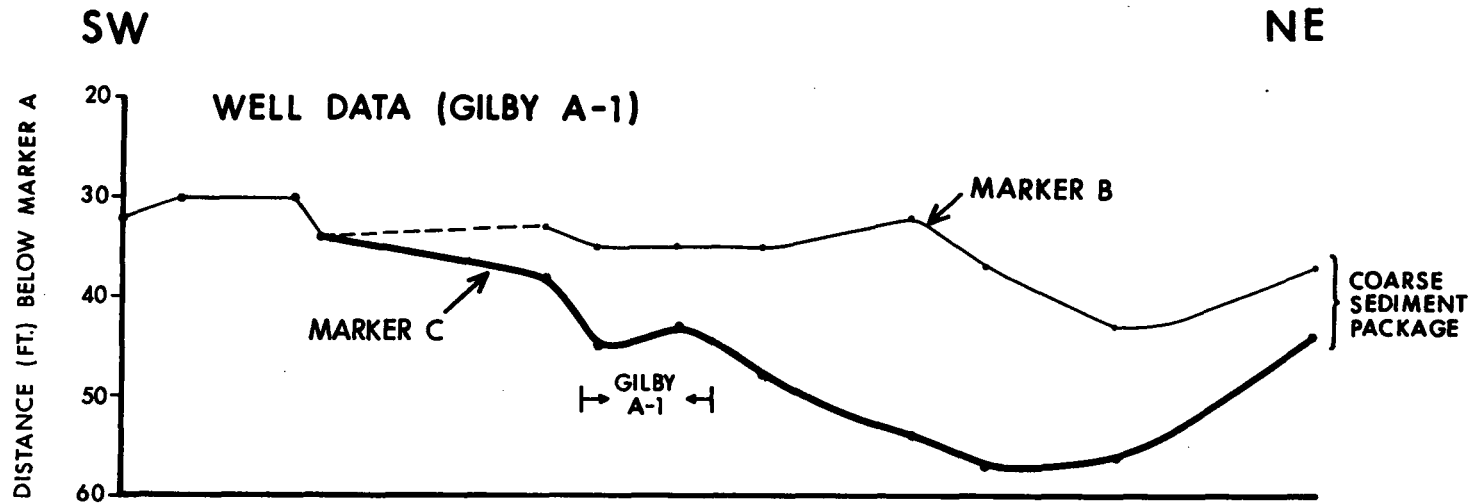


Fig. 6.3. Cross sections 6.3a and 6.3b, location shown on Figure 5.13. See text for discussion.

FIGURE 6-3



separation between upper marker A (which has been inferred to have been deposited horizontally and is used as the datum in all cross-sections, see Chapter 5) and the two markers which envelope the Viking coarse sediment package. The two markers are: marker C, which represents the base of the coarse sediment package, (this data is taken directly from Figure 5.13 - isopach of marker A to marker C) and marker B, which represents the top of the coarse sediment package (this data is taken from Figure 5.12 - isopach of the separation of markers B and C, or the thickness of the coarse sediment package). The separation between upper marker A and markers B and C is shown in feet along the left margin of all sections.

The upper cross-section in Figures 6.1, 6.2 and 6.3 was constructed using values only from actual resistivity well-log data which the line of section intersected (the round circles represent well locations from Figure 5.13 which are included in the upper sections). The lower cross-section in Figure 6.1, 6.2 and 6.3 was constructed using data taken from points of intersection between contour lines and the lines of section both from Figure 5.13. The lower cross-section in each figure was constructed using contour data, these sections contain more data points and generally appear smoother than the upper well-log data sections.

For the separation between markers A and C the value was simply taken from Figure 5.12 in the manner described

above. The separation between markers A and B was determined by plotting the thickness values of the coarse sediment package, equal to the marker B to C separation, from Figure 5.12. These values were taken from Figure 5.12 from the same positions where either: a) well-log locations which the line of section intersected in Figure 5.13 (upper cross-sections in Figures 6.1, 6.2 and 6.3; or b) contour lines and the lines of section from Figure 5.13 intersected (lower cross-sections in Figures 6.1, 6.2 and 6.3).

On all sections the positions (as mentioned above, relative to marker A) of marker B, representing the top of the coarse sediment package and marker C (heavy solid outline) representing the scoured surface or lower surface of the coarse sediment package are labelled. The single line to the left of the lines labelled marker B and C represents the coincident surface to these markers where no coarse sediment is found. The dotted lines above this surface represents the position of possible coarse sediment observed in core.

Location of Viking field boundaries are shown on each cross-section by vertical bars with "in-field" directed arrows. The vertical scale is shown in feet on the left of all cross-sections (labelled distance below marker A) and the horizontal scale is given on each figure in miles; vertical exaggeration is about 528x.

### 6.3.2. Discussion of Figures 6.1, 6.2 and 6.3

The upper surface of the coarse sediment package (marker B) gently undulates in all cross-sections. All sections demonstrate that the lower surface of the coarse sediment package (marker C) drops stratigraphically to the northeast beginning approximately to the southwest of the Gilby A and B field margins. Sections 6.1 and 6.3 (Figures 6.1 and 6.3 respectively) are similar in that the field areas Gilby B-1 and A-1 are situated at the position of the first stratigraphic drop. Further to the northeast (2 - 3 mi, 3.2 - 4.8 km) a second stratigraphic drop occurs, beyond this the scoured surface begins to rise stratigraphically again. Section 6.2 (Figure 6.2) differs from sections 6.1 and 6.3 in that at least 4 stratigraphic drops of the lower surface of the coarse sediment package (marker C) occur in 6.2. The first stratigraphic drop occurs to the southwest of the Gilby A-3 margin. The second stratigraphic drop coincides with the Gilby A-3 area. Towards the northeast are 2 stratigraphic drops separated by a significant 10 ft (3 m) stratigraphic rise of marker C. The location of the Gilby A and B fields on each section coincides with the steepest portion of the stratigraphic drop of marker C - the base of the coarse sediment.

The character of the coarse sediment package from resistivity logs observed through these sections (detail description in Chapter 5) change from "v-shaped" along the southwest field margins, to "blocky" at the central area of

the fields. To the northeast, outside of the field margins, the log character remains "blocky" but the maximum resistivity is often reduced to half of what it was within the fields. To the northeast of the Gilby A and B fields, the log character becomes "funnel-shaped".

The coarsest and best developed sandstones and conglomerates are observed in core, coincident with the "blocky" log response. The sandstones and conglomeratic facies identified in core would appear to be banked up against the steepest flank of the lower surface of the coarse sediment package. Towards the northeast beyond the field boundaries ("funnel-shaped" log response) the coarse sediment package is dominated by silt size sediment.

#### 6.4 Development and Infill of the Gilby Scour

Development of this scoured surface is problematic, a possible explanation for its development would have this area situated at or very near the shoreface. A rapid transgressive period or relative sea level rise could have resulted in erosion of the shoreface leaving the scoured topography. This topography being subsequently infilled by the Viking coarse sediment package during a relative drop in sea level in the (middle) Late Albian. Conversely, a rapid drop in sea level could have resulted in the development of the scoured topography by down-cutting in the study area. This was followed by scour topography infilling during

continued, though slower regression.

The coarse sediment package which infills the scour within the Gilby A and B field has from 1 to 3 individual coarsening-upward sequences (see Chapter 3). Each of these sequences may represent minor sea level fluctuations, with deposition occurring during regressive periods. The coarse sediment infilling of the scour probably occurred under influence of a longshore current system. Subsequent transgression resulted in the blanketing of the coarse sediment package with mudstone (Facies K).

Deposition of the pebble-veneer south of the Gilby A and B fields may be coeval with the scattered pebbles occurring at the base of the coarse sediment package within the Gilby fields (Chapter 3, section 3.4). This is apparent since in areas where the Skolithos burrows (Facies B) occur they are both infilled and overlain by chert pebbles, and in areas with no Skolithos burrows the base of the coarse sediment is composed of scattered chert pebbles. The thinness of the pebble veneer to the south of Gilby may be due to subsequent sea level fluctuations (during deposition of the coarse sediment package) which could have removed some of the pebbles leaving a portion as a thin veneer over the area. The area south of Gilby could have been subaerially exposed but evidence such as roots would have been removed.

The Viking coarse sediment package in the Willesden Green field may have been deposited prior to deposition at the Gilby fields. Since Willesden Green was landward

(during Viking Time) of the Gilby fields, deposition during a regressive period would likely have occurred at Willesden Green first.

It is unlikely that these Viking fields were deposited as an offshore sandbody such as an offshore bar since the sedimentology of the coarse sediment package does not exemplify the geometry of a positive bar feature (see Chapter 5). The contact of the lower surface of the coarse sediment package is erosive and abrupt with the lower siltstone (Facies A). An offshore bar would show a gradational coarsening-upward sequence. The capping conglomerates of the coarse sediment package are unsorted and show a chaotic fabric whereas in a barrier bar system reworking and sorting of the conglomerate might be expected. From the normalization procedure performed on the upper datum (marker A, see Chapter 5) and structure map of the upper datum the geometry of the lower surface of the coarse sediment package as shown in sections 6.1, 6.2 and 6.3 (Figures 6.1, 6.2 and 6.3) has a sigmoidal shape and represents at least one period of scour.

### 6.5 Development of the Viking Gilby A and B Fields

The Viking coarse sediment package (Facies C through J) in the Gilby A and B fields was deposited onto a scoured sigmoidal surface (recognized as Facies B) probably eroded during a change in relative sea level. The coarse sediment package was deposited and reworked by a longshore current system during a regressive period. The coarsest Viking sediment is concentrated along the most steeply dipping flank of the scour (the northeastern flank - dips of less than a degree). The Viking coarse sediment package "silts-out" to the northeast of the Gilby fields.

## REFERENCES

- Amajor, L. C., 1980. Chronostratigraphy, depositional patterns and environmental analysis of sub-surface Lower Cretaceous (Albian) Viking reservoir sandstones in central Alberta and part of southwestern Saskatchewan: Unpublished Ph.D Thesis, University of Alberta, Edmonton, 596 pp.
- Amajor, L. C., and Lerbekmo, J. F., 1980. Subsurface Correlation of Bentonite Beds in the Lower Cretaceous Viking Formation of South-Central Alberta. Bulletin of Canadian Petroleum Geologists, v. 28, no. 2, p. 149-172.
- Beach, F. K., 1955. Cardium, a turbidity current deposit: Bulletin of the Alberta Society of Petroleum Geologists, v. 3, p. 123-125.
- Beach, F. K., 1956, Reply to De Weil on turbidity current deposits: Bulletin of the Alberta Society of Petroleum Geologists, v. 4, no. 8, p. 175-177.
- Beach, F. K., 1962, Viking Deposition(discussion): Bulletin of the Alberta Society of Petroleum Geologists, v. 10, p. 210-212.
- Beaumont, E. A., 1984, Retrogradational shelf sedimentation: Lower Cretaceous Viking Formation, central Alberta: In Tillman, R. W. and C. T. Siemers, (eds.), Siliclastic Shelf Sediments: Society of Economic Paleontologists and Mineralogists, Tulsa, Oklahoma, Special Publication No. 34, p. 163-177.
- Berg, R. R, 1975, Depositional environment of Upper Cretaceous Sussex Sandstone, House Creek Field, Wyoming. American Association of Petroleum Geologists, Bulletin, v. 59, p. 2099-2110.
- Blatt, H., Middleton, G. V., Murray, R. C., 1980. Origin of sedimentary rocks: Prentice-Hall Inc., New Jersey, Second Edition, 782 pp.
- Boethling, F. C., 1977a, Increase in gas prices rekindles Viking-Sandstone interest: Oil and Gas Journal, v. 75, p. 196-200.
- Boethling, F. C., 1977b, Typical Viking Sequence: A marine sand enclosed with marine shales: Oil and Gas Journal, v. 75, p. 172-176.

- Brown, M. B., 1983. Two-Way and Multivary Frequency Tables - measures of association and the Log-Linear Model (complete and incomplete tables), In W. J. Dixon, chief editor, BMDP Statistical software, 1983 revised printing, University of California press, Los Angeles, California, p. 143-206.
- Caldwell, W. G. E., North, B. R., Stelck, C. R and Wall, J. H., 1978. A Foraminiferal Zonal Scheme for the Cretaceous System, in Stelck, C. R., ed., Western and Arctic Canadian Biostratigraphy: Geological Association of Canada, Sp. Paper 18, p. 496-575.
- Davis, J. C., 1973. Statistics and Data Analysis in Geology: John Wiley and Sons, Inc., New York, 550 pp.
- De Wiel, J. E., 1956, Viking and Cardium not turbidity current deposits, Bulletin of the Alberta Society of Petroleum Geologists, v. 4, p. 173-174.
- E.R.C.B., 1983, Alberta's Reserves of Crude Oil, Oil Sands, Gas, Natural Gas Liquids, and Sulphur at 31 December, 1983. ERCB Report 84-18.
- Evans, W. E., 1970, Imbricate linear sandstone bodies of Viking Formation in the Dodsland-Hoosier area of southwestern Saskatchewan, Canada. Bulletin of the American Association of Petroleum Geologists, Bulletin, v. 54, p. 469-486.
- Gammell, H. G., 1955, The Viking Member in central Alberta, Bulletin of the Alberta Society of Petroleum Geologists, v.3, p. 63-69.
- Glaister, R.P., 1959, Lower Cretaceous of southern Alberta and adjoining areas, Bulletin of the American Association of Petroleum Geologists, v. 43, p. 590-640.
- Hobson, J. P. Jr., Fowler, M. L., and Beaumont, E. A., 1982. Depositional and statistical exploration models, Upper Cretaceous offshore sandstone complex, Sussex Member, House Creek Field, Wyoming. Bulletin of the American Association of Petroleum Geologists, v. 66, p. 689-707.
- Jones, H. L., 1961b. Viking deposition in southwestern Saskatchewan with a note on the source of the sediments. Bulletin of the Alberta Society of Petroleum Geologists, v. 9, p. 231-244.
- Koldijk, W. S., 1976. Gilby Viking B: a storm deposit. In: Lerand M. M. (ed.), The sedimentology of selected clastic oil and gas reservoirs in Alberta. Canadian Society of Petroleum Geologists, p. 62-77.

- Kopp O. C, 1981, Cathodoluminescence petrography - a valuable tool for teaching and research, *Journal of Geological Education*, v. 29, p. 108.
- La Fon, N. A., 1981. Offshore bar deposits of Semilla Sandstone Member of Mancos Shale (Upper Cretaceous), San Juan Basin, New Mexico. *American Association of Petroleum Geologists, Bulletin*, v. 65, p. 706-721.
- Love A. M., 1959. The Gilby-Bentley Oil Field, Oil Fields of Alberta,
- Nickel, E., 1978, The present status of cathode luminescence as a tool in sedimentology: *Minerals Science Engineering*, v. 10, p. 73-100.
- Oliver, T. A., 1960. "The Viking-Cadotte Relationship", *Journal Alberta Society of Petroleum Geologist*, v. 8, n. 9, pp. 247-253.
- Pemberton, S. G. and Frey, R. W., 1983. Biogenic structures in Upper Cretaceous outcrops and cores: *Canadian Soc. of Petroleum Geologists, Conference on the Mesozoic of Middle North America, Field Trip Guidebook 8*, 161p.
- Pemberton, S. G. and Frey, R. W., 1984. Ichnology of storm-influenced shallow marine sequence: Cardium Formation (Upper Cretaceous) at Seebe, Alberta. *In: Stott, D.F and Glass D.J. (eds.), The Mesozoic of Middle North America. Calgary, Alberta, Canadian Society of Petroleum Geologists, Memoir 9*, p. 281-304.
- Reinson, G. E., Foscolos, A. E., and Powell, T. G., 1983. Comparison of Viking sandstone sequences, Joffre and Caroline Fields. *In: McLean, J. R. and Reinson, G. E. (eds.), Sedimentology of selected Mesozoic clastic sequences. Canadian Society of Petroleum Geologists*, p. 101-117.
- Robb, G. A., 1985. Sedimentology and Diagenesis of the Viking Formation, Garrington Field, Alberta. Unpublished M.Sc. thesis, University of Edmonton, p 181.
- Scholle, P. A., 1979. Memoir 28 - A Colour Illustrated Guide To Constituents, Textures, Cements, and Porosities of Sandstones and Associated Rocks. *American Association of Petroleum Geologists, Tulsa*,
- Seeling, A., 1978. The Shannon Sandstone, a further look at the environment of deposition at Heldt Draw Field, Wyoming. *Mountain Geologist*, v. 15, p. 133-144.

- Shelton, J. W., 1973, Models of sand and sandstone deposits: a methodology for determining sand genesis and trend: Viking Sandstone, Cretaceous, Joffre Field, Alberta, Bulletin of the Oklahoma Geological Survey, v. 118, p. 91-94.
- Simpson, F., 1975, Marine Lithofacies and Biofacies of the Colorado Group (Middle Albian to Santonian) in Saskatchewan, In Caldwell, W.G.E. (ed.), The Cretaceous system in the Western Interior of North America, Geological Association of Canada, Special Paper No. 13, p. 553-587.
- Slipper, S.E., 1918. Viking Gas Field, Structure of Area: Geological Survey Summary Department, 1917, Part C, p. 8c.
- Spearing, D. R., 1976. Upper Cretaceous Shannon Sandstone: an offshore shallow marine sand body. Wyoming Geological Association, 28th Annual Field Conference, Guidebook, p. 65-72.
- Stelck, C. R., 1958. "Stratigraphic Position of the Viking Sand", Journal Alberta Society Petroleum Geologists, v. 6, no. 1, pp. 2-7.
- Stelck, C. R., 1975, The Upper Albian Miliammina manitobensis zone in northeastern British Columbia: In Caldwell, W.G.E., (ed.), The Cretaceous system in the Western Interior of North America: Geological Association of Canada, Special Paper No. 13, P. 253-275.
- Swift, D. J. P., 1984. Response of the shelf floor to flow. In: Tillman, R. W., Swift, D. J. P., and Walker R. G. (eds.), Shelf Sands and Sandstone Reservoirs, Society of Economic Paleontologists and Mineralogists, Short Course 13.
- Swift, D. J. P., and Field, M. E., 1981, Evolution of a classic sand ridge field: Maryland Sector, North American inner shelf. Sedimentology, v. 28, p. 461-481.
- Swift, D. J. P., and Rice, D. D., 1984. Sandbodies on muddy shelves: a model for sedimentation in the Western Interior Seaway, North America. In: Tillman, R. W. and Siemers C. T. (eds.), Siliciclastic shelf sediments, Society of Economic Paleontologists and Mineralogists, Special Publication 34, p. 43-62.
- Tizzard, P.G., and J.G. Lerbekmo, 1975, Depositional history of the Viking formation, Suffield area, Alberta, Canada: Bulletin of the Canadian Society of Petroleum Geologists, v. 23, p. 715-752.

- Walker, R. G., 1983a. Cardium Formation 1. "Cardium, a turbidity current deposit" (Beach, 1955): A brief history of ideas. *Bulletin of Canadian Petroleum Geology*, v. 31, p. 205-212.
- Walker, R. G., 1983b. Cardium Formation 2. Sand body geometry and stratigraphy in the Garrington - Caroline - Ricinus area, Alberta - the "ragged blanket" model. *Bulletin of Canadian Petroleum Geology*, v. 31, p. 14-26.
- Walker, R. G., 1984a. Shelf and shallow marine sands. In: Walker R. G. (ed.), *Facies Models* (second edition), Geoscience Canada reprint series 1, p. 141-170.
- Walker, R. G., 1984b. Geological evidence for storm transportation and deposition on ancient shelves. In: Tillman, R. W., Swift, D. J. P., and Walker R. G. (eds.), *Shelf Sands and Sandstone Reservoirs*, Society of Economic Paleontologists and Mineralogists, Short Course 13, (in press).
- Walker, R. G., 1976. Cardium Formation at Ricinus Field, Alberta: a channel cut and filled by turbidity currents in the Cretaceous Western Interior Seaway. *American Association of Petroleum Geologists, Bulletin*.
- Weimer, R. J., 1983. Relation of unconformities, tectonics and sea-level changes, Cretaceous of Denver Basin and adjacent areas. In: Reynolds, M. and Dolly, E. (eds.) *Mesozoic paleogeography of west-central United States*. Denver, Colorado, Society of Economic Mineralogists and Paleontologists, Rocky Mountain Section, Special Publication, p. 359-376.
- Zinkernagel, U., 1978, Cathodoluminescence of quartz and its application to sandstone petrology, ch. 8. In Fuchtbauer, H, et al, *Contributions to Sedimentology*, Stuttgart, 1978.

APPENDIX 1: MARKOV CHAIN ANALYSIS - DATA AND RESULTS

# GILBY A - 1

PAGE 5 BMDP4F MARKOV CHAIN ANALYSIS OF GILBY A SOUTHEAST

\*\*\*\*\*  
TABLE PARAGRAPH 1

\*\*\*\*\* OBSERVED FREQUENCY TABLE  
ASTERISK INDICATES MISSING VALUE

BELOW	ABOVE												
	A	B	C	D1	D2	E1	E2	F	G	H	I	J	K
A	*												
B		*											
C			*										
D1				*									
D2					*								
E1						*							
E2							*						
F								*					
G									*				
H										*			
I											*		
J												*	
K													*
TOTAL	0	12	26	4	10	15	27	21	13	16	9	16	22

BELOW	ABOVE	TOTAL
A		0
B		12
C		26
D1		4
D2		10
E1		15
E2		27
F		21
G		13
H		16
I		9
J		16
K		22
TOTAL	191	191

TOTAL OF THE OBSERVED FREQUENCY TABLE IS 191  
SUMMED OVER 157 CELLS WITHOUT STRUCTURAL ZEROS

PAGE 6 BMDP4F MARKOV CHAIN ANALYSIS OF GILBY A SOUTHEAST

\*\*\*\*\*  
MODEL 1

100xL	D.F.	LIKELIHOOD-RATIO CHI-SQUARE	PROB	PEARSON CHI-SQUARE	PROB	ITER.
A,B	118	106.91	.0000	366.77	.0000	3

\*\*\*\*\* EXPECTED VALUES USING ABOVE MODEL  
ASTERISK INDICATES MISSING VALUE

BELOW	ABOVE												
	A	B	C	D1	D2	E1	E2	F	G	H	I	J	K
A	*												
B		*											
C			*										
D1				*									
D2					*								
E1						*							
E2							*						
F								*					
G									*				
H										*			
I											*		
J												*	
K													*
TOTAL	0	12.0	26.0	4.0	10.0	15.0	27.0	21.0	13.0	16.0	9.0	16.0	22.0

BELOW	ABOVE	TOTAL
A		0
B		12.0
C		26.0
D1		4.0
D2		10.0
E1		15.0
E2		27.0
F		21.0
G		13.0
H		16.0
I		9.0
J		16.0
K		22.0
TOTAL	191.0	191.0

PAGE 7 BMDP4F MARKOV CHAIN ANALYSIS OF GILBY A SOUTHEAST

\*\*\*\*\* CRITERION TO SELECT CELLS IS MAXIMUM STANDARDIZED DEVIATE = (OBS. - EXP.) / SQRT(EXP.)

STEP	CHISQUARE	D.F.	PROB	MAXIMUM DEVIATION	FOUND IN CELL	
					BELOW	ABOVE
0	106.91	118	.00000	9.266	A	B
1	246.73	109	.00000	5.179	G	J
2	227.67	108	.00000	4.950	C	E1
3	202.38	107	.00000	4.268	E1	D2
4	189.92	106	.00000	5.393	E1	C
5	162.12	105	.00029	3.793	J	K
6	149.47	104	.00277	3.530	J	G
7	139.40	103	.00985	3.323	A	C
8	136.11	102	.03164	3.591	B	C
9	119.80	101	.09766	3.641	B	E1
10	113.23	100	.17268	3.056	A	E1
11	109.49	99	.22132			

P-VALUE EXCEEDS SPECIFIED PROBABILITY LEVEL. STEPPING STOPS.

# GILBY A - 2

PAGE 5 BMDP4F MARKOV CHAIN ANALYSIS OF GILBY A GENERAL

\*\*\*\*\*  
 \*\*\*\*\*  
 \*\*\*\*\*

\*\*\*\*\* OBSERVED FREQUENCY TABLE \*\*\*\*\*  
 \*\*\*\*\*  
 \*\*\*\*\*

\*\*\*\*\*  
 \*\*\*\*\*  
 \*\*\*\*\*

	A	B	C	D1	D2	E	F	G	H	I	J	K	L	TOTAL
A	1	1	1	1	1	1	1	1	1	1	1	1	1	13
B	1	1	1	1	1	1	1	1	1	1	1	1	1	13
C	1	1	1	1	1	1	1	1	1	1	1	1	1	13
D1	1	1	1	1	1	1	1	1	1	1	1	1	1	13
D2	1	1	1	1	1	1	1	1	1	1	1	1	1	13
E	1	1	1	1	1	1	1	1	1	1	1	1	1	13
F	1	1	1	1	1	1	1	1	1	1	1	1	1	13
G	1	1	1	1	1	1	1	1	1	1	1	1	1	13
H	1	1	1	1	1	1	1	1	1	1	1	1	1	13
I	1	1	1	1	1	1	1	1	1	1	1	1	1	13
J	1	1	1	1	1	1	1	1	1	1	1	1	1	13
K	1	1	1	1	1	1	1	1	1	1	1	1	1	13
L	1	1	1	1	1	1	1	1	1	1	1	1	1	13
TOTAL	13	13	13	13	13	13	13	13	13	13	13	13	13	13

TOTAL OF 136 OBSERVED FREQUENCY TABLE IS  
 SUMMED OVER ALL CELLS WITHOUT STRUCTURAL ZEROS

PAGE 6 BMDP4F MARKOV CHAIN ANALYSIS OF GILBY A GENERAL

\*\*\*\*\*  
 \*\*\*\*\*  
 \*\*\*\*\*

MODEL

1000

D.P. 90  
 15.98 2.7731

LIKELIHOOD-RATIO  
 241.3044 2109

CHI-SQUARE  
 61.883 2.7174

\*\*\*\*\* AFFECTED VALUES USING ABOVE MODEL

\*\*\*\*\*  
 \*\*\*\*\*  
 \*\*\*\*\*

	A	B	C	D1	D2	E	F	G	H	I	J	K	L	TOTAL
A	1	1	1	1	1	1	1	1	1	1	1	1	1	13
B	1	1	1	1	1	1	1	1	1	1	1	1	1	13
C	1	1	1	1	1	1	1	1	1	1	1	1	1	13
D1	1	1	1	1	1	1	1	1	1	1	1	1	1	13
D2	1	1	1	1	1	1	1	1	1	1	1	1	1	13
E	1	1	1	1	1	1	1	1	1	1	1	1	1	13
F	1	1	1	1	1	1	1	1	1	1	1	1	1	13
G	1	1	1	1	1	1	1	1	1	1	1	1	1	13
H	1	1	1	1	1	1	1	1	1	1	1	1	1	13
I	1	1	1	1	1	1	1	1	1	1	1	1	1	13
J	1	1	1	1	1	1	1	1	1	1	1	1	1	13
K	1	1	1	1	1	1	1	1	1	1	1	1	1	13
L	1	1	1	1	1	1	1	1	1	1	1	1	1	13
TOTAL	13	13	13	13	13	13	13	13	13	13	13	13	13	13

PAGE 7 BMDP4F MARKOV CHAIN ANALYSIS OF GILBY A GENERAL

\*\*\*\*\* STOPPAGE CELL DILUTION IS NOT PERFORMED. P-VALUE OF MODEL FIT ( 6.7174 ) IS GREATER THAN CRITERION PROB ( .2500 )  
 NUMBER OF ITERATIONS WITHOUT CHANGE USED IN PRECEDING PARALLEL 1005  
 CPU TIME USED 3.499 SECONDS

\*\*\*\*\*  
 TABLE PARAGRAPH 1  
 \*\*\*\*\*

\*\*\*\*\* OBSERVED FREQUENCY TABLE 1

\*\*\*\*\*  
 ASTERISK INDICATES MISSING VALUE

	ABOVE											TOTAL
	A	B	C	D	E	F	G	H	I	J	K	
A	0	0	0	0	0	0	0	0	0	0	0	0
B	0	0	0	0	0	0	0	0	0	0	0	0
C	0	0	0	0	0	0	0	0	0	0	0	0
D	0	0	0	0	0	0	0	0	0	0	0	0
E	0	0	0	0	0	0	0	0	0	0	0	0
F	0	0	0	0	0	0	0	0	0	0	0	0
G	0	0	0	0	0	0	0	0	0	0	0	0
H	0	0	0	0	0	0	0	0	0	0	0	0
I	0	0	0	0	0	0	0	0	0	0	0	0
J	0	0	0	0	0	0	0	0	0	0	0	0
K	0	0	0	0	0	0	0	0	0	0	0	0
TOTAL	0	0	0	0	0	0	0	0	0	0	0	0

TOTAL OF THE OBSERVED FREQUENCY TABLE  
 SUMMED OVER 93 CELLS WITHOUT STRUCTURAL ZEROS

\*\*\*\*\*  
 MODEL 1  
 \*\*\*\*\*

MODEL 1  
 D.F. 26  
 LIKELIHOOD-RATIO 110.0  
 G-SQUARE 110.0  
 P-VALUE 0.0022

PERIODIC  
 CHANGES PERIOD 11.0  
 110.0  
 110.0

\*\*\*\*\* LEARNED VALUES USING ABOVE MODEL

\*\*\*\*\*  
 ASTERISK INDICATES MISSING VALUE

	ABOVE											TOTAL
	A	B	C	D	E	F	G	H	I	J	K	
A	0	0	0	0	0	0	0	0	0	0	0	0
B	0	0	0	0	0	0	0	0	0	0	0	0
C	0	0	0	0	0	0	0	0	0	0	0	0
D	0	0	0	0	0	0	0	0	0	0	0	0
E	0	0	0	0	0	0	0	0	0	0	0	0
F	0	0	0	0	0	0	0	0	0	0	0	0
G	0	0	0	0	0	0	0	0	0	0	0	0
H	0	0	0	0	0	0	0	0	0	0	0	0
I	0	0	0	0	0	0	0	0	0	0	0	0
J	0	0	0	0	0	0	0	0	0	0	0	0
K	0	0	0	0	0	0	0	0	0	0	0	0
TOTAL	0	0	0	0	0	0	0	0	0	0	0	0

\*\*\*\*\* CRITERION TO SELECT CELLS AS MAXIMUM STANDARDIZED DEVIATE = (93.1 - L.P.M.) / (3.041148 P.D.)

STEP MISSQUARE D.F. P-VAL MAXIMUM DEVIATION ALLOW FOUND IN CELL

1 122.33 55 0.0016 4.367 A 0

2 79.81 57 0.0169 3.131 J 1

3 144.2 54 0.0016

P-VALUE EXCEEDS SPECIFIED PROBABILITY LEVELS STEPPING STOPS

\*\*\*\*\*  
 TABLE PARAGRAPH 1  
 \*\*\*\*\*  
 \*\*\*\*\* OBSERVED FREQUENCY TABLE 1  
 ASTERISK INDICATES MISSING VALUE

		BELOW											TOTAL	
		A	B	C	O1	O2	E2	F	G	H	I	J	K	TOTAL
A		0	0	0	0	0	0	0	0	0	0	0	0	0
B		0	0	0	0	0	0	0	0	0	0	0	0	0
C		0	0	0	0	0	0	0	0	0	0	0	0	0
O1		0	0	0	0	0	0	0	0	0	0	0	0	0
O2		0	0	0	0	0	0	0	0	0	0	0	0	0
E2		0	0	0	0	0	0	0	0	0	0	0	0	0
F		0	0	0	0	0	0	0	0	0	0	0	0	0
G		0	0	0	0	0	0	0	0	0	0	0	0	0
H		0	0	0	0	0	0	0	0	0	0	0	0	0
I		0	0	0	0	0	0	0	0	0	0	0	0	0
J		0	0	0	0	0	0	0	0	0	0	0	0	0
K		0	0	0	0	0	0	0	0	0	0	0	0	0
TOTAL		0	0	0	0	0	0	0	0	0	0	0	0	0

TOTAL OF THE OBSERVED FREQUENCY TABLE IS 64  
 SUMMED OVR 132 CELLS WITHOUT STRUCTURAL ZEROS

\*\*\*\*\*  
 MODEL 1  
 \*\*\*\*\*

MODEL	D.F.	LIKELIHOOD-RATIO CHI-SQUARE	PROB	PEARSON CHI-SQUARE	PROB	ITER.
A.D.	99	118.59	.0075	141.79	.0031	5

\*\*\*\*\* EXPECTED VALUES USING ABOVE MODEL  
 ASTERISK INDICATES MISSING VALUE

		BELOW											TOTAL	
		A	B	C	O1	O2	E2	F	G	H	I	J	K	TOTAL
A		0	0	0	0	0	0	0	0	0	0	0	0	0
B		0	0	0	0	0	0	0	0	0	0	0	0	0
C		0	0	0	0	0	0	0	0	0	0	0	0	0
O1		0	0	0	0	0	0	0	0	0	0	0	0	0
O2		0	0	0	0	0	0	0	0	0	0	0	0	0
E2		0	0	0	0	0	0	0	0	0	0	0	0	0
F		0	0	0	0	0	0	0	0	0	0	0	0	0
G		0	0	0	0	0	0	0	0	0	0	0	0	0
H		0	0	0	0	0	0	0	0	0	0	0	0	0
I		0	0	0	0	0	0	0	0	0	0	0	0	0
J		0	0	0	0	0	0	0	0	0	0	0	0	0
K		0	0	0	0	0	0	0	0	0	0	0	0	0
TOTAL		0	0	0	0	0	0	0	0	0	0	0	0	0

\*\*\*\*\* CRITERION TO SELECT CELLS IS MAXIMUM STANDARDIZED DEVIATE = (OBS. - EXP.) / SQRT(EXP.)

STEP	CHISQUARE	D.F.	PROB	MAXIMUM DEVIATION	BELOW	FOUND IN CELL ABOVE
0	118.59	99	.00752			
1	108.12	98	.42163	4.099	A	B

P-VALUE EXCEEDS SPECIFIED PROBABILITY LEVEL. STEPPING STOPS.

\*\*\*\*\* EXPECTED VALUES USING ABOVE MODEL

ASTERISK INDICATES MISSING VALUE

		BELOW											TOTAL	
		A	B	C	O1	O2	E2	F	G	H	I	J	K	TOTAL
A		0	0	0	0	0	0	0	0	0	0	0	0	0
B		0	0	0	0	0	0	0	0	0	0	0	0	0
C		0	0	0	0	0	0	0	0	0	0	0	0	0
O1		0	0	0	0	0	0	0	0	0	0	0	0	0
O2		0	0	0	0	0	0	0	0	0	0	0	0	0
E2		0	0	0	0	0	0	0	0	0	0	0	0	0
F		0	0	0	0	0	0	0	0	0	0	0	0	0
G		0	0	0	0	0	0	0	0	0	0	0	0	0
H		0	0	0	0	0	0	0	0	0	0	0	0	0
I		0	0	0	0	0	0	0	0	0	0	0	0	0
J		0	0	0	0	0	0	0	0	0	0	0	0	0
K		0	0	0	0	0	0	0	0	0	0	0	0	0
TOTAL		0	0	0	0	0	0	0	0	0	0	0	0	0

NUMBER OF INTEGER WORDS OF STORAGE USED IN PRECEDING PROBLEM 1585  
 CPU TIME USED 3.948 SECONDS

GILBY B - 1

## APPENDIX 2: WELL LOCATIONS OF EXAMINED VIKING CORE

The locations of all Viking Formation core examined in this study are listed on the following page. These locations are shown in Figure 5.9 (p.174). Diagrammatic core descriptions of underlined core locations are included in appendix 3 (p.219).

## TWP. 39

9-27-39-28W43-35-39-28W4

14-9-39-2W5

## TWP. 40

12-1-40-1W514-1-40-1W5

8-3-40-1W5

16-9-40-1W510-10-40-1W512-10-40-1W5

4-11-40-1W5

12-11-40-1W5

4-12-40-1W5

2-16-40-1W510-16-40-1W512-16-40-1W58-17-40-1W510-17-40-1W5

16-18-40-1W5

2-19-40-1W5

8-19-40-1W5

10-19-40-1W5

12-19-40-1W5

16-19-40-1W5

4-20-40-1W5

2-30-40-1W54-30-40-1W5

11-33-40-1W5

10-24-40-2W5

16-24-40-2W5

4-25-40-2W5

10-26-40-2W5

12-32-40-2W5

6-2-40-3W5

10-2-40-3W5

15-22-40-3W5

15-2-40-4W5

13-4-40-4W5

5-9-40-4W5

7-9-40-4W5

3-18-40-4W5

7-22-40-4W5

## TWP. 41

2-5-41-2W5

6-5-41-2W5

2-6-41-2W5

6-8-41-2W5

4-9-41-2W5

4-2-41-3W512-2-41-3W5

4-3-41-3W5

12-3-41-3W510-7-41-3W5

4-8-41-3W5

10-8-41-3W5

12-8-41-3W5

2-9-41-3W5

4-9-41-3W512-9-41-3W5

10-10-41-3W5

2-17-41-3W5

4-18-41-3W510-30-41-3W5

14-16-41-4W5

16-18-41-4W5

10-32-41-4W5

10-34-41-4W510-35-41-4W54-36-41-4W5

10-10-41-5W5

12-11-41-5W5

## TWP. 42

4-3-42-4W5

4-4-42-4W5

10-4-42-4W5

2-5-42-4W512-5-42-4W5

4-6-42-4W5

4-8-42-4W5

16-9-42-4W5

10-17-42-4W510-2-42-5W57-10-42-5W54-12-42-5W5

### APPENDIX 3: DIAGRAMMATIC CORE DESCRIPTIONS

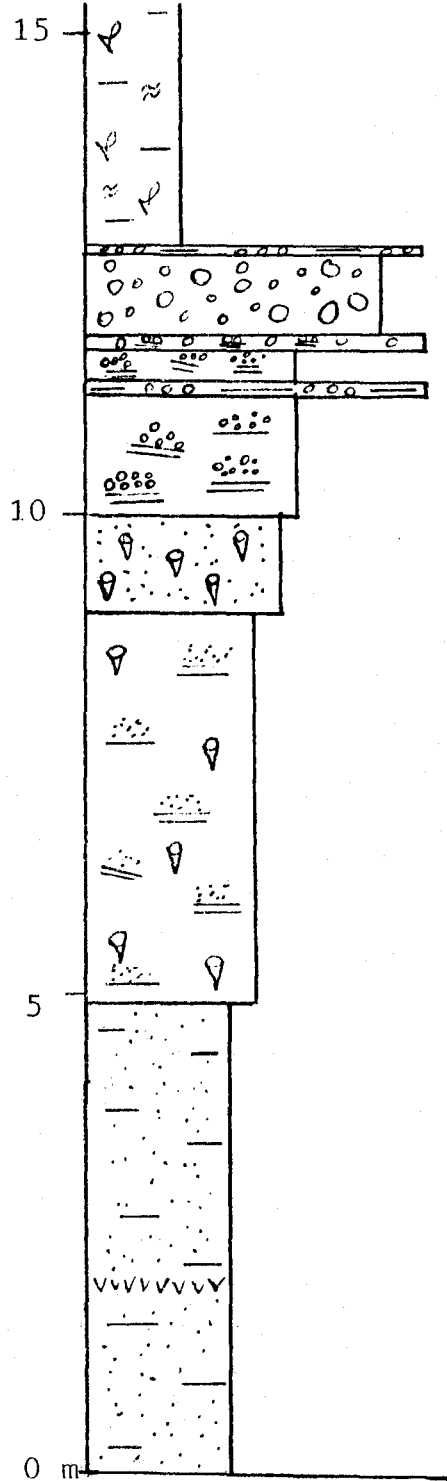
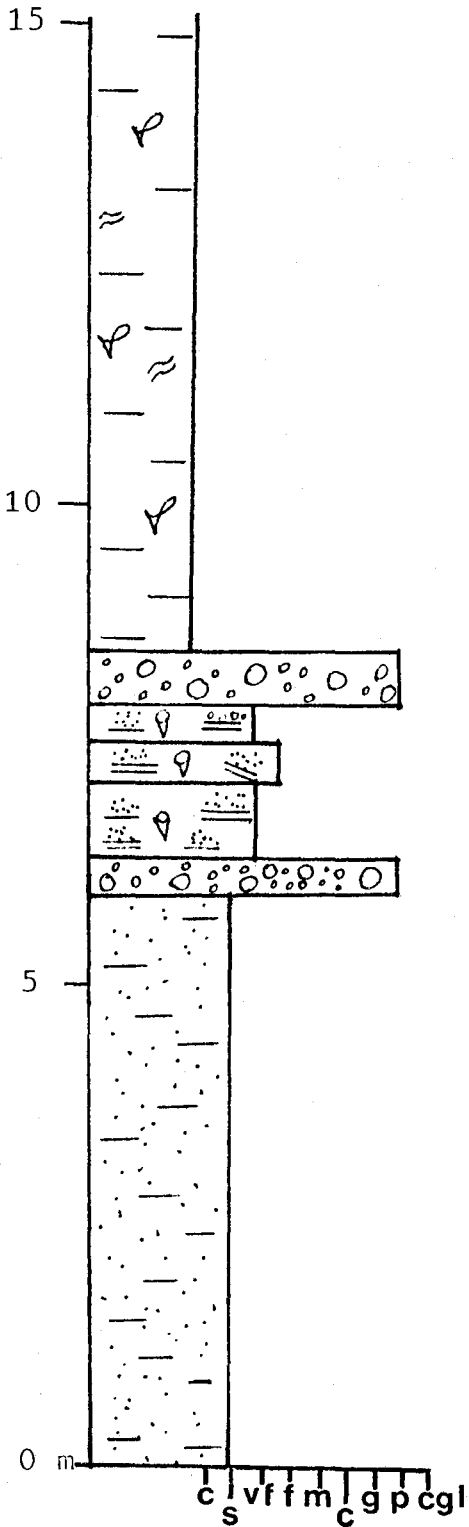
Diagrammatic core descriptions of the 44 of the 80 core examined in this study are included on the following pages. Facies symbols are identical to those in Figure 3.34 (p.77). Figure 5.9 (p.174) shows the locations of the of cores within the study area.

9-27-39-28W4

5442-5491'

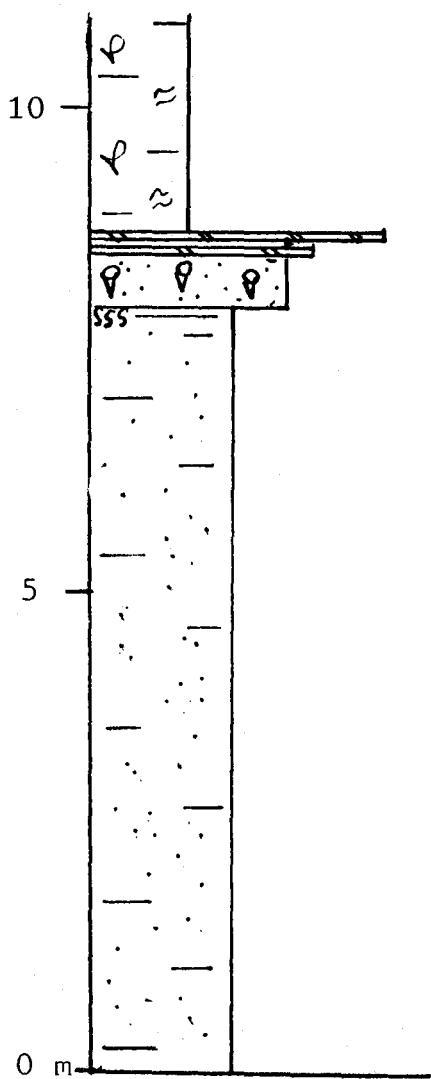
3-35-39-28-W4

5450-5499'



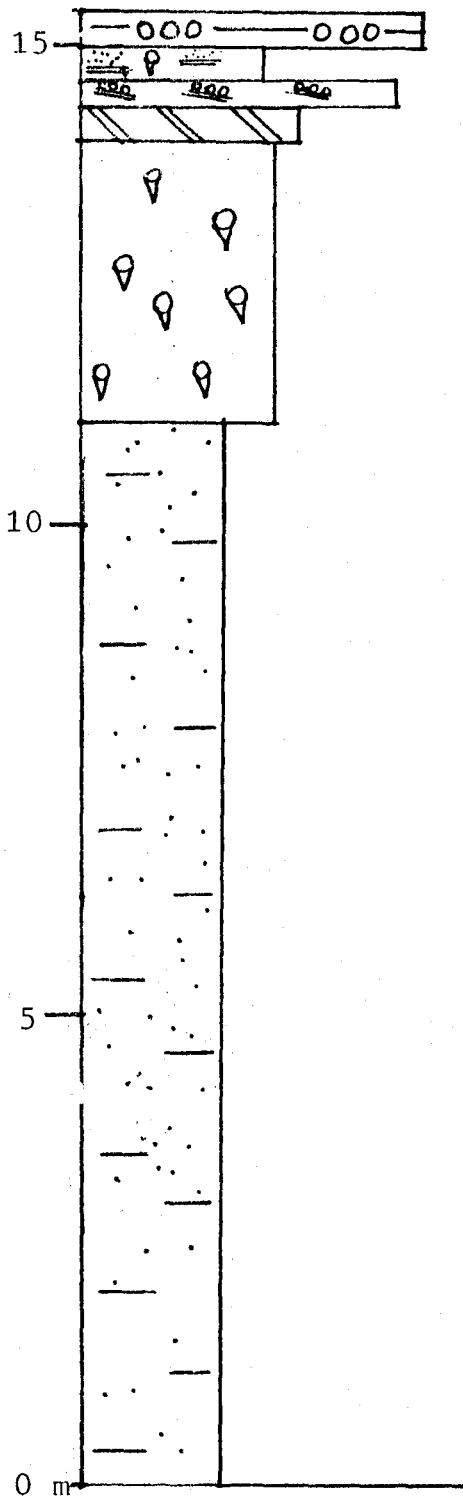
12-1-40-1W5

5475-5513'



14-1-40-1W5

5474-5527'



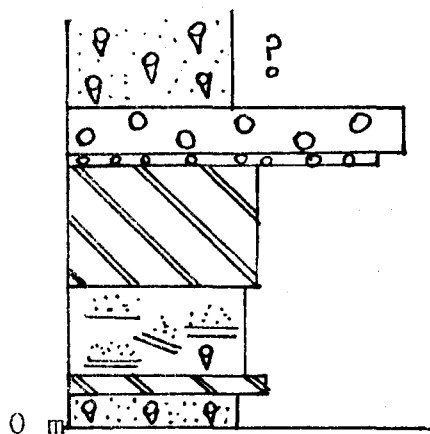
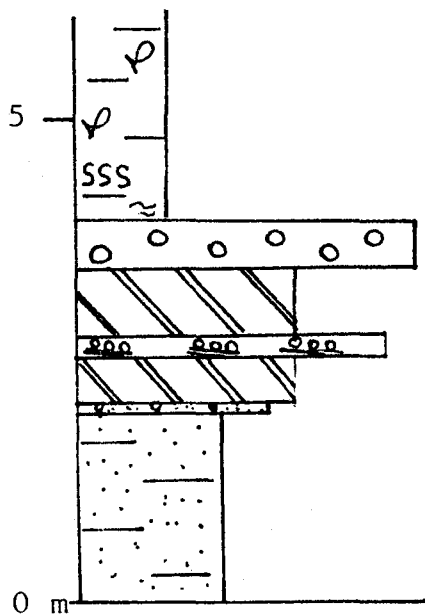


12-10-40-1W5

5493-5513'

12-11-40-1W5

5509-5522'

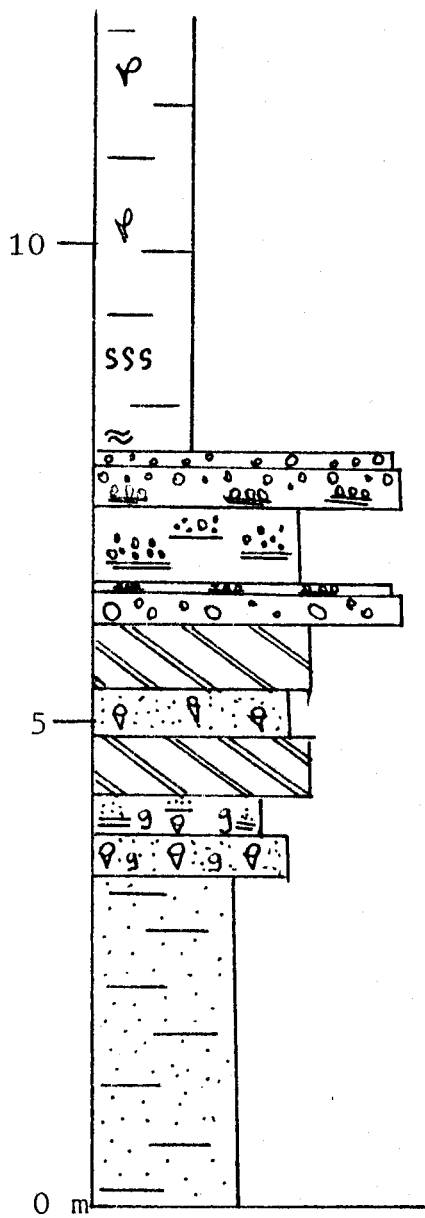
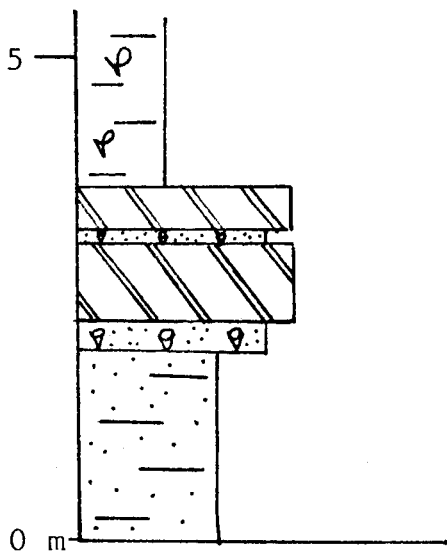


2-16-40-1W5

5559-5577'

10-16-40-1W5

5555-5595'



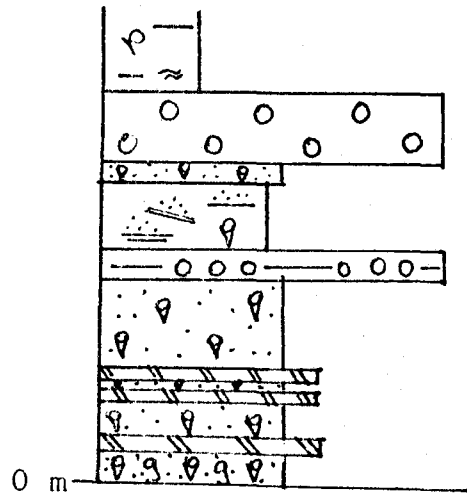
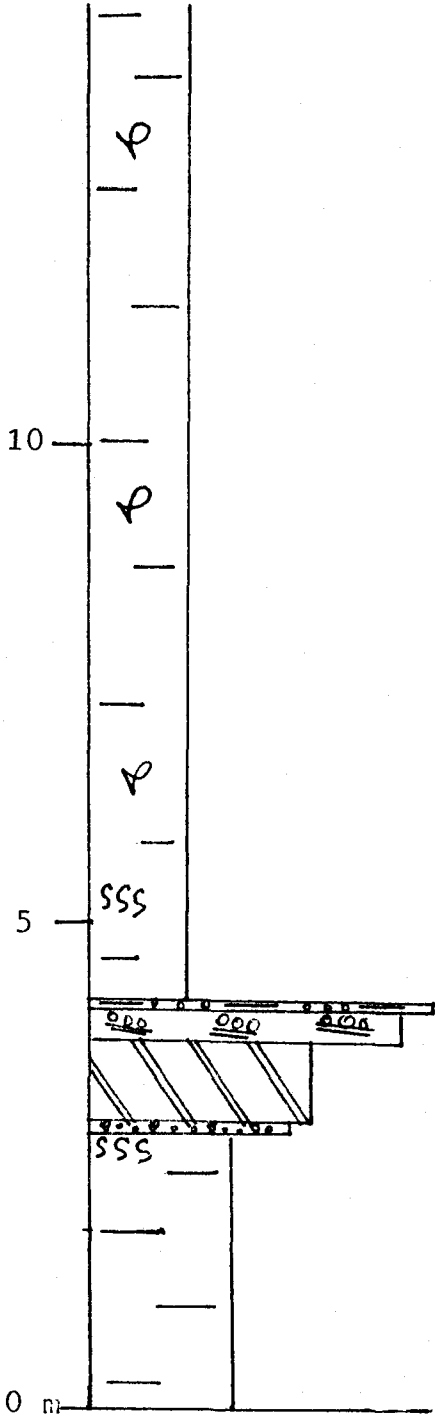


10-17-40-1W5

5635-5683'

8-19-40-1W5

5731-5746'

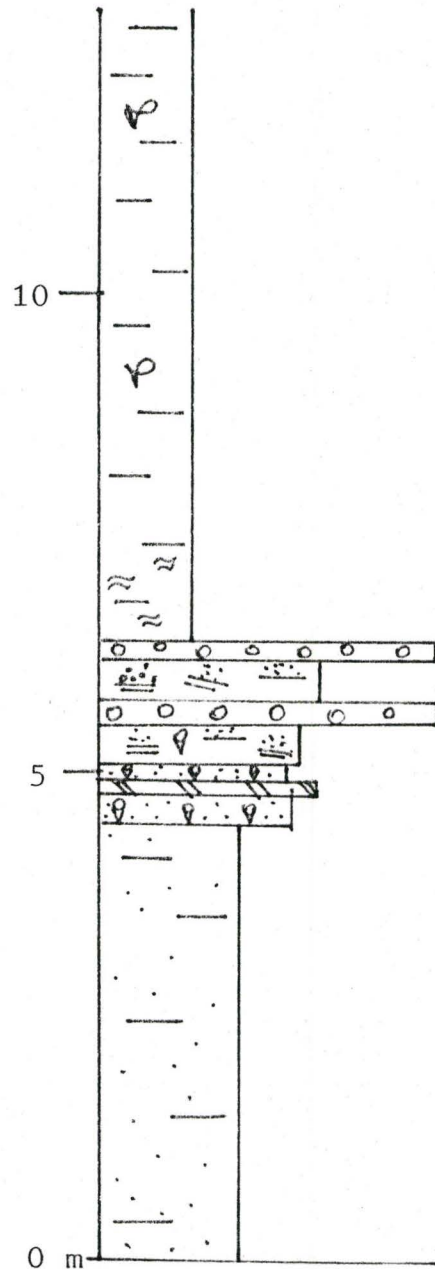
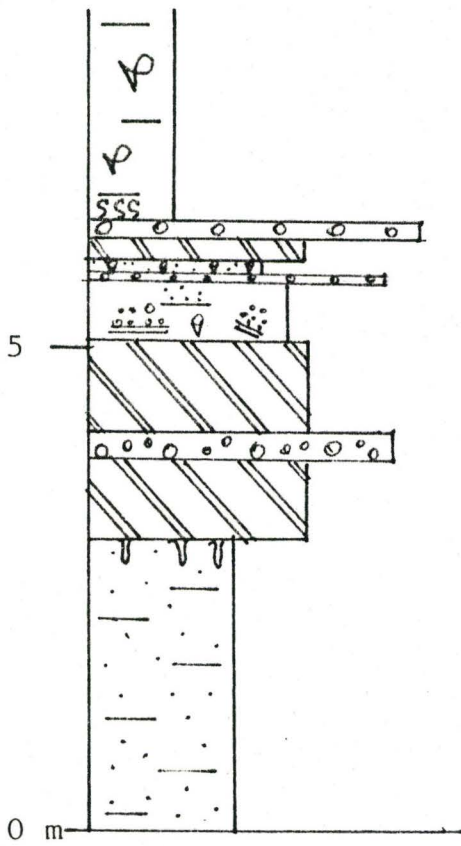


12-19-40-1W5

5704-5732'

2-30-40-1W5

5793-5836'

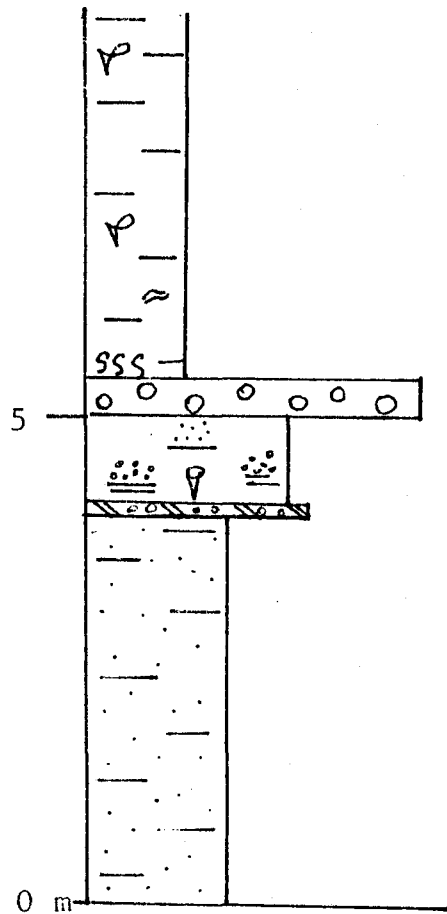
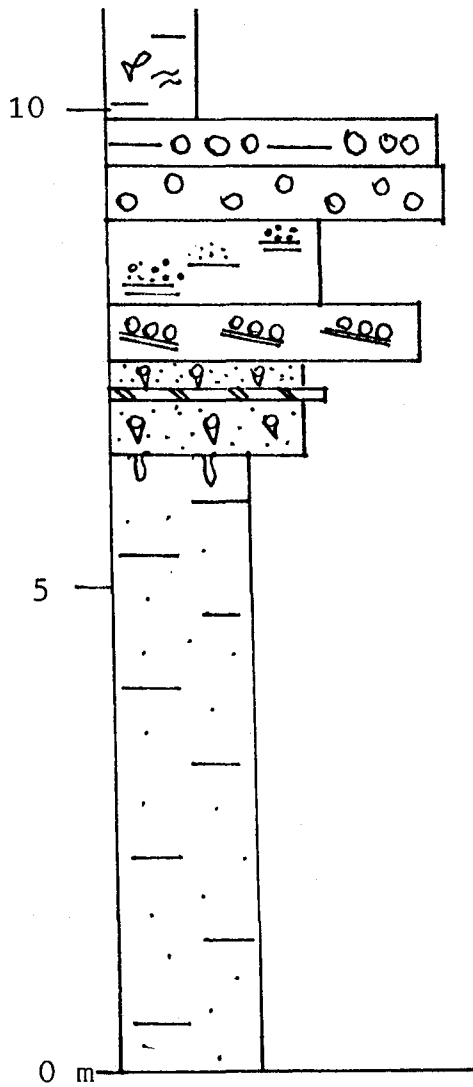


4-30-40-1W5

5733-5745'  
5746-5770'

10-24-40-2W5

5798-5828'

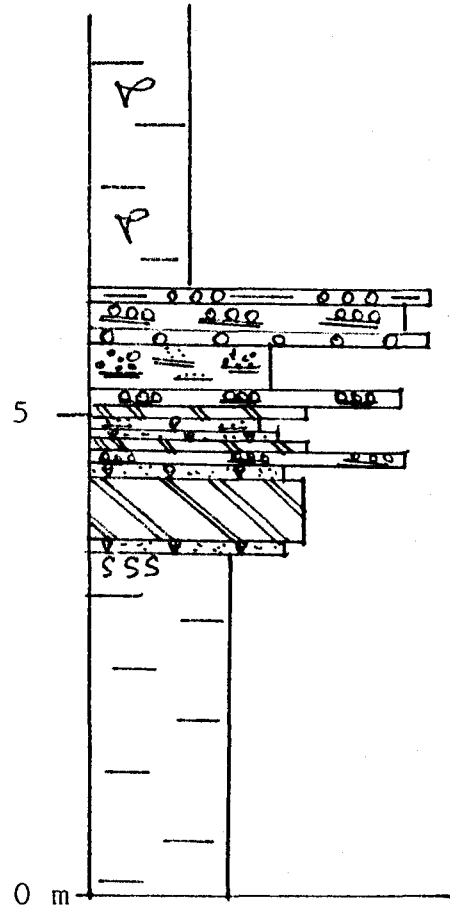
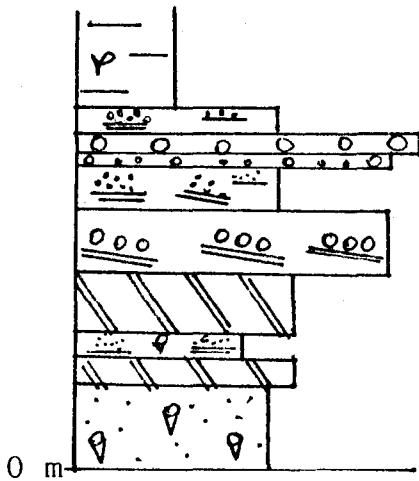


16-24-40-2W5

5753-5770'

4-25-40-2W5

5865-5895'



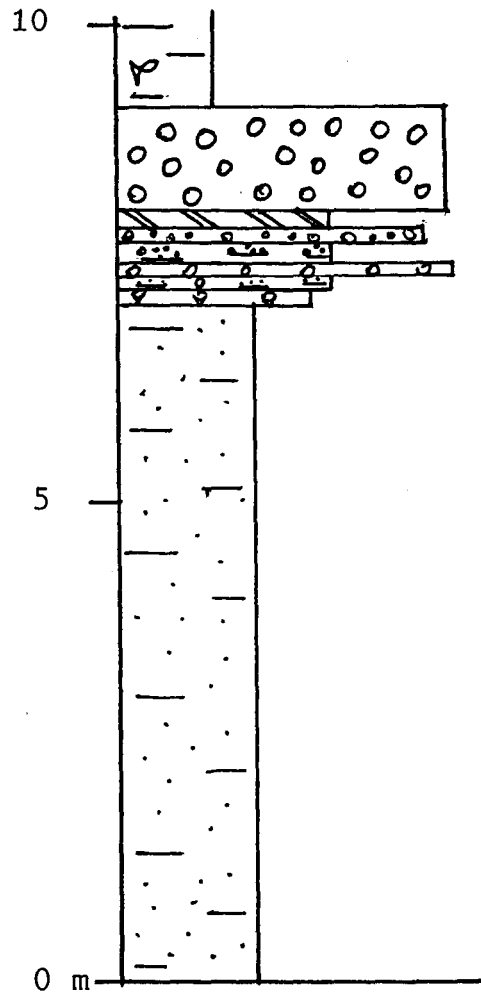
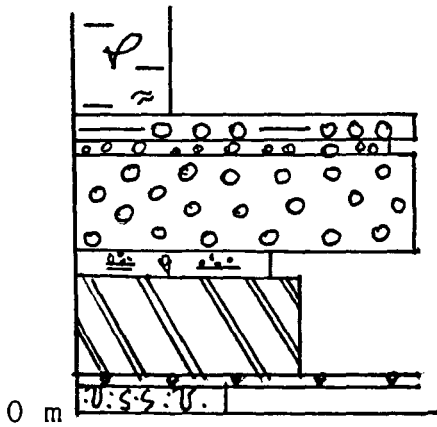


2-6-41-2W5

6043-6057'

4-2-41-3W5

6384-6418'



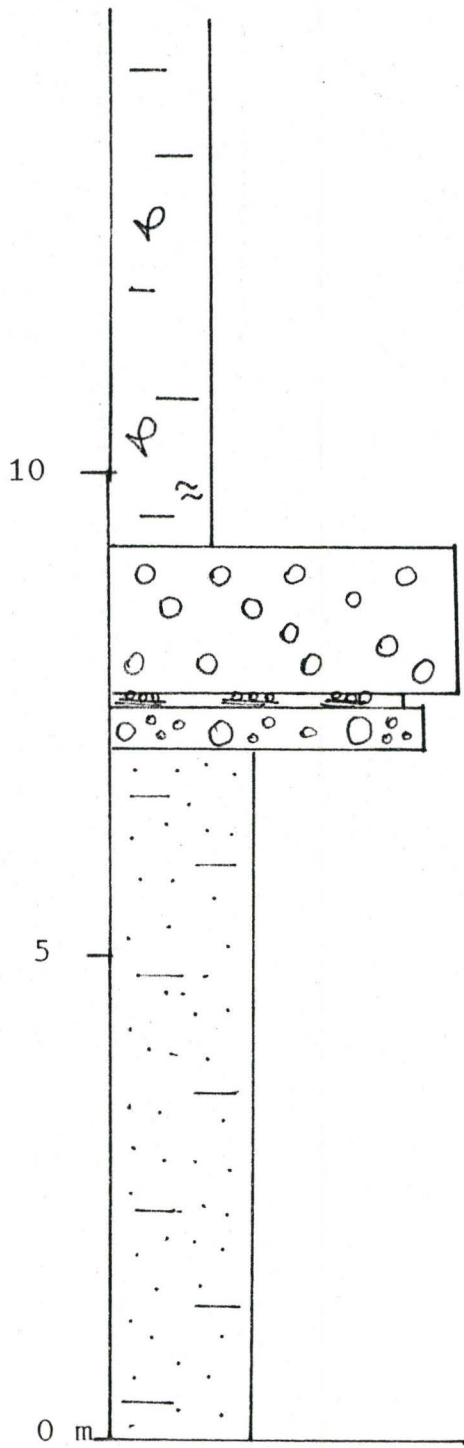
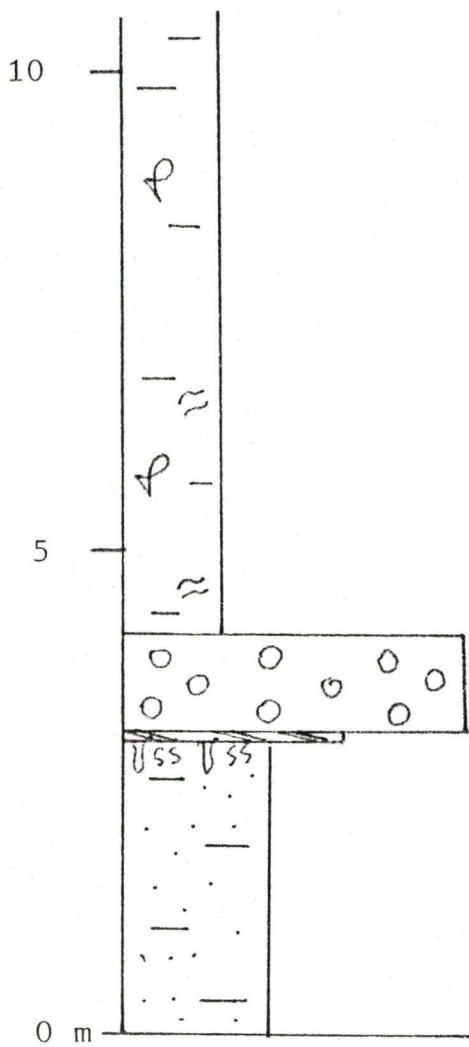


10-7-41-3W5

6292-6327'

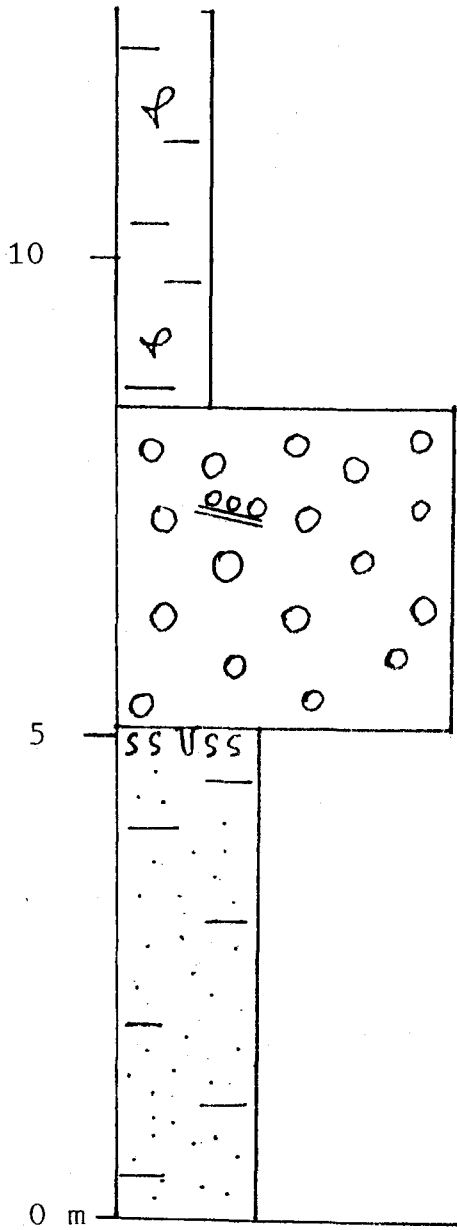
10-8-41-3W5

6243-6292'



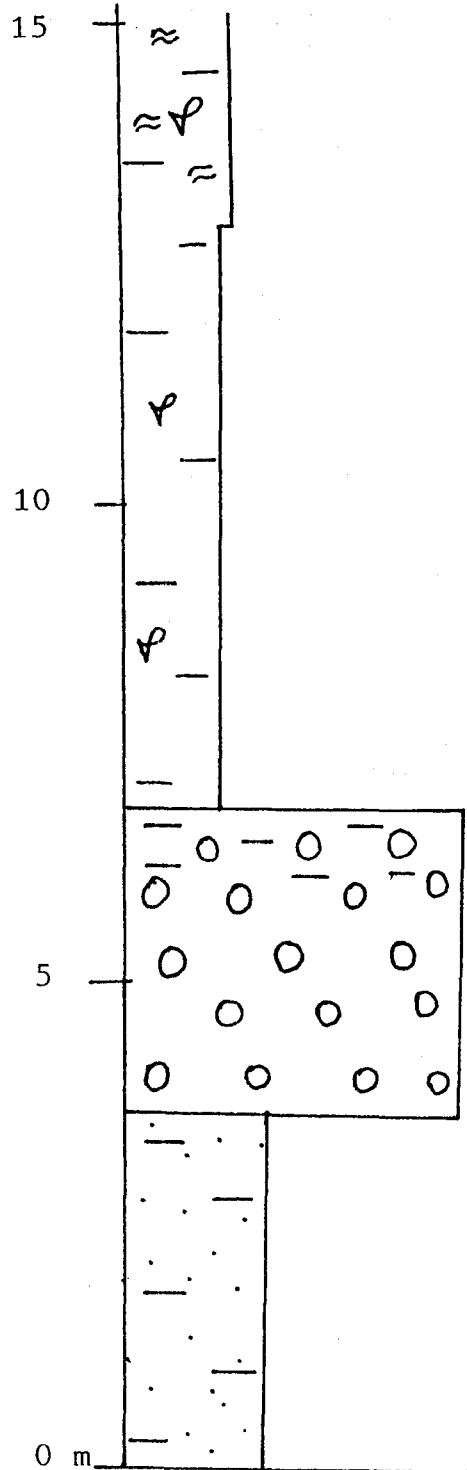
2-9-41-3W5

6240-6281'



4-9-41-3W5

6274-6324'

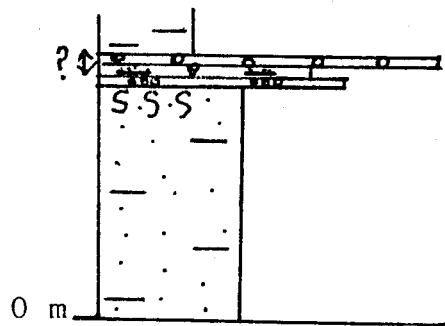
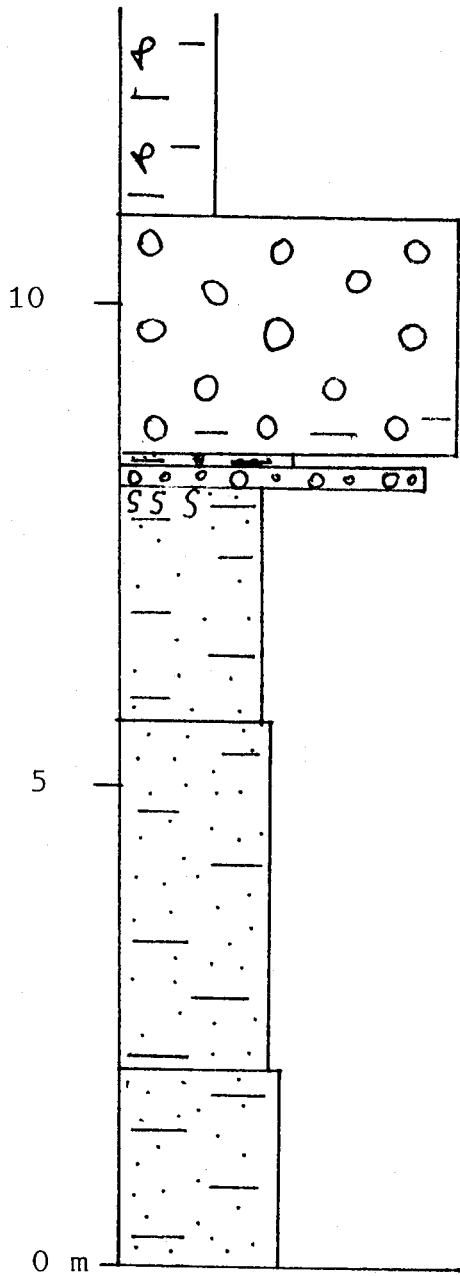


12-9-41-3W5

6307-6350'

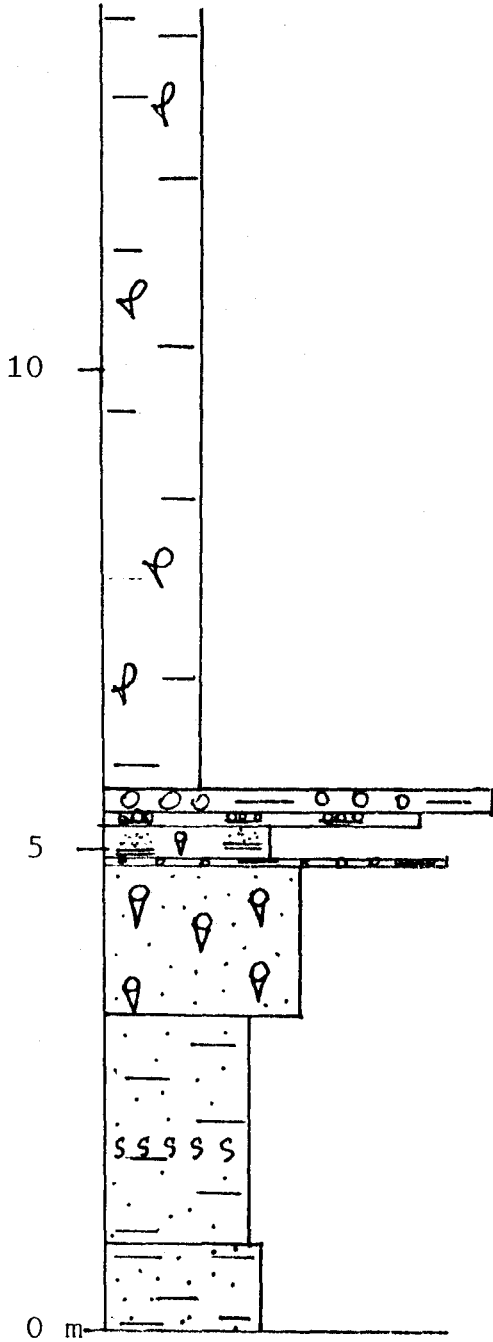
4-18-41-3W5

6365-6375'



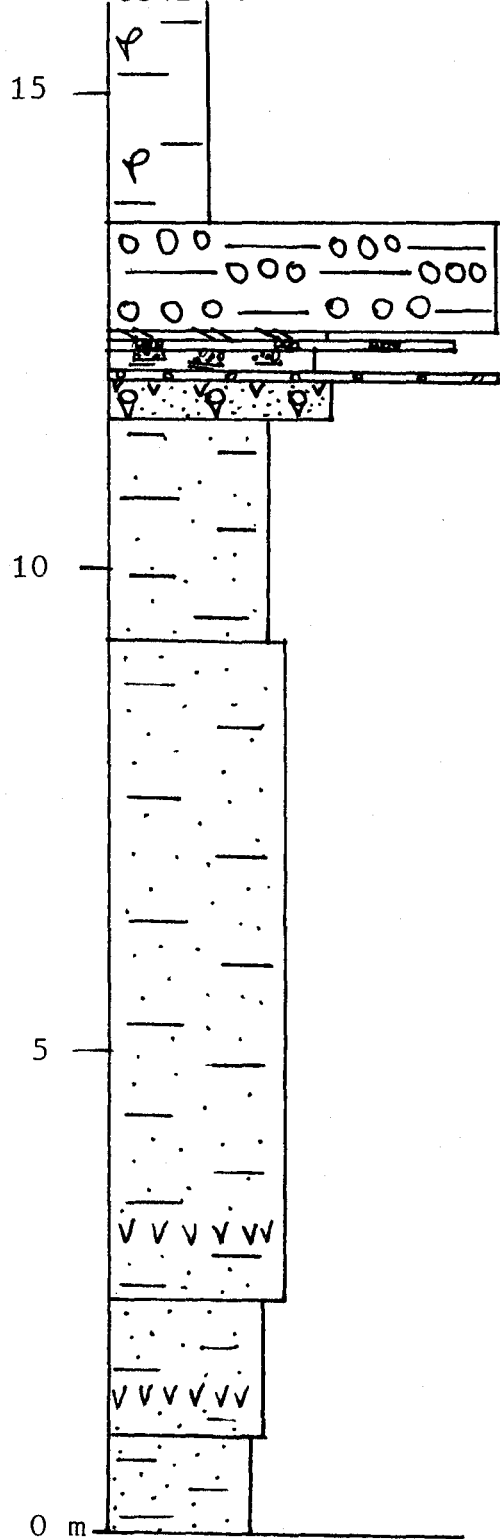
10-30-41-3W5

6302-6348'



10-34-41-4W5

6342-6395'

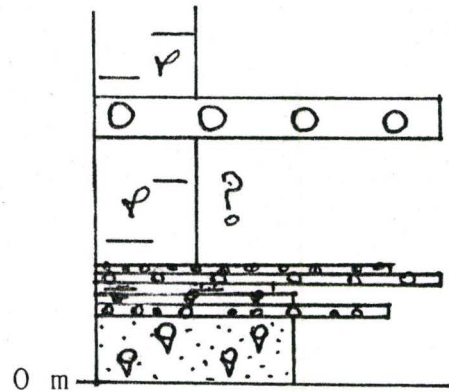
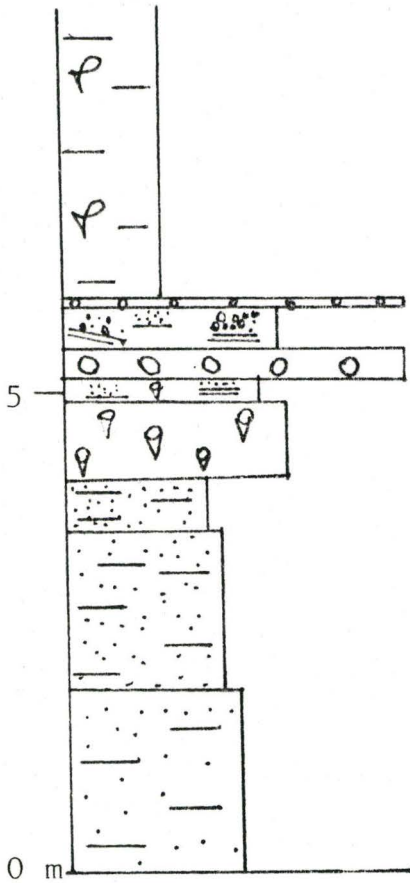


10-35-41-4W5

4-36-41-4W5

6280-6309'

6319-6332'

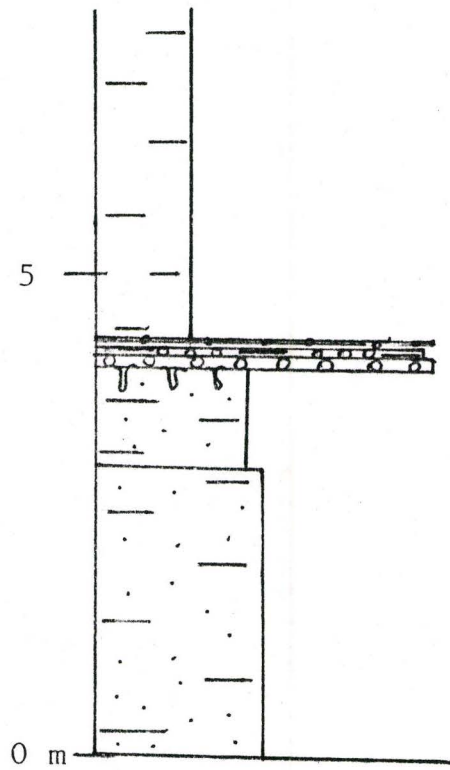
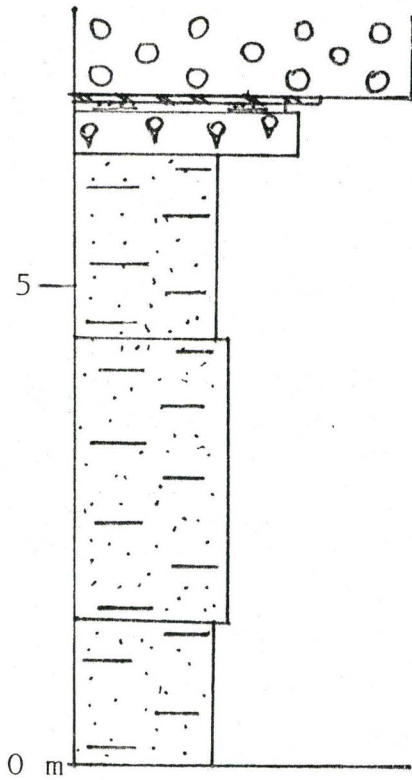


4-3-42-4W5

6351-6376'

2-5-42-4W5

6431-6456'

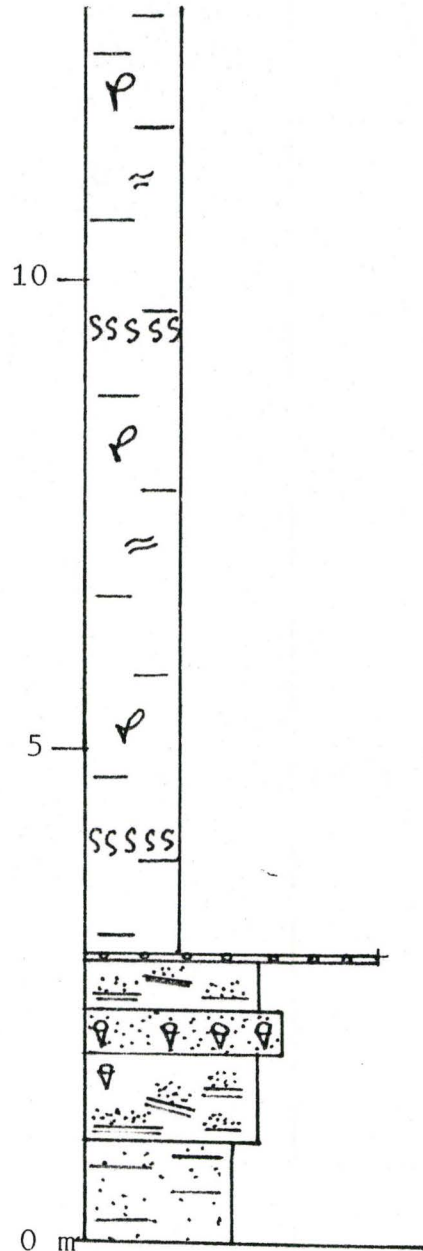
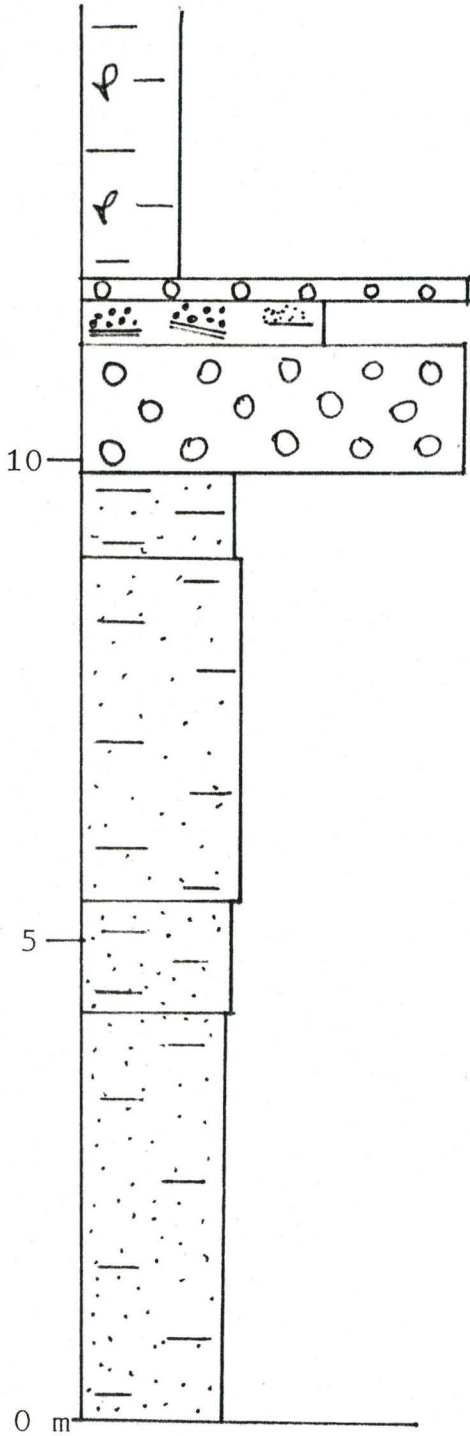


12-5-42-4W5

6422-6470'

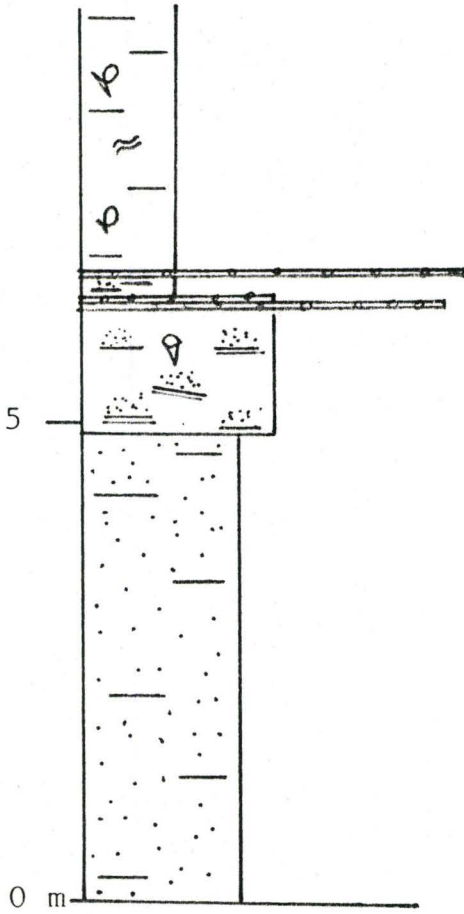
4-8-42-4W5

6405-6445'



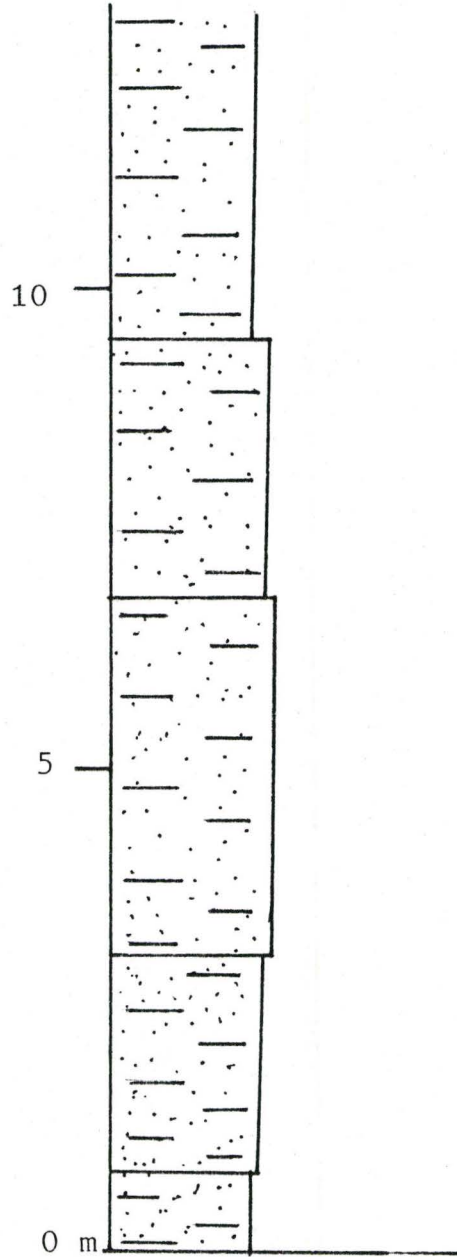
10-17-42-42W5

6345-6377'



10-2-42-5W5

6522-6565'



7-10-42-5W5

6547-6595'

4-12-42-5W5

6494-6535'

